Aus der

Berufsgenossenschaftlichen Unfallklinik

Klinik für Unfall- und Wiederherstellungschirurgie an der
Universität Tübingen

Exposure to Extremely Low-Frequency Pulsed Electromagnetic Fields Promotes Fracture Healing through Alleviating the Damage Caused by Cigarette Smoke and Modulating the Osteoimmune Microenvironment

**Thesis submitted as requirement to fulfill the degree
„Doctor of Philosophy" in Experimental Medicine (PhD)**

**at the
Faculty of Medicine
Eberhard Karls Universität
Tübingen**

by

Chen, Yangmengfan

2023

Dean: Professor Dr. B. Pichler

First reviewer: Professorin Dr. S. Ehnert
Second reviewer: Privatdozent Dr. B. Steinhilber
Third reviewer: Professor Dr. P. M. Loskill

Tag der Disputation: 07.08.2023

Table of Contents

Abbreviations

$[Ca^{2+}]_i$	intracellular calcium ion
1,25D	1,25-dihydroxyvitamin D3
AC	alternative current
ACVR	activin A receptor
ALK	activin receptor-like kinase
AP	alkaline phosphatase
BB	basal body
BMD	bone mineral density
BMP	bone morphogenic protein
BSA	bovine serum albumin
BSAP	bone-specific alkaline phosphatase
Ca^{2+}	calcium ion
cAMP	cyclic adenosine monophosphate
CH	chloral hydrate
COL1A1	collagen I
CS	cigarette smoke
CSE	cigarette smoke extract
CTX	Type I collagen C-terminal telopeptide
CV	ciliary vesicles
CXCL	CXC-chemokine ligand
DCFH-DA	2´, 7´ dichlorofluorescein-diacetate
DLL	delta-like
DLX 5	distal-less homeobox 5
ECM	extracellular matrix
EF	electronic field
EMF	electromagnetic field
ERK	extracellular signal-regulated kinase
EU	European Union
FAK	focal adhesion kinase
FBS	fetal bovine serum
FDA	food and drug administration
GAPDH	glyceraldehyde 3-phosphate dehydrogenase
GM-CSF	granulocyte macrophage-colony stimulating factor
GPCRs	G protein-coupled receptors
HH	hedgehog
HSCs	hematopoietic stem cells
Hz	hertz
IFN-γ	interferon gamma
IFT	intraflagellar transport
IGF	insulin-like growth factor
IL	interleukin
iNOS	inducible nitric oxide synthase

LPS	lipopolysaccharide
MAPK	mitogen-activated protein kinase
MF	magnetic field
MMPs	matrix metalloproteinases
MSC	mesenchymal stem cell
mT	millitesla
Mφ	macrophage
NETs	neutrophil extracellular traps
NK cell	natural killer cells
NSAID	non-steroidal anti-inflammatory drug
OCN	osteocalcin
OSX	osterix
PC1	polycystin-1
PDGF	platelet-derived growth factor
PEMF	pulsed electromagnetic field
PKA	protein kinase A
PMA	phorbol myristate acetate
RA	rheumatoid arthritis
RANKL	receptor Activator of NF-κB Ligand
RHW	rectified half-wave
ROS	reactive oxygen species
RT	room temperature
RTKs	receptor tyrosine kinases
RUNX2	runt-related transcription factor 2
SCP-1	single-cell-picked clone 1
SLC	small latent complex
SMO	smoothened
SRB	sulforhodamine B
T2DM	type 2 diabetes mellitus
TBS-T	tris-buffered saline-tween
Temff1	tomoregulin1
TEP	transepithelial potential difference
TGF-β	transforming growth factor-beta
TGF-β R	TGF-β receptor
TNF-α	tumor necrosis factor-alpha
UK	United Kingdom
US	United States of America
UV	ultraviolet
μT	microtesla

Figures

1. Introduction

Around 385 million years ago, when aquatic vertebrates migrated from the sea to the mainland, the skeletal system evolved. To avoid the DNA damage caused by ultraviolet (UV) light, hematopoietic stem cells (HSCs) gradually moved into the cortical bone (Tsukasaki and Takayanagi, 2019). Since then, our skeletal system and immune system have not been isolated, but are rather highly interrelated with each other in the bone marrow. The bone marrow is the main location for the generation and maintenance of HSCs and immune cells, and it provides a microenvironment for both systems to share a variety of molecules and cytokines to affect signaling pathways in the resident cells (Takayanagi, 2007). This microenvironment is more than an immune cell niche that unilaterally affects osteogenesis (Chen *et al.*, 2016). Instead, both the skeletal system and the immune system mutually regulate each other to reach a homeostatic steady state. For example, the depletion of CXC-chemokine ligand 12 (CXCL12) in osteoblasts affects the differentiation of B-lymphocytes (Greenbaum *et al.*, 2013) and increases levels of Notch ligand delta-like 4 (DLL4) in osteoblasts, which affects the differentiation of T-lymphocytes (Yu *et al.*, 2015). In turn, activating the immune response also affect osteoblasts (Chen *et al.*, 2021) and osteoclasts (Sato and Takayanagi, 2006), thereby indirectly influencing the skeletal system. Thus, a stable and harmonious osteoimmune microenvironment is important for the maintenance of bone homeostasis.

1.1 Bone and Bone Fracture

The human skeletal system has been under selection pressure throughout the long evolutionary journey (Medina-Gomez *et al.*, 2015). To maintain a healthy metabolic homeostasis of the skeletal system, there are 206 bones of very different shapes and sizes in adult human. They not only play a key role in consolidating our body (Brasinika *et al.*, 2020), protecting internal organs (Lee *et al.*, 2021), and supporting muscle attachment (Labusca *et al.*, 2015), the skeleton also acts as local storage depot of calcium, phosphate, and growth factors (Delany and Hankenson, 2009). These valuable merits originate from the structural features of bones. The bone structure is very compact and sophisticated; for instance, a long bone can be subdivided into five distinct regions:

1) Bone marrow: a semi-solid tissue in the trabecular bone that contains myelopoietic cells, erythropoietic cells, and stromal cells (*e.g.*, mesenchymal stromal cells (MSCs), osteoblasts, osteoclasts, and macrophages) (Fracchiolla *et al.*, 2017);

2) Trabecular bone: the central part of cancellous bone that functions as a distributor of the mechanical load (He *et al.*, 2019);

3) Cortical bone: the dense outer layer of bone. Both the cortical bone and trabecular bone determine the bone strength and bone mineral density (BMD) (Furst *et al.*, 2008);

4) Periosteum: a connective tissue covering the surface of cortical bone, which consists of both a fibrous layer and a cambial layer, and contains periosteal progenitor cells (Wang *et al.*, 2013); and

5) Cartilage: a highly specialized tissue at the end of the bone, which contributes to smooth and frictionless joint mobility (Muttigi *et al.*, 2016).

The sophisticated architecture and finely tuned function are of vital importance and can be affected in many diseases, *e.g.*, osteoarthritis (Belsue *et al.*, 2021) and osteoporosis (Pignolo *et al.*, 2021). If the structural continuity of a bone is partially or completely broken after a direct force or indirect stress, a bone fracture happens.

Notably, bone fractures are a global health issue and present a serious economic burden around the world. It has been reported that the global average cost in hospitals for the treatment of a hip fracture is around $ 10,075, and the total cost over a period of 12 months can reach up to $ 43,669 (Williamson *et al.*, 2017). In Europe (data from 27 EU countries + Switzerland and the UK), 4.3 million patients suffered from different types of fragility fractures in 2019, *i.e.*, hip fractures (826,708; 19%), vertebral fractures (662,544; 16%), forearm fractures (636,705; 15%), and other fractures (2,149,591; 50%) (Kanis *et al.*, 2021). The total direct costs were estimated to be € 56.9 billion (Kanis *et al.*, 2021). Along with the increase in disabilities and the prolonged recovery time, bone fractures impose heavy socioeconomic and health care burdens (Victoria *et al.*, 2009). Moreover, bone defects caused by injury, cancer, or other systemic diseases are one of the most serious diseases in our society (De Mattos *et al.*, 2012). Therefore, an effective, low cost, and integrated therapeutic option for bone fractures is an urgent clinical and social need.

1.2 The Healing Process of Bone Fracture

Although nature has endowed living beings with self-healing abilities, allowing them to repair damage when injured (Lai *et al.*, 2018), this ability is sometimes not sufficient to meet the demands of human life in modern society where people seek a high quality of life, attractive appearance, and sophisticated work, rather than simply surviving the harsh environment as other creatures do. To develop a satisfactory therapeutic option for fracture healing, it is important to understand the pathophysiologic fracture healing process. A fracture heals in a sophisticated and finely tuned way; a good outcome of fracture healing is the full reconstitution of bone continuity and function. To achieve this goal, intercellular communications between different cell types (*e.g.*, osteoblasts, osteoclasts, and macrophages) (Kaku and Komatsu, 2017), and interactions between cytokines and growth factors at the fracture site should proceed in a coordinated and ordered manner (Martin and Rodan, 2008). The healing process of bone fracture is subdivided into the 1) primary type and 2) secondary type. During primary fracture healing, there is only a small fracture gap and the ends of the fracture are closely repositioned, such that the bone is reestablished without callus formation. During primary fracture healing, neither resorption of the fracture end nor callus formation happens. Instead, osteoblasts synthesize and deposit new bone to fill the gap. However, primary fracture healing is rare, and the majority of fractures heal as the secondary (spontaneous) type (Cottrell *et al.*, 2016). Secondary fracture healing usually happens when bone fragments undergo motion without rigid fixation. This process is so complex that it requires the involvement of the periosteum, soft tissues, and various cell types at the fracture site (Bigham-Sadegh and Oryan, 2015). The process of secondary healing is divided into four overlapping phases (Fig. 1):

1) Inflammatory phase: immediately after the fracture happens, a hematoma forms and the inflammatory phase starts. The cells from interrupted peripheral and intramedullar blood, as well as the bone marrow, form a hematoma at the fracture site (Gerstenfeld *et al.*, 2003). The hematoma at the fracture site provides a hypoxic environment, thereby inducing cell activation, migration, and differentiation (Annamalai *et al.*, 2018). The hematoma not only forms a 3D platform for the cells involved in the repair process, but also releases various cytokines and growth factors to regulate angiogenesis and new bone formation at the fracture site (Street *et al.*, 2000). This phase takes 3 to 4 days until the initiation of soft callus

formation. The timeframe of the inflammatory phase may be altered in many pathological situations, *e.g.*, type 2 diabetes mellitus (T2DM) (Singh *et al.*, 2016), or cigarette smoking (Hao *et al.*, 2021), thus impairing fracture healing.

2) Soft callus formation: within a few days, the fracture site is populated with fibroblasts and MSCs, and the hematoma is gradually replaced by fibrin-rich granulation tissue (Marsell and Einhorn, 2011). On the one hand, granulation tissue provides a microenvironment for angiogenesis (Carano and Filvaroff, 2003) and chondrogenesis (Claes *et al.*, 2012), which are required to form the soft callus at the fracture ends. On the other hand, it provides a platform for the upcoming endochondral ossification (Loi *et al.*, 2016).
3) Hard callus formation: with the formation of a soft callus, chondrocytes gradually transform into hypertrophic chondrocytes and then undergo apoptosis (Marsell and Einhorn, 2011). Meanwhile, MSCs differentiate into osteoblasts to start intramembranous ossification and mineralization at the fracture ends to form a hard callus (Gerstenfeld *et al.*, 2006). Different from the soft callus, the formation of a hard callus tightly bridges the fracture ends with a certain degree of biomechanical stability, therefore, it usually marks the late stage of the repair phase (Lafuente-Gracia *et al.*, 2021).
4) Bone remodeling: After the formation of a hard callus, both resorption and formation are activated to sustain the bone mass and provide adequate mechanical strength. The process of bone remodeling follows Wolff's law, *i.e.*, the bone will be remodeled to be able to resist loading (Remedios, 1999, Wolf, 1995). Bone remodeling is initiated from 3 to 4 weeks after the fracture and takes several years to eventually achieve full biomechanical stability (Daish *et al.*, 2018). After this final phase of fracture healing, the continuity and stability of the bone will be completely restored.

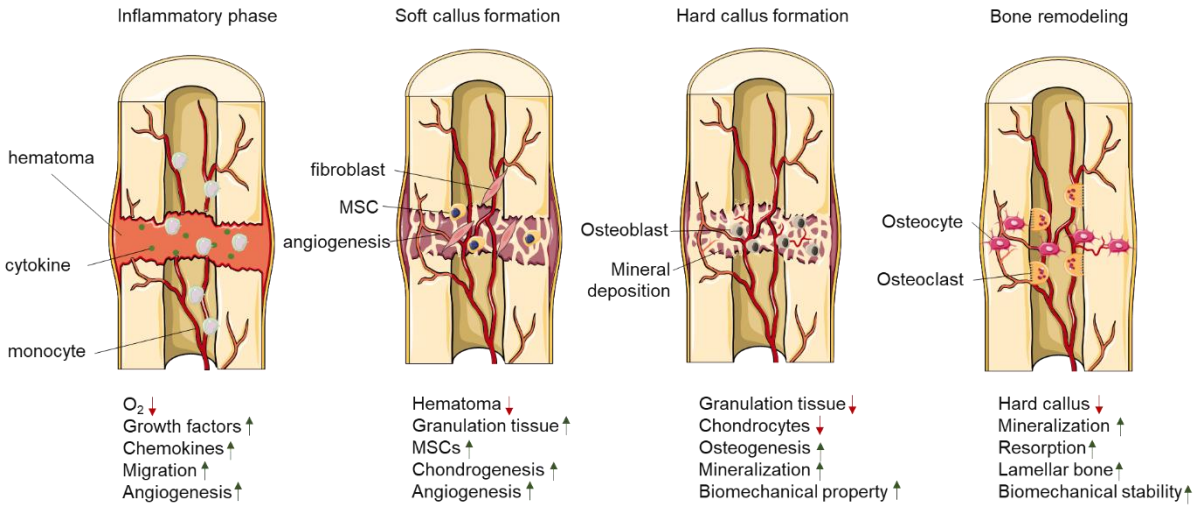

Figure 1: The healing process of a fractured bone is subdivided into four phases: 1) inflammatory phase, 2) soft callus formation, 3) hard callus formation, and 4) bone remodeling. Immediately after a bone fracture occurs, many immune cells, *e.g.*, neutrophils, lymphocytes, monocytes, and platelets, are attracted to the fracture site and form a hematoma. Immune cells in the hypoxic environment of the hematoma are activated and secrete many growth factors, cytokines, and chemokines. Subsequently, the hematoma is gradually replaced by granulation tissue. In this phase, fibroblasts and MSCs migrate to the fracture site, and angiogenesis and chondrogenesis are initiated, thus forming the soft callus. When the chondrocytes in the soft callus exhibit a hypertrophic morphology, they gradually undergo apoptosis. Then, mineral deposition increases, and the soft callus turns into a hard callus with limited biomechanical properties. In the end, the hard callus is degraded, and both osteoblastic mineralization and osteoclastic resorption are activated to remodel the new bone to form lamellar bone, which further enhances the biomechanical stability. Graphic elements were provided by Servier (smart.servier.com). This schematic diagram was graphically processed based on a previous study (Einhorn and Gerstenfeld, 2015).

1.3 Immune Cells in Bone Healing

As mentioned above, the immune system and skeletal system share an evolutionary homology. Especially macrophages are actively involved in all stages of the healing process (Loffler *et al.*, 2019). Immediately after the fracture happens, macrophages (Mφ) migrate to the fracture site and initiate the inflammatory phase, participating in the formation of soft callus and hard callus, and subsequently regulate the bone remodeling phase (Munoz *et al.*, 2020, Ehnert *et al.*, 2021). Mφ is a so-called versatile multifunctional cell type; which displays different phenotypes and activities depending on the surrounding microenvironment (Chen *et al.*, 2020). Following induction by interferon-γ (IFN-γ) (Orecchioni *et al.*, 2020), granulocyte macrophage-colony stimulating factor (GM-CSF) (Mily *et al.*, 2020), or lipopolysaccharide (LPS) (Porta *et al.*, 2009), Mφ exhibit pro-inflammatory activities (classically activated, M1 Mφ). Following induction by interleukin-4 (IL-4) (He *et al.*, 2020), interleukin-10 (IL-10) (Lopes *et al.*, 2016), or TGF-β (Zhang *et al.*, 2016), Mφ

also exhibit strong anti-inflammatory activities (alternatively activated, M2 Mφ) (Murray, 2017). The versatile and polarizable capability of Mφ multi-directionally affects fracture healing (Gibon *et al.*, 2016). In detail, Mφ with pro-inflammatory activity can secrete high amounts of pro-inflammatory cytokines (*e.g.*, IL-1β, IL-6, and IL-23), reactive oxygen species (ROS), inducible nitric oxide synthase (iNOS), and tumor necrosis factor (TNF-α) (Shapouri-Moghaddam *et al.*, 2018). As a result, the pro-inflammatory microenvironment created by M1 Mφ supports the clearance of pathogens (Makowski *et al.*, 2019), chemoattracts MSCs (Ishikawa *et al.*, 2014), and initiates MSC proliferation (Liao *et al.*, 2020). However, a prolonged and excessive inflammatory response could suppress MSC activity and impair fracture healing (Maruyama *et al.*, 2020). In contrast, Mφ with anti-inflammatory activity can secrete many anti-inflammatory cytokines and a variety of growth factors, *e.g.*, TGF-β (Liu *et al.*, 2018), IL-10 (Viola *et al.*, 2019), vascular endothelial growth factor (VEGF) (Lai *et al.*, 2019), platelet-derived growth factor (PDGF) (Glim *et al.*, 2013), osteopontin (OPN) (Raggi *et al.*, 2017), 1,25-dihydroxyvitamin D3 (1,25D) (Small *et al.*, 2021), and bone morphogenetic proteins (BMPs) (Huang *et al.*, 2021). As a result, Mφ with anti-inflammatory activity suppress excessive inflammation, and thus may induce extracellular matrix (ECM) deposition, and promote fracture healing (Zhang *et al.*, 2018). The active interaction between pro-inflammatory Mφ and anti-inflammatory Mφ are important to promote fracture healing and achieve a satisfactory medical outcome (Fig. 2).

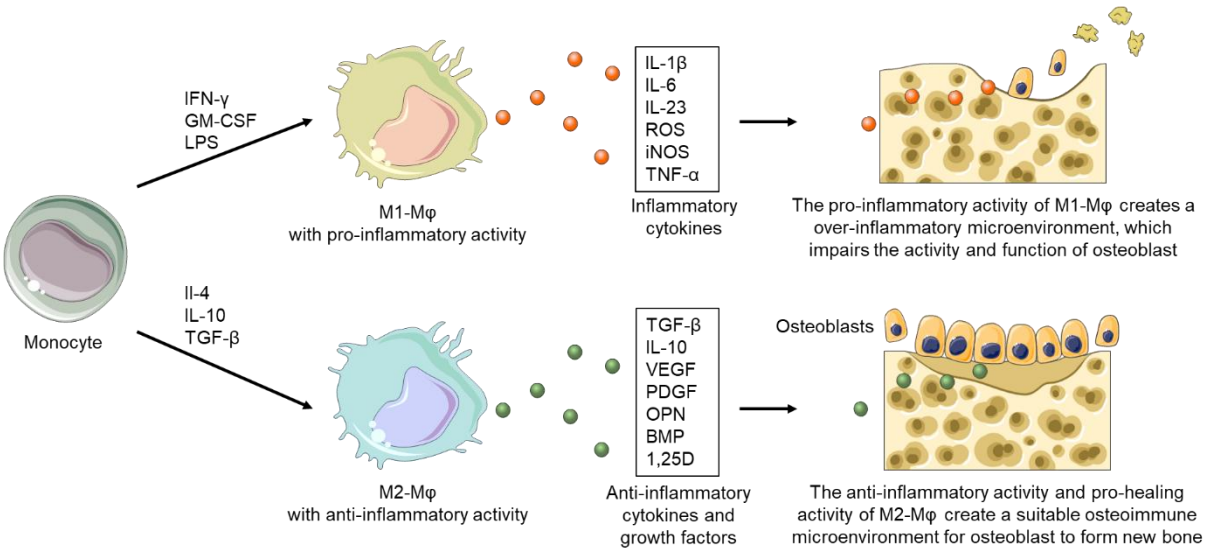

Figure 2: The important roles of monocytes in fracture healing: Immediately after a fracture occurs, monocytes from the peripheral blood migrate into the hematoma at the fracture site. Monocytes are activated by cytokines in the microenvironment and then polarize into Mφ with pro-inflammatory activity (M1 Mφ) or Mφ with anti-inflammatory activity (M2 Mφ). In detail, Mφ with

pro-inflammatory activity are induced by IFN-γ, GM-CSF, or LPS, then create an inflammatory microenvironment by secreting IL-1β, IL-6, IL-23, ROS, iNOS, and TNF-α. An excessive inflammatory response impairs cell viability and the differentiation capacity of osteoblasts and can induce apoptosis of osteoblasts. In contrast, Mφ with anti-inflammatory activity are induced by IL-4, IL-10, or TGF-β, then create an anti-inflammatory microenvironment by secreting various growth factors and anti-inflammatory mediators, *e.g.*, IL-10, TGF-β, VEGF, PDGF, OPN, BMP, and 1,25D. This microenvironment eliminates excessive inflammation and oxidative stress and thereby promotes cell viability and the osteogenic differentiation of osteoblasts, and enhances mineral deposition. Graphic elements were provided by Servier (smart.servier.com). This schematic diagram was graphically processed based on a previous study (Shen *et al.*, 2021).

1.4 Fracture Delayed Union and Non-union

Almost 2,500 years have passed since the earliest records of conservative fracture treatment from Hippocrates (Biz *et al.*, 2022). Since the industrial revolution of the 18th century, and the discovery of antibiotics in the early 20th century, fracture treatment has been greatly improved. However, the debate on the best therapy for fractures is far from being over (Biz *et al.*, 2022). In recent decades, although tremendous amounts of research have been conducted to promote fracture healing, fracture delayed union and non-union still occurs in approximately 5% to 10% of all cases. According to the American Food and Drug Administration (FDA), delayed fracture healing is defined as a fracture process that takes longer than 9 months and has no progressive signs of healing for more than 3 months (Nicholson *et al.*, 2021). The majority of fracture non-unions occur after long bone fractures, *e.g.*, forearm fracture, humerus fracture, femur fracture, and tibia fracture, in working-age males or elderly women (Mills *et al.*, 2017, Zura *et al.*, 2016, Mills and Simpson, 2013). The average costs for treating a long bone fracture non-union is approximately CN$ 11,800 (Busse *et al.*, 2005), US$ 11,333 (Beaver *et al.*, 1997), or £ 29,204 (Patil and Montgomery, 2006). Thus, the treatment of fracture delayed union and non-union poses a tremendous financial burden on health care systems (Hak *et al.*, 2014). Generally, risk factors for developing fracture non-union include both local and general factors. Among the local factors, open fractures with surrounding soft tissue injury are considered one of the most critical local risk factors of non-union (Schemitsch *et al.*, 2012). Other local risk factors such as bone loss (Keating *et al.*, 2005), bone displacement and comminution (Zura *et al.*, 2016), multiple fractures with polytrauma (Metsemakers *et al.*, 2015), or implant-related infection rarely occur (Mills *et al.*, 2016). However, to prevent fracture non-union by surgical intervention, surgeons should place more attention on general and often modifiable risk factors (Nicholson *et al.*, 2021). Most studies report that cigarette smoking is a major general

risk factor for fracture healing, *e.g.*, it impairs endochondral ossification, exacerbates peripheral arterial disease, and induces perioperative complications (Hernigou and Schuind, 2019). In a systematic review that included 1,221 fractures, it was reported that the average healing time of non-smokers and smokers was 24.1 weeks and 30.2 weeks, respectively, with the overall ratio of non-union in smokers being 12% higher than in nonsmokers (Scolaro *et al.*, 2014). Other general risk factors that may delay fracture healing and lead to fracture non-unions are increased age (Bhandari *et al.*, 2012), T2DM (Zura *et al*., 2016), obesity (Zura *et al*., 2016), and the long-term application of non-steroidal anti-inflammatory drugs (NSAID) (Hernandez *et al.*, 2012). Considering that fracture delayed union or non-union is often accompanied by many risk factors and disorders, novel therapies aiming to promote fracture healing while ameliorating risk factors are urgently required.

1.5 A Promising Treatment for Fracture Non-union: Extremely Low-Frequency Pulsed Electromagnetic Field (ELF-PEMF)

To develop a promising treatment for fracture non-union, we focused on magnetic fields (MF), which exist everywhere in our daily life, *e.g.*, microwaves, radio waves, visible lights, and x-rays (Fig. 3). There is a wide variety of classifications for MF, such as the origin (permanent magnets or electromagnetic fields), production (natural fields or artificial fields), status (static field or dynamic field), and ionization ability (ionizing or non-ionizing radiation) (Wang and Zhang, 2017). Of these, extremely low-frequency pulsed electromagnetic fields (ELF-PEMF, frequency <300 Hz) have received substantial attention in regenerative medicine (Yuan *et al.*, 2018). The reasons can be mainly described as:

1) ELF-PEMF has many advantages as a clinical treatment, *e.g.*, its safety (non-invasive and non-ionizing) and convenience (low cost and home implementation) (Bassett, 1993). As early as 1978, Bassett *et al.* first reported the therapeutic effects of ELF-PEMF exposure in treating bone fractures (Bassett *et al.*, 1978). Subsequently, increasing evidence demonstrated the therapeutic effects of ELF-PEMF exposure on fracture healing (Shi *et al.*, 2013, Ziegler *et al.*, 2019), osteoporosis (Li *et al.*, 2018), spinal fusion (Foley *et al.*, 2008), and osteoarthritis (Dundar *et al.*, 2016, Ehnert *et al.*, 2019). Nevertheless, the mechanisms behind have not yet been fully investigated.

2) The physical properties of ELF-PEMF provide many possibilities to treat different diseases in a tuned and multidimensional way. In detail, the generation of ELF-PEMF

follows Faraday's Law, which states that EMF are generated when electrons move at an accelerated velocity, and a change in EF or MF can generate each other mutually (Ross *et al.*, 2015). Therefore, ELF-PEMF have many physical parameters that can be modulated, *e.g.*, waveform, frequency, amplitude, burst width, pulse width, and duration (Ehnert *et al.*, 2019). Thus, the controllable properties of an ELF-PEMF could be a target for precise regulation to be used to treat specific diseases.

3) EMF combine the merits of both EF and MF. In detail, EF are easy to modulate and can directly exert electric forces on charged molecules and organelles (Ross *et al.*, 2015) to mediate cell migration by directly regulating the dynamics of microfilaments and microtubules (Finkelstein *et al.*, 2004). MF have a strong penetrating ability that can easily be transferred into cells and tissues to influence biochemical reactions (Funk *et al.*, 2009). Therefore, a modulable exogenous EMF is theoretically feasible to penetrate the tissue at the fracture site to regulate endogenous EMF and thus support healing of the fractured bone (Ross *et al.*, 2015).

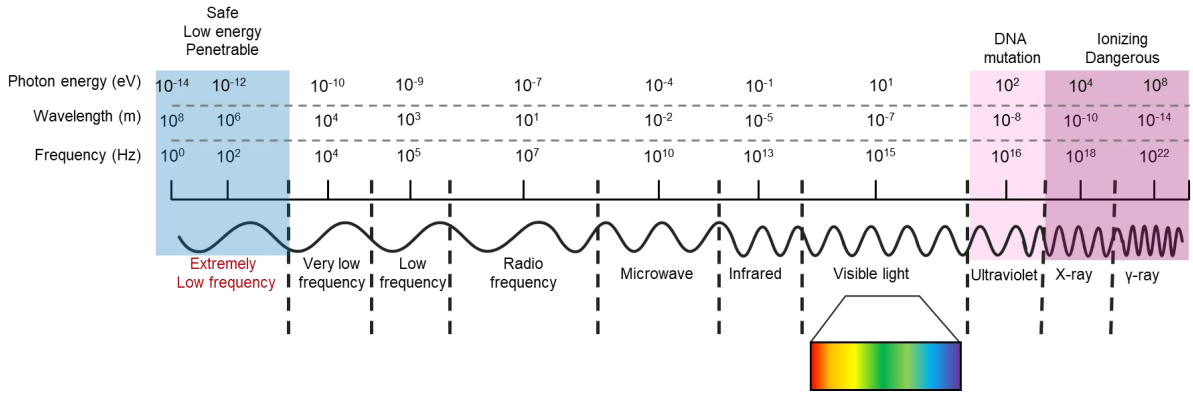

Figure 3: Schematic illustration of the EMF spectrum: EMF are divided into many types based on their physical characteristics *e.g.*, frequency, wavelength, or photon energy. According to the EMF frequency, EMF are subclassified into extremely low-frequency EM waves, very low-frequency EM waves, low-frequency EM waves, radio waves, microwaves, UV/visible/infrared light, X-ray, and γ-rays. Among the variety of EMF, extremely low-frequency EMF have been used as a promising treatment for fracture healing because of their safety, low energy, and penetrance. This schematic diagram was graphically processed based on our previous study (Ehnert *et al.*, 2019).

1.6.1 ELF-PEMF Directly Promote Fracture Healing

In the human body, especially in the musculoskeletal system, physiological EMF are omnipresent because of the piezoelectric phenomenon. During movement of the musculoskeletal system, the frequency of local physiological EMF ranges from 5 Hz to 30 Hz (Antonsson and Mann, 1985). In the case of trauma, the endogenous electric potential has been reported to be lower at the wound site and higher in healthy tissue, which generates a transepithelial potential difference (TEP) (Song *et al.*, 2002).

During the healing process, TEPs around the wound would stimulate the healing process and then gradually disappear after the wound is completely healed (Becker *et al.*, 1962). Inspired by this pathophysiological phenomenon, we intended to apply EMF to support the piezoelectric phenomenon during the healing process to achieve a satisfactory outcome.

The role of ELF-PEMF in fracture healing has received lots of attention in recent decades. It has been reported that ELF-PEMF exposure with specific parameters and strategies exhibited different biological effects. For instance, 75 Hz PEMF can activate Notch signaling to upregulate the levels of runt-related transcription factor 2 (Runx2), osterix (OSX), and distal-less homeobox 5 (DLX5), to induce osteogenic differentiation of human MSCs (Bagheri *et al.*, 2018); 15 Hz sinusoidal EMF exposure increases the activity of extracellular signal-regulated kinase (ERK), cyclic adenosine monophosphate (cAMP), and cAMP-dependent protein kinase A (PKA) (Yong *et al.*, 2016); 15 Hz PEMF exposure has been reported to rescue glucocorticoid induced-anabolic activity in bone by upregulating Wnt1, Wnt3a, and Wnt10b (Cai *et al.*, 2020). Moreover, in a clinical trial including 43 women with postmenopausal osteoporosis, ELF-PEMF exposure significantly increased the levels of bone-specific alkaline phosphatase and β-catenin, while decreasing collagen degradation (type I collagen C-terminal telopeptide (CTX)) and the receptor activator of NF-κB ligand/ osteoprotegerin (RANKL/OPG) ratio (Catalano *et al.*, 2018).

The therapeutic effects of ELF-PEMF on fracture healing have been proven by many researchers; however, there has been little solid evidence to explain how MSCs perceive and transfer EMF signals into biological signals. Theoretically, several prerequisites should be reached in terms of ELF-PEMF therapy: 1) a specific organelle should function as a receptor to perceive these EMF signals, 2) a critical transduction event that can convert an EMF signal into a biochemical signal at the molecular level, 3) an effective and fast signaling pathway that can transmit this molecular signal to the nucleus (Temiyasathit and Jacobs, 2010). Therefore, we aim to provide a clear and systematic investigation of the mechanisms in this project, not only regarding the biological significance, but also to improve the therapeutic effects of ELF-PEMF on fracture healing.

1.6.2 ELF-PEMF May Promote Fracture Healing Through Indirectly Modulating the Immune Response

As mentioned above, the healing process of a fracture requires the involvement of many different cell types. Immediately after the fracture, various immune cells are recruited to the fracture site, where they regulate the activities of MSCs and osteoblasts during fracture healing (Baht *et al.*, 2018). Thus, controlling immune cell function at the fracture site may provide us with an alternative option to promote fracture healing and prevent fracture non-union.

There are many methods to regulate the immune system, but many treatments for immune dysregulation usually have systemic side effects, *e.g.*, infections caused by infliximab (Aringer *et al.*, 2009) or hypertension caused by cyclosporine (Bascones-Martinez *et al.*, 2014). Such systemic side-effects may be prevented using a treatment that can modulate immune cell function locally at the site of fracture. One option could be exposure to ELF-PEMF. Considering the versatile activities of Mφ during fracture healing, it is promising to modulate the Mφ (Fig. 4). For instance, a specific ELF-PEMF that can induce pro-inflammatory activity in Mφ could be applied to create an inflammatory microenvironment in the early stage of fracture healing to help clear pathogens and cellular debris; another ELF-PEMF that can induce anti-inflammatory activity in Mφ could be used reduce inflammation and promote tissue regeneration.

However, evidence about the immunomodulatory functions of ELF-PEMF are still missing.

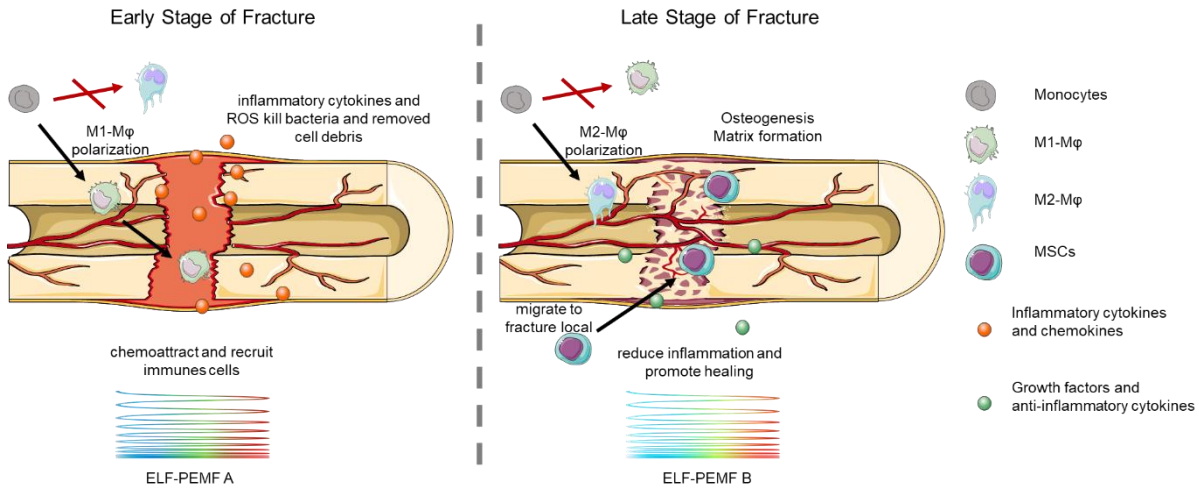

Figure 4: To achieve the temporal regulation of the immune environment, we intend to use one field in the early stage of fracture healing, to differentiate monocytes into Mφ with pro-inflammatory activity, which chemoattract more immune cells to secrete inflammatory cytokines and ROS to kill bacteria, initiate signaling pathways, and clear cell debris. At a late stage of fracture healing, we

use another field to differentiate monocytes into Mφ with anti-inflammatory activity, which can secrete many anti-inflammatory cytokines, and a variety of growth factors to reduce inflammation and promote healing. Graphic elements were provided by Servier (smart.servier.com). This schematic diagram was graphically processed based on a previous study (Lv *et al.*, 2021).

1.6 The Molecular Mechanism Behind the Therapeutic Effects of ELF-PEMF

Even though ELF-PEMF have considerable potential to promote fracture healing, the molecular mechanisms responsible for this are still largely unknown. This work focused on the effects of ELF-PEMF on different pathways involved in fracture healing.

1.6.1 TGF-β and BMP Signaling Pathway

Transforming growth factor-β isoforms (TGF-βs), as well as the bone morphogenic proteins (BMPs), belong to the TGF-β superfamily. The members of this superfamily and the related cellular signaling pathways are important in the fracture healing process and can be modulated by specific mechanical stimuli (Hiepen *et al.*, 2020).

In the TGF-β signaling pathway, the TGF-β receptor is a heterotetrameric complex of serine/threonine kinases, *i.e.*, TGF-β RI/ALK5 and TGF-β RII, which is located on the surface of the plasma membrane (Clement *et al.*, 2013). The ligands of the TGF-β receptor are subclassified into three highly homologous subtypes TGF-β1, TGF-β2, and TGF-β3 (Yue and Mulder, 2001). In canonical TGF-β signaling, binding of the ligand will activate TGF-β RII to phosphorylate TGF-β RI, which then phosphorylates Smad2/3. The phospho-Smad2/3 can then form a complex with Smad4 and pass through the nuclear membrane to modulate the expression of genes involved in cell proliferation, migration, and differentiation (Wu *et al.*, 2016). In addition to canonical or Smad-dependent TGF-β signaling, TGF-βs may also induce non-canonical signaling pathways, such as NFκB signaling (Luo, 2017) and ERK/MAPK signaling (Clement *et al.*, 2013). The related BMPs can be subclassified into more than 20 subtypes; this is the largest subfamily of the TGF-β superfamily (Hong *et al.*, 2009). In canonical BMP signaling, binding of a ligand activates BMPRII (*i.e.*, ACVR2A and ACVR2B) to phosphorylate BMPRI (*i.e.*, ALK1, 2, 3, and 6) (Dituri *et al.*, 2019). Then, phospho-BMPRI will phosphorylate relevant effector proteins of the BMP signaling pathway, *e.g.*, Smad1/5/8. Phosphorylated Smad1/5/8 can then

bind to Smad4, and pass through the nuclear membrane, where it exerts complex functions as a transcription factor (Rahman *et al.*, 2015).

Immediately after a bone is fractured, or the balance of the bone homeostasis is broken under certain stimuli, *e.g.*, matrix metalloproteinases (MMPs) (Lu *et al.*, 2011), glucocorticoid treatment (Hartmann *et al.*, 2016), reactive oxygen species (ROS) (Eble and de Rezende, 2014), or cigarette smoke extract (CSE) (Aspera-Werz *et al.*, 2019), the ECM will be degraded. ECM linked-inactive TGF-β will be released and thus activated, leading to a local increase in active TGF-β (Horiguchi *et al.*, 2012). This high concentration of TGF-β strongly enhances the recruitment and proliferation of MSCs and osteoprogenitor cells (Li *et al.*, 2013). As a result, TGF-β provides the fracture site with a fundamental and essential premise for initiating healing, *i.e.,* sufficient cell numbers. However, prolonged and excessive TGF-β may also block the activity of BMPs (Li *et al.*, 2012, Ehnert *et al.*, 2012, Xu *et al.*, 2020), which are required at later stages of the fracture healing process. With decreasing concentrations of TGF-β, BMP signaling is activated (Martini *et al.*, 2020), which induces the expression of molecules that favor osteogenesis and matrix mineralization, *e.g.*, OSX (Liu *et al.*, 2020) or OCN (Wei *et al.*, 2020). It has been reported that TGF-β at a low concentration enhances BMP2 expression in a Smad3-dependent manner (Xu *et al.*, 2020), prolongs the effective period of BMPs (Asparuhova *et al.*, 2018), and increases BMP osteogenic activity (Li *et al.*, 2012). This led to the hypothesis that patients with bone fractures that show disordered interactions between TGF-βs and BMPs may eventually suffer from delayed union or non-union (Li *et al.*, 2012, Ehnert *et al.*, 2012). Interestingly, ELF-PEMF exposure has been reported to upregulate the gene expression of *BMP2* and *BMP9* (Bodamyali *et al.*, 1998), to increase the expression of *BMPRI* and *BMPRII* (Xie *et al.*, 2016), and to activate the BMP signaling pathway (Yan *et al.*, 2015). However, few studies have investigated the influence of ELF-PEMF on the TGF-β signaling pathway during the early stage of fracture healing.

Thus, by knowing the ELF-PEMF parameters for specific signaling pathways, TGF-β signaling or BMP signaling may be actively targeted. In the case of fracture healing, an ELF-PEMF specifically activating TGF-β signaling may be beneficial at early stages of the healing process, while an ELF-PEMF promoting BMP signaling may be beneficial at late stages of the healing process (Fig. 5).

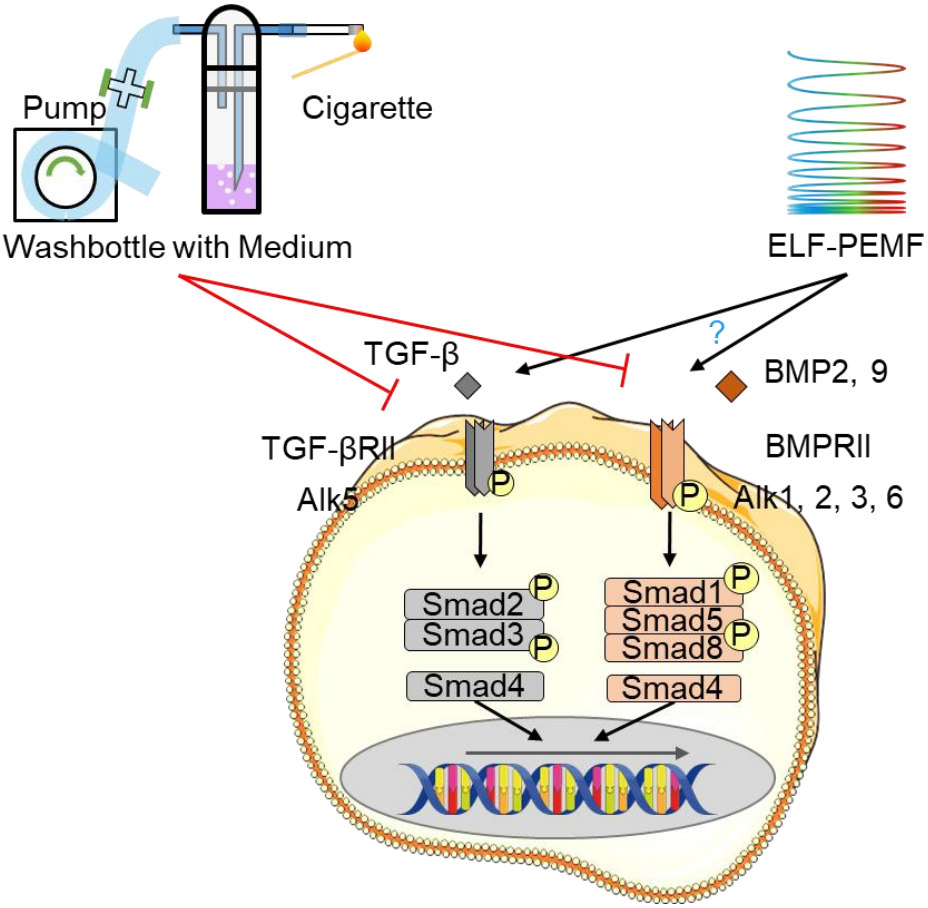

Figure 5: Overview of the working hypothesis. Cigarette smoke extract (CSE) can impair cell viability and osteogenic differentiation of MSCs by inhibiting both TGF-β signaling and BMP signaling. In contrast, ELF-PEMF can be used to restore both TGF-β and BMP signaling pathways, thus rescuing MSC viability and differentiation capacity. Graphic elements were provided by Servier (smart.servier.com).

1.6.2 Piezo1: The Mechanosensitive and Voltage-sensitive Calcium Ion (Ca^{2+}) Channel

In 2010, piezo1 and piezo2 were first described in a neuroblastoma cell line, where they functioned as mechanically activated cation channels (Coste *et al.*, 2010). These two members of the piezo family are expressed across a variety of cell types and tissues. Piezo1 is mainly located at the plasma membrane of many cell types, *e.g.*, vascular endothelial cells (Douguet *et al.*, 2019), monocytes/macrophages (Walmsley, 2019), and chondrocytes (Zhao *et al.*, 2020). In contrast, piezo2 is mainly expressed in sensory neurons; therefore, it is beyond the scope of the current project (Jiang *et al.*, 2021). Piezo1 is a non-selective calcium ion (Ca^{2+}) channel. It can be activated by many mechanical stimuli, *e.g.*, shear stress or compression (Ranade *et al.*, 2014, Cox *et al.*, 2016). It was recently reported that piezo1 is also voltage-sensitive (Moroni *et al.*, 2018). Since piezo1 is a Ca^{2+} channel, the activation of piezo1 can induce Ca^{2+}

influx into the cell. As a secondary messenger, increased intracellular Ca^{2+} ($[Ca^{2+}]_i$) affects many signaling pathways and biological activities (Monteith *et al.*, 2017).

Deficiency of piezo1 may result in a wide range of diseases, *e.g.*, developmental defects of blood vessels (Ranade *et al.*, 2014), generalized lymphatic dysplasia (Fotiou *et al.*, 2015), or dehydrated stomatocytosis (Alper, 2017). In the skeletal system, piezo1 deficiency may lead to osteoporosis (Zhou *et al.*, 2020), and the deletion of piezo1 in MSCs (piezo1^{Prx1}) severely impairs mouse skeletal growth and development (Wang *et al.*, 2020). Deletion of piezo1 in Runx2-expressing cells (piezo1^{Runx2}) impairs long bone growth in mice (Hendrickx *et al.*, 2021). Therefore, piezo1 is considered as an essential skeletal mechanosensor that mediates force detection in the skeletal system (Liu *et al.*, 2022), inducing physiological processes, *e.g.*, skeletal growth and development (Fig. 6). Taken together, piezo1 is an important protein on the plasma membrane to perceive and translate mechanical stimuli into biological signals by altering the $[Ca^{2+}]_i$ concentration.

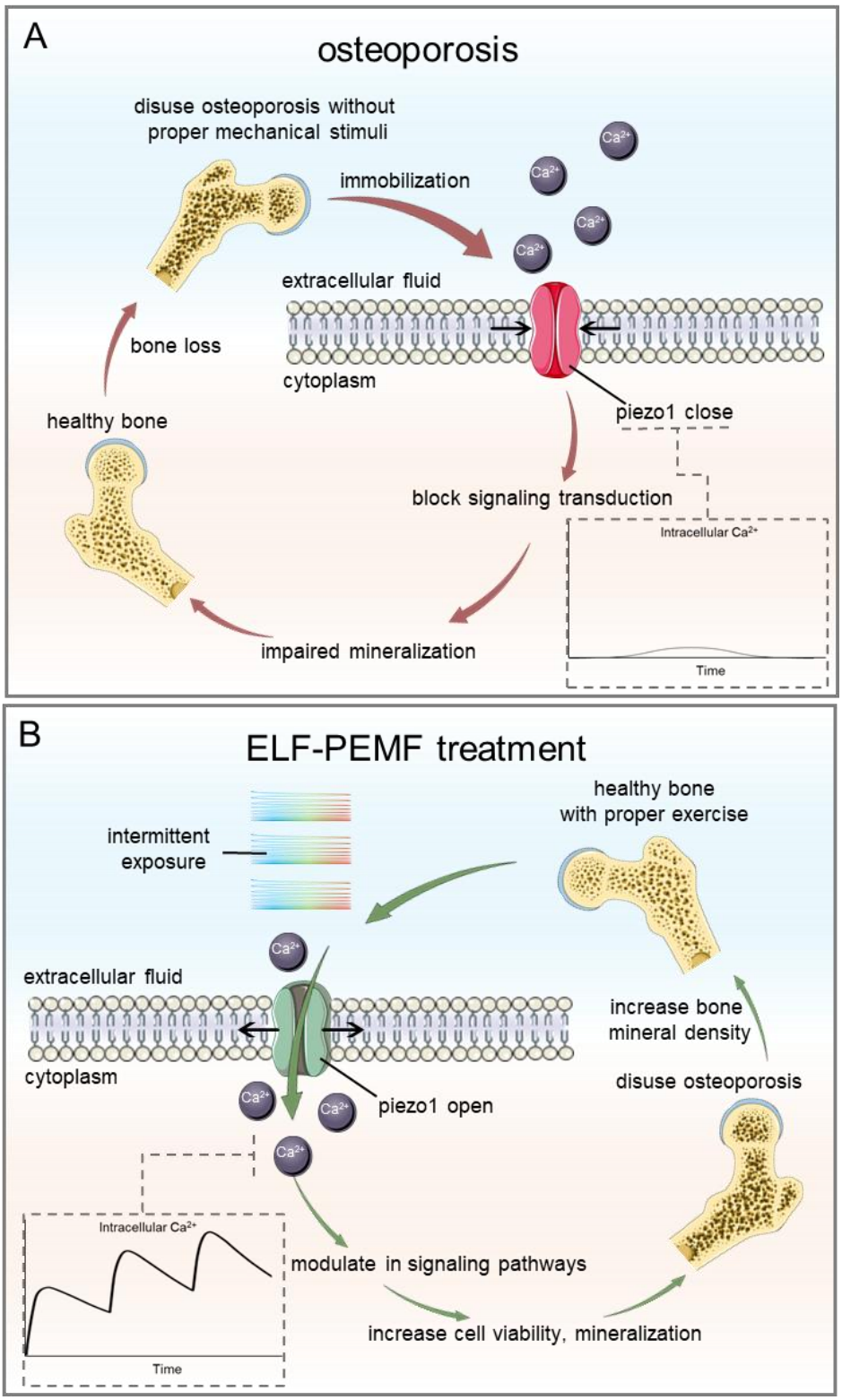

Figure 6: Piezo1 is located on the cellular membrane of SCP-1 cells and modulates the influx of calcium ions (Ca^{2+}). (A) Without proper extracellular mechanical stimuli, Ca^{2+} cannot influx into cells through piezo1. Ca^{2+} is a critical second messenger in cells. The lack of Ca^{2+} influx blocks signal transduction, thus impairing maturation of osteoprogenitors, and accelerating bone loss. In turn, the limited mobility caused by the poor skeletal condition will further block the mechanical stimuli on piezo1, thus aggravating osteoporosis. (B) To solve this challenge, physiotherapy, *e.g.*, ELF-PEMF, could be applied to simulate the mechanical stimuli from performing exercise. Therefore, we intended to explore if ELF-PEMF could activate piezo1, induce Ca^{2+} influx, regulate signaling pathways, and increase cell viability and mineralization. As a result, the bone mineral

intensity may increase disuse osteoporosis patients. Graphic elements were provided by Servier (smart.servier.com). This schematic diagram was graphically processed based on a previous study (Peng *et al.*, 2021).

1.6.3 Primary Cilium: The Mechanosensory Organelle

The primary cilium is a microtubule-based non-motile organelle that exists in nearly all eukaryotic cells (Tonna and Lampen, 1972). The primary cilium provides mechanosensitive ability to many tissues and organs, *e.g.*, the kidney (Yoder *et al.*, 2002), endothelium (Zaragoza *et al.*, 2012), liver (Masyuk *et al.*, 2008), and tumors (Menzl *et al.*, 2014). Moreover, the primary cilium functions as a critical mechanosensor and plays a pivotal role during the healing process in the musculoskeletal system, *e.g.*, bone (Temiyasathit *et al.*, 2012, Sreekumar *et al.*, 2018) and cartilage (McGlashan *et al.*, 2006, Aspera-Werz *et al.*, 2019). The primary cilium protrudes from the plasma membrane like an antenna. This special shape allows the detection of extracellular physicochemical signals (Prevo *et al.*, 2017). The primary cilium is assembled with nine outer microtubules, which is different from motile cilia, which contain an additional pair of central microtubules. The absence of the two inner microtubules and other axonemal components provides the primary cilium with a greater movement range and chemotactic ability than motile cilia (Schwartz *et al.*, 1997, Higgins *et al.*, 2019).

In addition to the morphological advantages, the perceptive ability of the primary cilium also benefits from the receptors and channels located on the ciliary membrane (Seeger-Nukpezah and Golemis, 2012). As the scheme shows (Fig. 7), Hedgehog (Hh) receptors (He *et al.*, 2014), G protein-coupled receptors (GPCRs) (Mykytyn and Askwith, 2017), calcium channels (Saternos *et al.*, 2020), Wnt receptors (Zhang *et al.*, 2015), receptor tyrosine kinases (RTKs) (Lemmon and Schlessinger, 2010), transforming growth factor-β (TGF-β) receptors (Nickel *et al.*, 2018), and bone morphogenetic protein (BMP) receptors (Heldin and Moustakas, 2016) are constantly or temporally located on the ciliary membrane (Anvarian *et al.*, 2019).

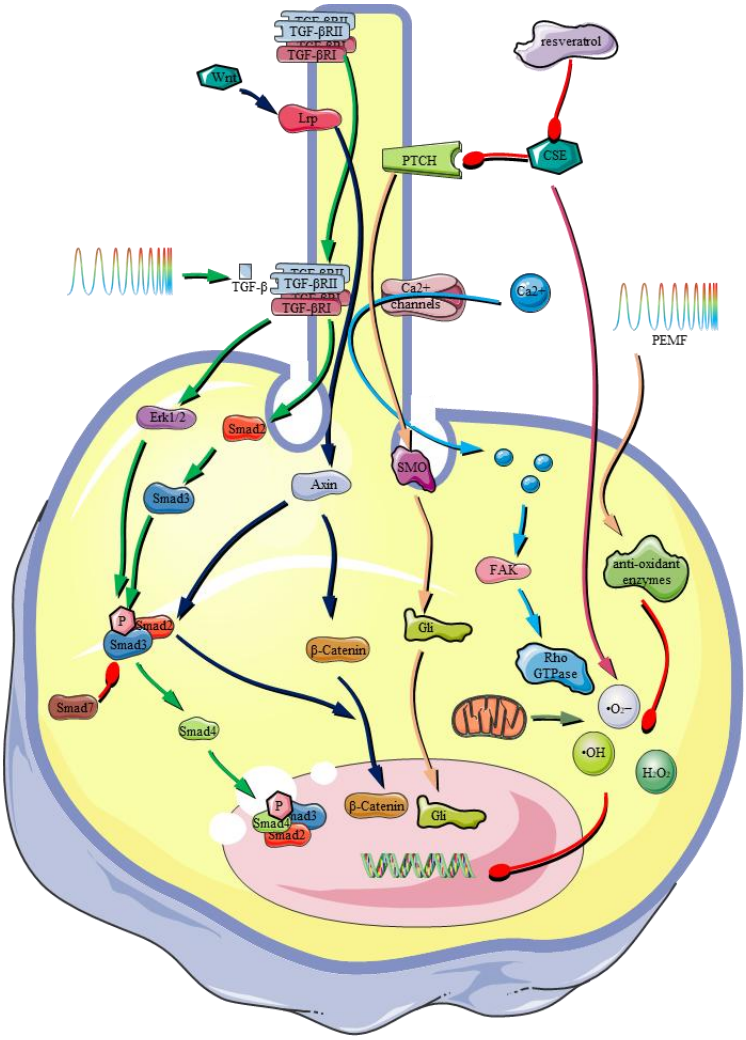

Figure 7: Schematic illustration of the important role that the primary cilium plays in receiving extracellular physiochemical stimuli and transducing them by various signaling pathways. Graphic elements were provided by Servier (smart.servier.com). This schematic diagram was graphically processed based on a previous review (Anvarian *et al.*, 2019).

Therefore, the presence of a primary cilium facilitates osteogenesis by 'translating' mechanical stimuli into biochemical signals. For example, fluid flow has been shown to induce osteogenesis in osteocytic MLO-Y4 cells with intact primary cilia. However, damaging the primary cilia structure with chloral hydrate (CH) or IFT88 siRNA significantly decreased the OPG/RANKL ratio and inhibited osteogenesis (Malone *et al.*, 2007). Furthermore, the knockdown of polycystin-1 (PC1), which is a component of primary cilia, reduced the gene expression of Runx2, osteocalcin (OCN), and OSX (Wang *et al.*, 2014). In turn, mechanical stimulation significantly increased alkaline phosphatase (AP) activity and the mineralization of osteoblasts with intact primary cilia (Ehnert *et al.*, 2017). Moreover, the critical role of the primary cilium in osteogenic differentiation results from its high correlation with the cell cycle

(Fig. 8). Even though it has been recognized that the synthesis and morphology of the primary cilium are essential factors involved in the therapeutic effects of ELF-PEMF on fracture healing (Chen *et al.*, 2021), the molecular mechanism is poorly understood.

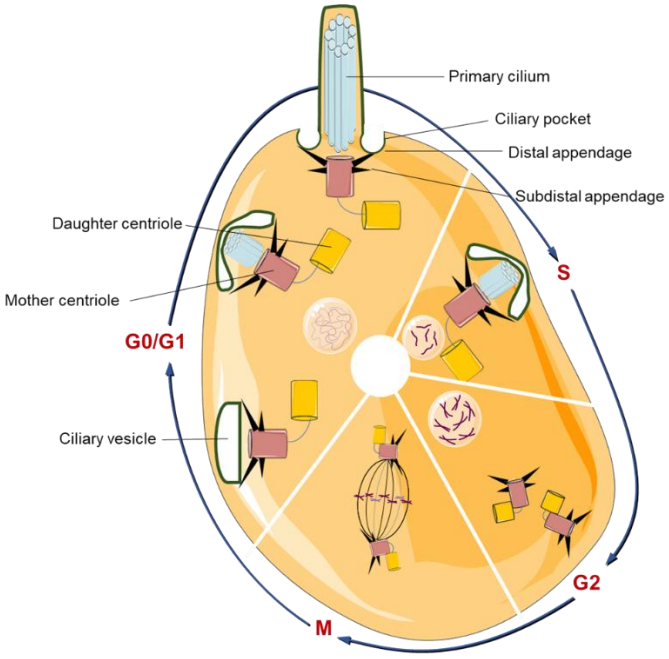

Figure 8: The process of ciliogenesis in osteocytes strongly correlates with the cell cycle. During the G0/G1 phase, the centrosome moves beneath the cell membrane, and the mother centriole that was used for axoneme nucleation transforms into the basal body (BB) and initiates ciliogenesis.(Kobayashi and Dynlacht, 2011) Then, primary cilia start to be degraded in the G2 phase and S phase. This phenomenon occurs because the centrioles are duplicating and preparing to form the mitotic spindle pole in the M phase (Ford *et al.*, 2018). Most osteocytes stay in G0/G1 with matured primary cilia (Kaku and Komatsu, 2017). The primary cilium of osteocytes touches the lacuna tightly because the length of the primary cilia (2-9 μm) is much longer than the lacunar space (0.1-3 μm) (Jacobs *et al.*, 2010). Moreover, when the primary cilium receives ELF-PEMF signals, osteocytes can communicate with surrounding cells through gap junctions (Jacobs *et al.*, 2010). Hence, the length of the primary cilium is most important for its function as 1) if the length of the primary cilium is too short to touch the wall of the lacuna, osteocytes cannot perceive mechanical forces, and 2) longer primary cilia have a larger surface area, more receptors, and ion channels, and are thus more sensitive to extracellular signals (Yuan and Yang, 2016). Graphic elements were provided by Servier (smart.servier.com). This schematic diagram was graphically processed based on a previous review (Avidor-Reiss and Gopalakrishnan, 2013).

1.7 Aims and Objectives

As described above, ELF-PEMF may have considerable potential to support fracture healing and prevent fracture non-union. However, there are still many challenges to be handled before the efforts in this research field can bring benefits to patients. These challenges can be generally categorized into three parts: 1) to figure out the effective parameters and strategies of ELF-PEMF exposure; 2) to evaluate the biological effects of specific ELF-PEMF; 3) to clarify the molecular mechanism. This project targets the above challenges by fulfilling the objectives below:

- Screening of parameters and strategies:

  •**Aim 1: Identification of suitable ELF-PEMF parameters and exposure strategies.** In order to identify suitable ELF-PEMF parameters, all experiments will first be performed in a blinded manner. The ELF-PEMF with blinded parameters will be used to stimulate the target cells (macrophages and SCP-1 cells) and cellular activities will be evaluated. Afterward, the effect of the four most effective ELF-PEMF on target cell function will be further analyzed to obtain one or two representative ELF-PEMFwith the desired cellular effects. Similarly, the exposure strategy is also an important factor influencing the therapeutic effects of ELF-PEMF. Therefore, different exposure strategies will be additionally tested, which includes exposure duration and exposure interval. For screening the exposure duration, the therapeutic effects of 7 min, 15 min, 30 min, 60 min, and 90 min daily ELF-PEMF exposure will be compared. For screening different expsoure intervals, effects of continuous exposure (without exposure interval) and intermittent exposure (with several exposure intervals) on cellular activities, *e.g.*, cell viability, will be compared.

With the achievement of the above objectives, suitable ELF-PEMF parameters and exposure strategies will be identified and used to investigate the biological effects and possible underlying mechanisms.

- Evaluation of the biological effects

  •**Aim 2: Characterization of ELF-PEMF effects on MSC viability and function.** MSCs represent the first osteogenic cells that inifiltrate the fracture site, where they proliferate and differentiate. Therefore, the effects of the identified ELF-PEMF on cell attachment, spreading, migration, cell number,

and cell viability of MSCs shall be characterized. Furthermore, both the expression of osteogenic differentiation markers and mineral deposition will be evaluated.

- **Aim 3: Characterization of ELF-PEMF effects on macrophage activity.** In addition to the direct effects of the ELF-PEMF on MSCs, the effect of immune cells regulating fracture healing shall be analyzed. Here, the focus will be on macphages, as they are active throughout the entire fracture healing process. In detail, immune cells will be exposed to the identified ELF-PEMF, then the cellular phenotype and the pro- or anti-inflammatory activity will be evaluated at the levels of gene expression and protein expression. Furthermore, the effect of the immunemodulation on MSCs, *e.g.*, migration, proliferation, and AP activity, will be characterized using an indirect co-culture approach.

- Exploration of the molecular mechanism

  - **Aim 4: ELF-PEMF effects on TGF-β/BMP signaling.** Considering the important role of TGF-β/BMP signaling in tissue regeneration, we will explore if ELF-PEMF exposure can activate TGF-β/BMP signaling to promote new bone formation. To achieve this aim, we intend to evaluate gene expression, protein expression, and phosphorylation states of Smads. Since receptors of TGF-β/BMP are located on primary cilia, we will also evaluate the structure of primary cilia.

  - **Aim 5: Effects of ELF-PEMF on Ca^{2+} signaling.** As a critical intracellular secondary messenger, Ca^{2+} plays an important role in regulating biological activities. In this study, we will explore the influence of ELF-PEMF on gene expression and function of a novel Ca^{2+} channel, *i.e.*, piezo1. Moreover, we will investigate if piezo1-induced Ca^{2+} influx affects the osteogenic differentiation of SCP-1 cells, the intracellular concentration and kinetics of Ca^{2+} will be measured and analyzed.

2. Results

2.1 Modulation of Macrophage Activity by Pulsed Electromagnetic Fields in the Context of Fracture Healing

(CHEN, Y., MENGER, M. M., BRAUN, B. J., SCHWEIZER, S., LINNEMANN, C., FALLDORF, K., RONNIGER, M., WANG, H., HISTING, T., NUSSLER, A. K. & EHNERT, S. 2021. Modulation of Macrophage Activity by Pulsed Electromagnetic Fields in the Context of Fracture Healing. Bioengineering (Basel), 8)

2.1.1 Summary and Major Findings

It has been widely recognized that delayed fracture healing or fracture non-union represents a great burden to patients and society. To identify an effective treatment to promote fracture healing immediately after surgical repositioning of the fracture, the focus of this study was on modulating immune responses during the healing process. In bone fracture healing, macrophages, with their long life-span and high degree of plasticity, participate both in early inflammation as well as later in differentiation and remodeling. Therefore, macrophages represent an ideal target to be influenced by ELF-PEMF. The aim of this study was to screen for specific ELF-PEMF that can modulate the activity of macrophages and indirectly regulate SCP-1 cell function. With a blinded screening of 22 different ELF-PEMF, two fields (fields A and B) were identified that could diversely modulate the activity of macrophages. Field A exhibited pro-inflammatory capacity, characterized by increased ROS levels and enhanced protein levels of phospho-Stat1 and CD86 in exposed macrophages, which then secreted many pro-inflammatory cytokines and chemokines. Contrarily, field B exhibited pro-healing and anti-inflammatory capacity, characterized by enhanced protein levels of arginase I and increased secretion of many anti-inflammatory cytokines and growth factors by the exposed macrophages. As the secreted cytokines, chemokines, and growth factors accumulated in the conditioned medium from the exposed macrophages, the conditioned medium was used to stimulate SCP-1 cells to investigate the effect on MSCs. Our data indicate that the conditioned medium from field B showed stronger effects on migration and ECM formation by SCP-1 cells than field A. In contrast, field A created an inflammatory environment that could favor the killing of pathogens and removal of debris at the fracture site.

Overall, this study partially achieved project **aims 1 and 3**. This work indicated that specific ELF-PEMF can modulate the activity of macrophages in a way that may provide patients with a promising adjuvant treatment to promote fracture healing.

Limitations and next steps: This study mainly focused on the immune response and the intercellular communications during fracture healing. It lacks insights into the activity of osteoblasts and the molecular mechanism. Therefore, we needed to conduct a second study to better understand ELF-PEMF therapy.

2.1.2 Personal Contribution

I was responsible for the experiments of this study; I was the main person who performed the data analysis and visualization. I was also highly involved in the design of the experiments and preparation of the original manuscript draft.

bioengineering

MDPI

Article

Modulation of Macrophage Activity by Pulsed Electromagnetic Fields in the Context of Fracture Healing

Yangmengfan Chen [1], Maximilian M. Menger [1], Benedikt J. Braun [1], Sara Schweizer [1], Caren Linnemann [1], Karsten Falldorf [2], Michael Ronniger [2], Hongbo Wang [3], Tina Histing [1], Andreas K. Nussler [1] and Sabrina Ehnert [1,*]

[1] Siegfried Weller Research Institute, BG Trauma Center Tübingen, Department of Trauma and Reconstructive Surgery, University of Tübingen, Schnarrenbergstr. 95, D-72076 Tübingen, Germany; chenyangmengfantj@163.com (Y.C.); mmenger@bgu-tuebingen.de (M.M.M.); bbraun@bgu-tuebingen.de (B.J.B.); sara.schweizer80@googlemail.com (S.S.); caren.linnemann@student.uni-tuebingen.de (C.L.); thisting@bgu-tuebingen.de (T.H.); andreas.nuessler@gmail.com (A.K.N.)

[2] Sachtleben GmbH, Haus Spectrum am UKE, Martinistraße 64, D-20251 Hamburg, Germany; falldorf@citresearch.de (K.F.); ronniger@citresearch.de (M.R.)

[3] Union Hospital, Tongji Medical College, Huazhong University of Science and Technology, 1277 Jiefang Ave, Wuhan 430022, China; whbdf@yahoo.com

* Correspondence: sabrina.ehnert@gmail.com; Tel.: +49-7071-606-1065

Abstract: Delayed fracture healing and fracture non-unions impose an enormous burden on individuals and society. Successful healing requires tight communication between immune cells and bone cells. Macrophages can be found in all healing phases. Due to their high plasticity and long life span, they represent good target cells for modulation. In the past, extremely low frequency pulsed electromagnet fields (ELF-PEMFs) have been shown to exert cell-specific effects depending on the field conditions. Thus, the aim was to identify the specific ELF-PEMFs able to modulate macrophage activity to indirectly promote mesenchymal stem/stromal cell (SCP-1 cells) function. After a blinded screening of 22 different ELF-PEMF, two fields (termed A and B) were further characterized as they diversely affected macrophage function. These two fields have similar fundamental frequencies (51.8 Hz and 52.3 Hz) but are emitted in different groups of pulses or rather send–pause intervals. Macrophages exposed to field A showed a pro-inflammatory function, represented by increased levels of phospho-Stat1 and CD86, the accumulation of ROS, and increased secretion of pro-inflammatory cytokines. In contrast, macrophages exposed to field B showed anti-inflammatory and pro-healing functions, represented by increased levels of Arginase I, increased secretion of anti-inflammatory cytokines, and growth factors are known to induce healing processes. The conditioned medium from macrophages exposed to both ELF-PEMFs favored the migration of SCP-1 cells, but the effect was stronger for field B. Furthermore, the conditioned medium from macrophages exposed to field B, but not to field A, stimulated the expression of extracellular matrix genes in SCP-1 cells, i.e., *COL1A1*, *FN1*, and *BGN*. In summary, our data show that specific ELF-PEMFs may affect immune cell function. Thus, knowing the specific ELF-PEMFs conditions and the underlying mechanisms bears great potential as an adjuvant treatment to modulate immune responses during pathologies, e.g., fracture healing.

Keywords: extremely low frequency pulsed electromagnetic fields (ELF-PEMFs); macrophages; mesenchymal stem/stromal cells; extracellular matrix; fracture healing

Citation: Chen, Y.; Menger, M.M.; Braun, B.J.; Schweizer, S.; Linnemann, C.; Falldorf, K.; Ronniger, M.; Wang, H.; Histing, T.; Nussler, A.K.; et al. Modulation of Macrophage Activity by Pulsed Electromagnetic Fields in the Context of Fracture Healing. *Bioengineering* **2021**, *8*, 167. https://doi.org/10.3390/bioengineering8110167

Academic Editor: Danièle Noël

Received: 29 September 2021
Accepted: 27 October 2021
Published: 29 October 2021

Publisher's Note: MDPI stays neutral with regard to jurisdictional claims in published maps and institutional affiliations.

Copyright: © 2021 by the authors. Licensee MDPI, Basel, Switzerland. This article is an open access article distributed under the terms and conditions of the Creative Commons Attribution (CC BY) license (http://creativecommons.org/licenses/by/4.0/).

1. Introduction

Almost every human on earth experiences one or more fractures during life. Although the treatment options for fractures have been greatly developed, 5% to 10% of all fractures still result in delayed healing or even non-union [1]. Consequently, fractures

are a major cause of disability, morbidity, and even mortality, particularly in elderly patients leading to a high economic burden [2].

Fracture healing is a complex and dynamic process that can be divided into three partially overlapping phases: inflammation phase, reparative phase, and remodeling phase. The complex and excellently tuned process during fracture healing requires the involvement of various cell types [3]. Neutrophils, arriving within a few hours at the fracture site, represent the first line of defense. They play a crucial role in resolving the formed hematoma and initiating inflammatory responses. Monocytes/macrophages represent a large proportion of the immune cells present at the injury site throughout the entire healing phase; however, their activation status is changing [4]. After a fracture occurs, monocytes/macrophages are recruited to the injury site, where they differentiate into macrophages within 2 to 3 days [5]. Unlike monocytes, macrophages show high plasticity. After receiving adequate stimuli, macrophages may easily change their activity and function, exhibiting either pro-inflammatory or anti-inflammatory and pro-healing activities [6,7]. Macrophage function is largely mediated by factors such as cytokines, growth factors, and chemokines, which they secrete depending on their activation status. Thus, macrophages are involved in controlling the different phases of the healing process by adapting their phenotype [8]. The differentially activated macrophages are mutually exclusive and involved in the whole healing process [9]. In the acute inflammatory phase, pro-inflammatory macrophages are important. These cells infiltrate the site of injury not only to detect and remove pathogenic microbes and cellular debris but also to initiate various signaling pathways required for the subsequent repair phase. In the chronic inflammatory and reparative phase, the tissue-resident macrophages exhibit anti-inflammatory and pro-healing activities to reduce hyper-inflammation and promote tissue regeneration. Later, during tissue remodeling, a controlled amount of pro-inflammatory macrophages are required [4]. Therefore, regulating the immune microenvironment at the site of injury by modulating macrophage activity is crucial for fracture healing [10].

Disorders in macrophage activity are highly related to the failure of fracture healing. For example, unrestrained and persistent pro-inflammatory macrophages may lead to impaired fracture healing, particularly in patients with rheumatoid arthritis (RA), chronic obstructive pulmonary disease (COPD), diabetes mellitus (DM), liver fibrosis/cirrhosis, and systemic lupus erythematosus (SLE) [11]. However, the suppression of inflammation also arrests the process of fracture healing [12,13]. Therefore, neither a hyper-inflammatory state nor an immune-suppressive state alone can contribute to successful fracture healing. The key factor to successful fracture healing is a dynamic and suitable immune microenvironment at the injury site. Thus, the modulation of inflammatory responses may offer great therapeutic options to support the healing of fractures and soft tissues.

Exposure to extremely low frequency pulsed electromagnetic fields (ELF-PEMF) is a non-invasive, penetrable, and patient-friendly treatment. Therefore, ELF-PEMFs are a promising adjuvant treatment to dynamically regulate the local immune microenvironment and promote healing processes. In recent years, ELF-PEMF was proven to effectively support fracture healing and bone regeneration (overview see [14]). Positive effects to the proposed mechanisms on osteoblasts [15], mesenchymal stem/stromal cells (MSCs) [16], chondrocytes [17], and intervertebral disc cell [18] function have been reported. However, there has been little research focused on the immune-regulatory ability of ELF-PEMFs [19], even though the importance of osteoimmunology is generally acknowledged. The reported effects of the ELF-PEMFs on macrophages are diverse. When employing different readout parameters, some reports show pro-inflammatory effects [20–22], while others reported anti-inflammatory [23], or even immune-suppressive [24], effects of the ELF-PEMFs. Interestingly, the ELF-PEMFs in these four studies all had a fundamental frequency of 50 Hz but varied in their magnetic field density and pulse pattern.

Earlier reports suggested that each cell type responds to ELF-PEMFs with specific fundamental frequencies and pulse burst patterns. While an ELF-PEMF with a fundamental frequency of 16 Hz was shown to improve the function of osteoblasts [15,25], another ELF-PEMF (comparable intensity) with a fundamental frequency of 26 Hz also affected osteoclast function [16]. Studies on primary rat calvaria cells showed that not only the fundamental frequency but also the waveform and pulse burst pattern might be relevant [26,27]. Thus, in an initial blinded screening, the effect of 22 ELF-PEMFs, with different fundamental frequencies, waveforms and pulse burst patterns on macrophage activation, were tested. Among these, two ELF-PEMF were chosen to further characterize their distinct effect on macrophage activity and function. This includes direct effects on macrophages: (i) expression of phenotypic markers; (ii) formation of reactive oxygen species (ROS) as an inflammatory response; and (iii) secretion of cytokines, growth factors and chemokines, as well as the expected effects that the treated macrophages have on MSCs during fracture healing: (i) migration and (ii) formation of extracellular matrix (ECM) components.

2. Materials and Methods

If not specified, reagents, culture media, and medium supplements were purchased from Merck (Darmstadt, Germany).

2.1. Human Material

All experiments involving human materials strictly adhered to the Declaration of Helsinki (1964) in its latest amendment and were approved by the Ethics Committee of the University Clinic Tübingen (541/2016BO2 approved 09.08.2016). PBMCs were isolated from the venous blood of healthy volunteers. Blood was obtained with the signed informed consent of the donors.

2.2. Isolation of Peripheral Blood Mononuclear Cells (PBMCs)

PBMCs were isolated from fresh EDTA blood. Venous blood was collected in EDTA tubes (S-Monovette, Sarstedt, Sarstedt, Germany) and directly used for density gradient centrifugation. A total of 6 mL of blood was carefully layered on 6 mL of Lympholyte-poly Cell Separation Medium (Cedarlane, Burlington, ON, Canada). Samples were centrifuged for 35 min at 500 g without a break at room temperature. The PBMC (upper) layer was transferred to a new tube. After washing twice with PBS, the cells were counted and seeded at a concentration of 5×10^5 cells/mL in an RPMI 1640 medium with 2% autologous plasma [28]. Experiments were performed at 37 °C (5% CO_2, humidified atmosphere).

2.3. ELF-PEMF Device and Exposure

The ELF-PEMF devices (Somagen®, Sachtleben GmbH, Hamburg, Germany) are medical devices certified according to European law (CE 0482, compliant with EN ISO 13485:2016 + EN ISO 14971:2012). The device generates an AC magnetic field, here ELF-PEMF, via applicators (coils). Furthermore, the applicators distort the local earth magnetic DC-field, yielding inhomogeneous DC-field conditions [25]. In this study, 22 ELF-PEMF conditions have been tested in a blinded manner. The 22 ELF-PEMF all have a similar intensity (with a magnetic field amplitude between 6 and 282 μT at 6 mm above the applicator) but different fundamental frequencies, emitted in different pulse burst patterns (pulses in send–pause intervals) [14]. The two ELF-PEMFs identified to modulate macrophage function have fundamental frequencies close to each other (field A: 51.8 Hz and field B: 52.3 Hz) but differ in their pulse burst pattern. The daily ELF-PEMF exposure was 7 or 30 min. Unblinding of the ELF-PEMF conditions was done after all experiments were finished and evaluated.

2.4. Western Blot

PBMCs were lysed in an ice-cold RIPA buffer (50 mM TRIS, 250 mM NaCl, 2% NP40, 2.5 mM EDTA, 0.1% SDS, 0.5% DOC, and protease/phosphatase inhibitors: 1 µg/mL Pepstatin, 5 µg/mL Leupeptin, 1 mM PMSF, 5 mM NaF, and 1 mM Na_3VO_4). The lysate was centrifuged (14,000 ×g, 10 min) to remove cell debris. Protein concentration was determined by micro-Lowry; 25 µg of total protein were separated by SDS-PAGE (10% acrylamide-bisacrylamide gels, 100 V, 180 min) then transferred to nitrocellulose membranes (100 mA, 180 min). Ponceau staining was used to confirm protein separation and transfer; 5% BSA was used to block unspecific binding sites. Then, membranes were incubated with primary antibodies against CD86, Arginase 1 (sc-28347, sc-20150 from Santa Cruz Biotechnology, Heidelberg, Germany), phospho-Stat1 (7649 from Cell Signaling Technologies, Danvers, MA, USA), and GAPDH (G9545 from Sigma-Aldrich, Munich, Germany) diluted in TBST, overnight at 4 °C. The following day, the membranes were incubated with the corresponding HRP-labeled secondary antibodies (1:10,000 in TBST) for 2 h at room temperature. After washing, target proteins were visualized with an enhanced chemiluminescent (ECL) substrate solution (1.25 mM Luminol, 0.2 mM p-Coumaric acid, 0.03% H_2O_2 in 100 mM TRIS, pH = 8.5), and the chemiluminescent signals were detected with a CCD camera. Signal intensities were quantified using ImageJ software [25].

2.5. DCFH-DA Assay

Oxidative stress was detected using a 2′, 7′-dichlorofluorescein diacetate (DCFH-DA) assay, detecting different reactive oxygen species. Freshly isolated PBMCs were incubated with 10 µM DCFH-DA for 25 min at 37 °C. Cells were washed once with PBS. Then cells were exposed to the ELF-PEMF, and positive control cells were stimulated with 0.001% H_2O_2. For a time course of 20 min, the increase in fluorescence (ex/em = 485/520 nm) was detected with the omega microplate reader, the slope representing an accumulation of O_2^-, H_2O_2, HO and $ONOO^-$ [29].

2.6. Human Cytokine Array C5 with Media Conditioned by PBMC Exposed to ELF-PEMFs

The human Cytokine Array C5 (RayBiotech, Peachtree Corners, GA, USA) was used to characterize media conditioned by PBMCs. Briefly, PBMCs (5×10^5 cells/mL) were exposed to the different ELF-PEMF then cultured for 24 h at 37 °C (5% CO_2, humidified atmosphere). Cells were removed from the conditioned media by centrifugation (1,000 g, 10 min). The array was performed according to the manufacturer's instructions. Chemiluminescent signals were detected with the ChemoCam and quantified using ImageJ software. The data were normalized to the internal controls [28].

2.7. Culture and Differentiation of SCP-1 Cells

This study used the human immortalized mesenchymal stem cell line SCP-1, kindly provided by Professor Matthias Schieker, as an osteogenic precursor cell. The SCP-1 cells were cultured in α-MEM medium (Gibco, Darmstadt, Germany) supplemented with 5% fetal bovine serum (FBS) in a water-saturated atmosphere of 5% CO_2 at 37 °C. The osteogenic function was induced with a differentiation medium (α-MEM medium supplemented with 1% FBS, 200 µM L-ascorbate-2-phosphate, 5 mM β-glycerol-phosphate, 25 mM HEPES, 1.5 mM $CaCl_2$, and 100 nM dexamethasone) mixed 1:1 with a conditioned medium from ELF-PEMF exposed PBMCs. The SCP-1 cells themselves were not exposed to the ELF-PEMF.

2.8. Cell Migration Assay

Cell migration was evaluated using the cell migration assay kit (tebu-bio GmbH, Offenbach, Germany). Sterilized stoppers were placed in 96-well plates before seeding the SCP-1 cells at a concentration of 4×10^5 cells/mL. After 24 h, the stoppers were removed from

the wells, and the cells were washed 3 times with PBS. Then, the growth medium and conditioned medium from ELF-PEMF exposed PBMCs were added in a 1:1 ratio. Immediately, an image was taken with the microscope to document the time point 0 h. After 48 h, SRB staining was performed for better visualization of SCP-1 cells. The "gap closure" in the microscopic images was calculated and analyzed using ImageJ software [28].

2.9. Sulforhodamine B (SRB) Staining

Adherent cells were fixed with ice-cold 99% EtOH for at least 1 h at −20 °C. After washing the plates with tap water, the cells were covered with SRB solution (0.4% SRB in 1% acetic acid) for 30 min. The unbound SRB was removed by washing with 1% acetic acid [28].

2.10. RNA Isolation and RT-PCR

Total mRNA was isolated by phenol–chloroform extraction. The obtained mRNA was dissolved in DEPC water. The total mRNA content was determined photometrically (λ = 260 nm, 280 nm, and 320 nm) with the omega microplate reader, and mRNA integrity was confirmed using agarose gel electrophoresis. The total mRNA was converted into cDNA using the First Strand cDNA Synthesis Kit (Thermo Fisher Scientific, Sindelfingen, Germany) according to the manufacturers' instructions. RT-PCR was carried out using the 2× Red Taq Mastermix (Biozym, Oldendorf, Germany) [25]. Optimized PCR conditions for each primer set are given in Table 1. Primers were designed with the help of primer-BLAST with the respective gene bank accession number listed in the table.

Table 1. List of primers, their sequences, and the corresponding PCR conditions.

Target	Gene Bank Accession Number	Sequence Forward Primer	Sequence Reverse Primer	T_a [°C]	# of Cycles	Amplicon Size [bp]
RPL13a	NM_012423.3	AAGTACCAGG CAGTGACAG	CCTGTTTCCGT AGCCTCATG	56	30	100
Biglycan	NM_001711.5	CGCCTCGTGT CTCTGCTGGC	GCGGATGCGG TTGTCGTGGA	64	35	501
Versican	NM_001164098.1	AATGCCGTCT GCAGGGTGCC	GGCCGCAAGC GACTGTTCCT	64	35	306
Collagen 1A1	NM_000088.3	CAGCCGCTTC ACCTACAGC	TTTGTATTCAAT CACTGTCTTGCC	56	35	83
Fibronectin	NM_002026.2	CCCCATTCCAG GACACTTCTG	GCCCACGGTA ACAACCTCTT	60	35	203

2.11. Statistical Analysis

Results are presented as box plots (min. to max.) with individual data points. Each experiment was repeated at least three times (N ≥ 3) with a minimum of three independent replicates ($n \geq 3$). The exact number of biological (N) and technical replicates (n) for each experiment is given in the figure legends. Statistical analyses were performed using the GraphPad Prism software version 8. Data sets were compared using a non-parametric Kruskal–Wallis test, followed by Dunn's multiple comparison test. A p-value below 0.05 was considered statistically significant.

3. Results

3.1. ELF-PEMFs Exposure Modulates Macrophage Differentiation.

In this study, the effect of 22 different ELF-PEMFs on macrophage activity was screened in a blinded manner in a two-step procedure. The ELF-PEMFs had comparable intensities but different fundamental frequencies ranging from 3.3 Hz to 90.60 Hz, emitted in pulses or bursts in send–pause intervals (pulse burst pattern). In the first screening step,

freshly isolated PBMCs were activated with 200 nM PMA and directly exposed to the different ELF-PEMFs for 7 min each. After 24 h, activation of macrophages was judged by attaching the cells to culture plastic. Furthermore, a possible effect of the macrophage conditioned medium on SCP-1 cell migration was considered (Figure 1). The number of ELF-PEMFs was reduced to four in a second screening step, and a second duration of exposure (30 min) was added for each. Of the four ELF-PEMF (blinded), two ELF-PEMFs (termed A and B) showed opposing effects on macrophage function and were therefore further investigated for unblinding.

In the screening, two ELF-PEMF were included, which showed positive effects on osteoblast function [15,25,29] and osteoclast function in earlier studies [16]. These two ELF-PEMF, however, did not seem to affect macrophages in our setting.

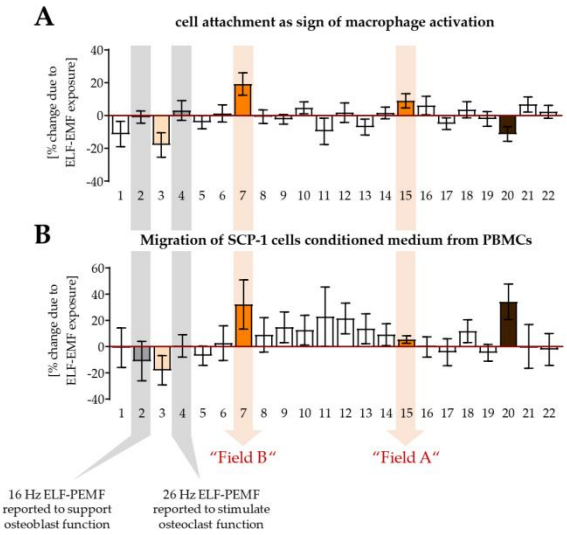

Figure 1. Screening of 22 different ELF-PEMF on macrophage function. Freshly isolated PBMCs (N = 7) were stimulated with 200 nM PMA and exposed to the different ELF-PEMFs for 7 min each in a blinded manner. (**A**) After 24 h, cell attachment was determined by Hoechst 33342 staining, and (**B**) conditioned medium was collected and added (1:1) to SCP-1 cells in a migration assay. The ELF-PEMF effects are displayed as fold of control (without ELF-PEMF exposure). After unblinding, field #2 was identified as the ELF-PEMF, which showed positive effects on osteoblast function in earlier studies [15,25,29] and field #4 was identified as the ELF-PEMF, which additionally stimulated osteoclast function in earlier studies [16]. Fields #3, #7, #15, and #20 were further investigated, of which #7 and #15 showed diverse effects on macrophage function—termed field A and field B in the following experiment.

As previously described, freshly isolated PBMCs were activated with 200 nM PMA and directly exposed to the two ELF-PEMFs for 7 min or 30 min each. After 24 h, cells were lyzed, and markers of pro-and anti-inflammatory macrophages were detected by Western blot (Figure 2). Exposure to field A significantly increased the protein levels of phosphorylated Stat1 (2.9-fold with $p = 0.0084$/2.8-fold with $p = 0.0396$) and CD86 (2.0-fold with $p = 0.0013$/1.6-fold with $p = 0.0193$), which are markers for pro-inflammatory macrophages (Figure 2B,C). Inversely, exposure to field B significantly increased (2.6-fold with $p = 0.0027$/2.5-fold with $p = 0.0034$) the protein levels of Arginase I, a marker for anti-

inflammatory macrophages, known to support healing processes (Figure 2D). Interestingly, extending the exposure time from 7 min to 30 min could not increase the observed effect.

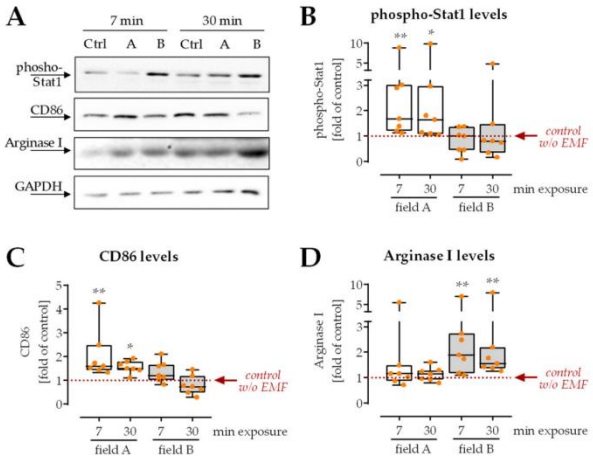

Figure 2. Macrophage differentiation is altered after single exposure to ELF-PEMFs. Freshly isolated PBMCs were exposed to the two ELF-PEMFs for 7 min or 30 min, respectively. After 24 h, markers of pro-and anti-inflammatory macrophages were detected by Western blot. (**A**) Representative Western blot images. All uncropped Western blot images are shown in Supplementary Figure S1. (**B**,**C**) As markers of pro-inflammatory macrophages, protein levels of phosphorylated Stat1 and CD86 were determined. (**D**) As markers of anti-inflammatory and pro-healing macrophages, protein levels of Arginase I were determined. N = 7, *n* = 3. Data were compared by non-parametric Kruskal–Wallis test, followed by Dunn's multiple comparison test: * $p < 0.05$, and ** $p < 0.01$ as compared to control cells without ELF-PEMF exposure.

3.2. Exposure to Field A Leads to the Formation of Intracellular Reactive Oxygen Species (ROS).

As a marker of inflammation, intracellular ROS levels were detected. It can already be determined that 7 min exposure to field A, but not exposure to field B, significantly increased the amount of intracellular ROS (1.4-fold with $p = 0.0004$) in freshly isolated PBMCs activated with 200 nM PMA (Figure 3).

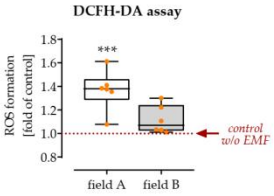

Figure 3. Intracellular ROS levels were regulated after single exposure to ELF-PEMFs. To detect intracellular reactive oxygen species (ROS), cells were incubated with a DCFH-DA probe before exposure to the ELF-PEMFs for 7 min. Produced ROS was quantified by the green fluorescence formed. N = 6, *n* = 3. Data were compared by non-parametric Kruskal–Wallis test, followed by Dunn's multiple comparison test: *** $p < 0.001$ as compared to control cells without ELF-PEMF exposure.

3.3. Field A and Field B Diversely Regulate the Secretion of Cytokines, Growth Factors, and Chemokines by Macrophages.

The paracrine effect of macrophages on neighboring cells, e.g., mesenchymal stem/stromal cells (MSCs) and other immune cells in the fracture site, is essential for the healing outcome [4]. Freshly isolated PBMCs were activated with 200 nM PMA and directly exposed to the two ELF-PEMFs for 7 min or 30 min each. After 24 h, cells in the conditioned medium were collected, and secreted factors were detected with the human Cytokine Array C5 (RayBiotech, Peachtree Corners, GA, USA). The resulting heat maps show that exposure to field A and field B diversely regulated the secretion of cytokines, growth factors, and chemokines in the macrophages. Many important pro-inflammatory cytokines, e.g., interleukin-1 beta (IL-1β), IL-3, interferon-gamma (IFN-γ), or Oncostatin M (OSM), were elevated in a conditioned medium from macrophages that were exposed to field A (Figure 4A). Inversely, many anti-inflammatory cytokines, e.g., IL-10, transforming growth factor-beta (TGF-β) isoforms, insulin-like growth factor (IGF), and their binding proteins (IGFBPs), were elevated in conditioned medium from macrophages that were exposed to field B (Figure 4A,B). Including angiogenin, these factors secreted by macrophages after exposure to field B have been reported to enhance regeneration during tissue repair [3]. Similar to the cytokines and growth factors, secretion of chemokines was selectively induced upon exposure to filed A and B (Figure 4C), which may affect cell invasion into the injury site. Interestingly, prolonging the exposure time from 7 min to 30 min seemed to intensify the observed effect.

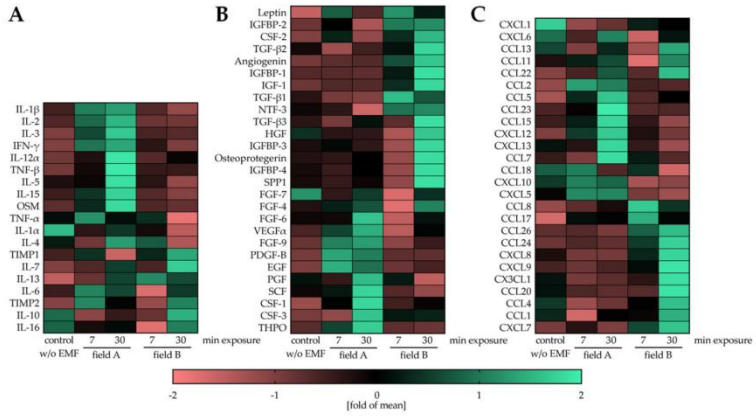

Figure 4. Cytokines, growth factors and chemokines secreted by PBMCs after exposure to the ELF-PEMFs. Freshly isolated PBMCs (N = 5) were stimulated with 200 nM PMA and exposed to the two ELF-PEMF for 7 min or 30 min, respectively. After 24 h, the conditioned medium was collected, pooled and analyzed (n = 3) for secreted factors using the human Cytokine Array C5 (RayBiotech, Peachtree Corners, GA, USA). Data were normalized with the standard score (z-score) method. Data are presented as heat maps: (**A**) Heat map of cytokines related to immune function and inflammation; (**B**) Heat map of cytokines and growth factors involved in repair and healing processes; and (**C**) Heat map of chemokines.

3.4. Factors Secreted by Macrophages Exposed to the Two ELF-PEMF Stimulated Migration of SCP-1 Cells

To investigate how the ELF-PEMF induced alterations in the macrophages cytokine secretion affect migration of MSCs, a migration assay with SCP-1 cells (immortalized human bone marrow-derived MSCs [30]) was performed (Figure 5). For the entire

migration phase (48 h), a macrophage conditioned medium (1:1 ratio) was added to the SCP-1 cells. Cells invading into the migration zone were visualized with SRB staining, and "gap closure" was determined with the help of ImageJ software. The quantitative results indicated that conditioned medium from macrophages exposed for 7 min to field B already promoted the migration of SCP-1 cells (1.7-fold with $p = 0.0390$). In line with the data from the human Cytokine Array *C5* conditioned medium from macrophages exposed for 30 min to field B, had even stronger effects on the migration of SCP-1 cells (1.7-fold with $p = 0.0050$). In contrast, the presence of conditioned medium from macrophages exposed to field A failed to significantly promote migration of SCP-1 cells (1.5-fold with $p = 0.0731$ and 1.5-fold with $p = 0.0902$).

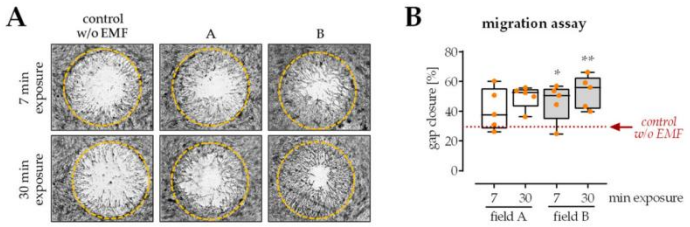

Figure 5. Migration of SCP-1 cells cultured with conditioned medium from macrophages exposed to the ELF-PEMFs. Freshly isolated PBMCs ($n = 5$) were stimulated with 200 nM PMA and exposed to the two ELF-PEMF for 7 min or 30 min, respectively. After 24 h, a conditioned medium was collected and added (1:1) to SCP-1 cells in a migration assay. (**A**) Representative images of the migration assay after 48 h. Cells invading the migration zone were visualized by Sulforhodamine B staining. (**B**) The uncovered area in the migration zone was measured with ImageJ software to quantify the migration assay. Data were compared by non-parametric Kruskal–Wallis test, followed by Dunn's multiple comparison test: * $p < 0.05$ and ** $p < 0.01$ as compared to control conditions (without ELF-PEMF exposure).

3.5. Conditioned Medium from Macrophages Exposed to Field B Induced Extracellular Matrix Formation in SCP-1 Cells

Directly upon invasion into the tissue, MSCs start producing extracellular matrix components. A well-organized matrix formation at an early stage decides the outcome of tissue regeneration. To investigate this aspect, SCP-1 cells were cultured in the presence of the different macrophage conditioned media for 1 week. Then, the gene expression of matrix proteins *collagen 1A1*, *fibronectin*, *biglycan*, and *versican*, was evaluated (Figure 6A). Results showed that the conditioned medium from macrophages exposed to field A did not affect the expression of *collagen 1A1*, *fibronectin*, *biglycan*, and *versican*. In contrast, the conditioned medium from macrophages exposed to field B induced expression of *collagen 1A1* (2.2-fold with $p < 0.0001$), *fibronectin* (1.3-fold with $p = 0.0106$), and *biglycan* (1.7-fold with $p = 0.0004$), however, mostly with the shorter ELF-PEMF exposure (7 min not 30 min). Similarly, the expression of *versican* was not affected in SCP-1 cells cultured in the presence of a conditioned medium from macrophages exposed to field B (Figure 6B–D).

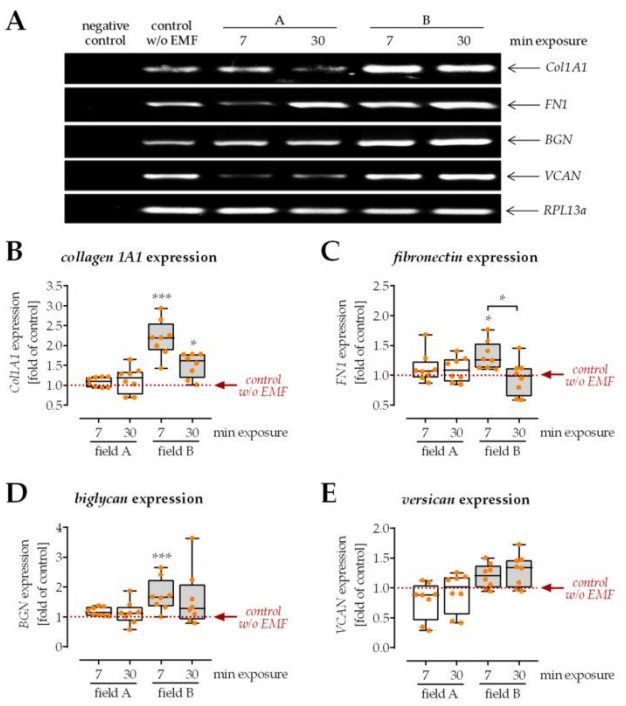

Figure 6. Gene expression of matrix proteins in SCP-1 cells cultured with conditioned medium from macrophages exposed to the ELF-PEMFs for 1 week. Freshly isolated PBMCs ($n = 5$) were stimulated with 200 nM PMA and exposed to the two ELF-PEMF for 7 min or 30 min, respectively. After 24 h, the conditioned medium was collected and added (1:1) to differentiate SCP-1 cells. (**A**) Representative images of the RT-PCR. All uncropped agarose gel images are shown in Supplementary Figure S2. ImageJ software was used to quantify signal intensities of (**B**) *collagen 1A1* (*Col1A1*); (**C**) *fibronectin* (*FN1*); (**D**) *biglycan* (*BGN*); and (E) *versican* (*VCAN*). *RPL13a* was used as a housekeeping gene for normalization. Data were compared by non-parametric Kruskal–Wallis test, followed by Dunn's multiple comparison test: * $p < 0.05$ and *** $p < 0.001$ as compared to control conditions (without ELF-PEMF exposure).

4. Discussion

Bone marrow is the major reservoir for immune cells in the human body, playing a crucial role in the innate immune response [31]. Locally, bone cells and immune cells tightly communicate and cooperate to form an 'osteoimmune micro-environment' [32]. Immediately after a bone is fractured, disruption of blood vessels leads to the formation of a hematoma at the injury site. Within hours to days, a large variety of immune cells, e.g., neutrophils, monocytes, macrophages, T-cells, and others, invade the hematoma [33]. Besides the immediate pathogen defense, immune cells orchestrate the following healing process mainly by secreting cytokines, growth factors and chemokines. Macrophages are present throughout the entire healing process and can change their activation status upon demand [3,4]. The high plasticity of the macrophages [9], in combination with their long life span at the fracture site [34], identifies macrophages as possible target cells when

attempting to temporally modulate the osteoimmune micro-environment for therapeutic purposes, i.e., when exploring the effects of different ELF-PEMFs.

In our blinded screening, we identified two ELF-PEMF that have diversely affected macrophage function. Unblinding revealed that the fundamental frequencies of these two ELF-PEMF are very close to each other, namely 51.8 Hz for field A and 52.3 Hz for field B. In literature, another 50 Hz ELF-PEMF induced anti-oxidative defense mechanism in LPS challenged THP-1 cells (mononuclear), thus initiating an anti-inflammatory reaction often associated with the M2 phenotype [23]. Yet other 50 Hz ELF-PEMFs induced ROS and thus pro-inflammatory responses in mouse macrophages [20,21], a functional response associated with the M1 phenotype. Similarly, another 50 Hz ELF-PEMF affected the immune response of monocyte-derived macrophages towards pathogens by modulating, amongst others, intracellular NO [24]. These findings are all in line with our initial assumption that different cell types respond to a specific range of fundamental frequencies. However, this does not explain why the two fields have opposing effects on the macrophages. In one study, the magnetic field density of the 50 Hz ELF-PEMF was altered (0.5–1.5 mT), which had an effect on the phagocytic activity of the macrophages [21]. This is in line with another report, which showed increased phagocytic activity and IL-1β release in mouse macrophages exposed to 50 Hz ELF-PEMF (1 mT) for 45 min [22]. In the latter study, ELF-PEMF exposure also induced ROS formation in the macrophages; however, ROS formation was independent of the chosen magnetic field density (0.05–1 mT) [22]. In our experiments, the produced ELF-PEMFs were inhomogeneous over the Somagen® applicator; the intensities of our two fields were similar. Their major difference between field A and field B was the pattern in which the pulses and bursts were emitted. The so-called send–pause intervals, suggesting that this could be a crucial factor in our experiments.

The screening also included ELF-PEMFs that have shown effects on osteoblasts (16 Hz [15,25]) and osteoclasts (26 Hz [16]) in previous studies. These two ELF-PEMFs did not affect macrophages in our screening, further underlining the idea of a frequency "window" for different cell types [35]. For example, the 16 Hz ELF-PEMF induced osteoblast function in patients undergoing high tibia osteotomies. However, no effect on osteoclast inflammatory markers was observed [36]. By changing the frequency "window", other cells might be addressed. This offers the possibility to target specific cells in different pathologies. With regard to macrophages, suppress or induce inflammation when required. An example is the two ELF-PEMF investigated here: CD86 and phospho-Stat1 are two common markers for pro-inflammatory macrophages [37]. Our data show an increase of CD86 and phospho-Stat1 after exposure of PMA-stimulated PBMCs to field A but not after exposure to field B. Arginase I, a common marker for anti-inflammatory macrophages, in turn, was increased after exposure of PMA-stimulated PBMCs to field B, but not after exposure to field A. These effects were not enhanced by prolonging the duration of the exposure. These data indicated that exposure to field A triggers macrophages towards a pro-inflammatory phenotype. In contrast, the exposure to field B triggers macrophages towards an anti-inflammatory and pro-healing phenotype [37].

To further investigate the proposed contrary effects of the two ELF-PEMF on macrophages, ROS production was determined. An accumulation of ROS is frequently observed in pro-inflammatory macrophages and is directly associated with the cells' phagocytic activity [38,39]. In line with the previous observation, only exposure to field A, but not field B, led to an increased accumulation of ROS in the ELF-PEMF exposed macrophages. The diverse effects of our two ELF-PEMF fields clearly showed that ELF-PEMF conditions are critical for the cell-specific effect. In macrophages, ROS are mainly formed by NADPH oxidases (NOX) [39], but also as a downstream product of the TLR signaling pathway [40]. In macrophages, NOX2-dependent mitochondrial ROS have direct antimicrobial activity, while ROS generated by several other NOX enzymes are supposedly involved in combating infections with protozoan parasites. Whether ROS regulate inflammatory responses of macrophages seems to be dependent on factors, e.g., type and cellular localization of the ROS and the respective stimuli [41,42]. It was

described that stimulation via TLRs leads to an increase in mitochondria-derived ROS (mtROS), mainly O_2, produced by complex I and III and its downstream product H_2O_2. Upon release into the cytoplasm, mtROS caused the dimerization of the NFκB essential modulator NEMO, subsequent activation of NFκB signaling and increased production of inflammatory cytokines [43]. Other reports show that cytoplasmically released mtROS may disrupt the interaction of the thioredoxin-interacting protein with thioredoxin, favoring the assembly of the NRLP3 inflammasome and subsequent activation of caspase-1 and related release of IL-1β and IL-18 [44]. These pro-inflammatory effects of mtROS are thought to be independent of NOX2 activity [45]. In contrast, following phagocytosis, NOX2 is activated to produce phagosomal ROS. By inactivating cathepsins L and S, phagosomal ROS inhibits excessive proteolysis of engulfed proteins, thus supporting the presentation of antigens by major histocompatibility complex class II molecules. These examples show that a tightly controlled increase in cellular ROS, a condition termed oxidative eustress [46], is an important regulator for immunological processes [47].

To verify the immune-regulatory ability of ELF-PEMFs, we performed the human Cytokine Array C5 to identify cytokines, growth factors, and chemokines secreted by the ELF-PEMF exposed macrophages. Compared to unstimulated (no ELF-PEMF) macrophages, exposure to field A stimulated the secretion of pro-inflammatory cytokines and exposure to field B stimulated the secretion of anti-inflammatory cytokines and growth factors known to support healing processes. In contrast to the phenotypic markers, elongation of the exposure duration from 7 min to 30 min enhanced the observed effect. For example, secretion of IL-10, a factor promoting the formation of a bone matrix [48], strongly increased only when macrophages were exposed for 30 min to field B. The same holds for the TIMP1 and TIMP2–secretion of both tissue inhibitors for matrix metalloproteinases (MMPs) was strongly upregulated when macrophages were exposed for 30 min to field B. This is of special interest, as patients with delayed fracture healing and non-union frequently show elevated activity of MMPs and decreased levels of TIMPs [49]. However, timing has to be considered when considering to increase secretion of TIMPs by exposure to field B—prolonged inhibition of MMPs, especially MMP9, was reported to result in defective endochondral ossification, diminished ECM remodeling, and delayed vascularization during skeletal healing [50]. This thought is fostered by the results on osteoprotegerin. The soluble antagonist for receptor activator of NF-κB ligand suppresses osteoclastogenesis, which is critically required in the bone remodeling phase [51]. Interestingly, the two ELF-PEMF induce the secretion of different angiogenic factors in macrophages. Exposure to the more anti-inflammatory field B induced factors, e.g., angiogenin, which besides angiogenesis, is also involved in various physiological and pathological processes through regulating cell proliferation, survival, migration, invasion, and/or differentiation [52]. In contrast, exposure to the more pro-inflammatory field A stimulated macrophages to secrete factors, e.g., vascular endothelial growth factor (VEGF). Here, the timing of the ELF-PEMF exposure seems to be critical when considering to increase secretion of VEGF by exposure to field A–while a rapid (few days) increase in VEGF serum levels is desired directly after a fracture. Prolonged elevation in VEGF serum levels is associated with delayed fracture healing and fracture non-unions [53]. A similar curve to VEGF was reported for transforming growth factor-beta (TGF-β). A rapid increase after fracture is required for successful fracture healing, but also its rapid decline after a few days [54]. There are several pathologies that regulate TGF-β levels–chronically elevated TGF-β levels are found in patients with chronic inflammation, e.g., patients with diabetes mellitus, COPD, liver- or kidney- fibrosis/cirrhosis, frequently displaying secondary osteoporosis with increased fracture risk and delayed fracture healing. One possible reason might be a reduced sensitivity of the bone cells towards mechanical stimulation [55]. Reduced TGF-β levels are found, for example, in smokers, which is associated with poor fracture healing [56]. Exposure to field B strongly increased the secretion of all three TGF-β isoforms. Thus, it is feasible to use exposure to field B not only

considering the timing of the ELF-PEMF exposure after the fracture but also the patients' current condition and medical history.

Besides its immune-modulatory function, TGF-β also acts as a chemokine and induces the expression of ECM proteins [57]. Thus, it was not surprising that the secretome of macrophages exposed to field B better stimulated migration of SCP-1 cells than the secretome of macrophages exposed to field A. Secretome from macrophages with the prolonged (30 min) ELF-PEMF exposure was more potent to induce SCP-1 cell migration than secretome from macrophages with the shorter (7 min) ELF-PEMF exposure. This can be explained by the results from the human Cytokine Array C5, showing enhanced secretion of cytokines, chemokines and growth factors when the duration of the ELF-PEMF exposure was prolonged.

When arriving at the fracture site, MSC ideally induces ECM synthesis, maturation, and subsequent mineral deposition [58]. In the correct composition, the formed ECM then provides a suitable niche for MSCs, regulates several intracellular signaling pathways, and thus controls the proliferation and maturation of MSCs [59]. As expected from the increased TGF-β content in the secretome of macrophages exposed to field B, the expression of collagen 1A1, fibronectin and biglycan was increased in SCP-1 cells. Expression of versican showed an inverse trend, being downregulated in SCP-1 cells cultured with secretome of macrophages exposed to field A. These results also indicate that the shorter 7 min exposure to field B was sufficient to produce enough cytokines and growth factors to exert a positive effect on ECM production in SCP-1 cells.

5. Conclusions

In summary, this study demonstrated that ELF-PEMFs with specific parameters might act immune-regulatory. Using these specific ELF-PEMFs as an adjuvant treatment to modulate the osteoimmune micro-environment at a fracture site is promising to promote fracture healing. However, not only the individual history and thus needs of the patients have to be considered, but also the duration and timing of the treatment have to be critically controlled. An ability to online measure the relevant factors, e.g., by suitable sensors and analytics, and then modify the ELF-PEMF conditions accordingly could be a future perspective to individualize care and accelerate healing, requires further research.

Supplementary Materials: The following are available online at www.mdpi.com/article/10.3390/bioengineering8110167/s1, Figure S1: Uncropped Western Blot Images. Western blot images shown in Figure 2A are shown inverse (black on white) as in the manuscript. Other membranes are summarized not inverse, Figure S2: Uncropped Agarose Gel Electrophoresis Images shown in Figure 6A and other rounds. As size marker PUC19 was used. Each round showing bands for Collagen 1A1 (83 bp), RPL13a (100 bp), Fibronectin (203 bp), Versican (306 bp), Biglycan (501 bp), and Decorin genomic DNA (>500 p).

Author Contributions: Conceptualization, S.E.; methodology, Y.C., C.L., M.R. and S.E.; software, B.J.B., H.W., T.H. and A.K.N.; formal analyses, Y.C.; investigation, Y.C. and S.S.; resources, M.M.M., K.F., M.R., H.W., T.H. and A.K.N.; data curation, S.E.; writing—original draft preparation, Y.C. and S.E.; writing—review and editing, all authors; visualization, Y.C. and S.E.; supervision, S.E. and A.K.N.; project administration, A.K.N.; funding acquisition, A.K.N. and S.E.; All authors have read and agreed to the published version of the manuscript.

Funding: S.E. received funding from the German Research Foundation (DFG EH 471/2). Y.C. received support from the China Scholarship Council (201906160085) to cover his living expenses.

Institutional Review Board Statement: The study was conducted according to the guidelines of the Declaration of Helsinki and approved by the Ethics Committee of the University Clinic Tübingen (541/2016BO2 approved 09.08.2016).

Informed Consent Statement: Informed consent was obtained from all healthy volunteers who donated blood (pseudonymized) for cell isolation in this study.

Data Availability Statement: The datasets generated during and/or analyzed during the current study are available from the corresponding author on reasonable request.

Acknowledgments: The authors would like to thank Sachtleben GmbH, which provided the ELF-PEMF devices (Somagen®) and the background on the physical parameters. The authors would like to thank M. Schieker, who provided us with the SCP-1 cells. The data presented in this manuscript were obtained during the Ph.D. work of Y.C. and the Bachelor work of S.S. The authors would like to thank Alicia Geier and Lina Afflerbach for their excellent technical assistance.

Conflicts of Interest: The authors declare no conflict of interest. Sachtleben GmbH provided the ELF-PEMF devices (Somagen®) and the background on the physical parameters but were not involved in the study design or the data evaluation.

References

1. Holmes, D. Non-union bone fracture: A quicker fix. *Nature* **2017**, *550*, S193, doi:10.1038/550S193a.
2. Castronuovo, E.; Pezzotti, P.; Franzo, A.; Di Lallo, D.; Guasticchi, G. Early and late mortality in elderly patients after hip fracture: A cohort study using administrative health databases in the Lazio region, Italy. *Bmc. Geriatr.* **2011**, *11*,1–9.
3. Bucher, C.H.; Lei, H.; Duda, G.N.; Volk, H.D.; Schmidt-Bleek, K. *The Role of Immune Reactivity in Bone Regeneration*; IntecOpen Limited: London, UK, 2016; pp. 169–194.
4. Schlundt, C.; El Khassawna, T.; Serra, A.; Dienelt, A.; Wendler, S.; Schell, H.; van Rooijen, N.; Radbruch, A.; Lucius, R.; Hartmann, S.; et al. Macrophages in bone fracture healing: Their essential role in endochondral ossification. *Bone* **2018**, *106*, 78–89.
5. Park, J.E.; Barbul, A. Understanding the role of immune regulation in wound healing. *Am. J. Surg.* **2004**, *187*, 11–16.
6. Wynn, T.A.; Vannella, K.M. Macrophages in tissue repair, regeneration, and fibrosis. *Immunity* **2016**, *44*, 450–462.
7. Okabe, Y.; Medzhitov, R. Tissue biology perspective on macrophages. *Nat. Immunol.* **2016**, *17*, 9–17.
8. Behm, B.; Babilas, P.; Landthaler, M.; Schreml, S. Cytokines, chemokines and growth factors in wound healing. *J. Eur. Acad. Dermatol. Venereol.* **2012**, *26*, 812–820.
9. Chen, Y.; Guan, M.; Ren, R.; Gao, C.; Cheng, H.; Li, Y.; Gao, B.; Wei, Y.; Fu, J.; Sun, J.; et al. Improved Immunoregulation of Ultra-Low-Dose Silver Nanoparticle-Loaded TiO2 Nanotubes via M2 Macrophage Polarization by Regulating GLUT1 and Autophagy. *Int. J. Nanomed.* **2020**, *15*, 2011–2026.
10. Mosser, D.M.; Edwards, J.P. Exploring the full spectrum of macrophage activation. *Nat. Rev. Immunol.* **2008**, *8*, 958–969.
11. Claes, L.; Recknagel, S.; Ignatius, A. Fracture healing under healthy and inflammatory conditions. *Nat. Rev. Rheumatol.* **2012**, *8*, 133–143.
12. George, M.D.; Baker, J.F.; Leonard, C.E.; Mehta, S.; Miano, T.A.; Hennessy, S. Risk of Nonunion with Nonselective NSAIDs, COX-2 Inhibitors, and Opioids. *J. Bone Jt. Surg. Am.* **2020**, *102*, 1230–1238.
13. Liu, Y.Z.; Akhter, M.P.; Gao, X.; Wang, X.Y.; Wang, X.B.; Zhao, G.; Wei, X.; Wu, H.J.; Chen, H.; Wang, D.; et al. Glucocorticoid-induced delayed fracture healing and impaired bone biomechanical properties in mice. *Clin. Interv. Aging* **2018**, *13*, 1465–1474.
14. Ehnert, S.; Schroter, S.; Aspera-Werz, R.H.; Eisler, W.; Falldorf, K.; Ronniger, M.; Nussler, A.K. Translational Insights into Extremely Low Frequency Pulsed Electromagnetic Fields (ELF-PEMFs) for Bone Regeneration after Trauma and Orthopedic Surgery. *J. Clin. Med.* **2019**, *8*, 2802. doi.org/10.3390/jcm8122028.
15. Ehnert, S.; Falldorf, K.; Fentz, A.K.; Ziegler, P.; Schroter, S.; Freude, T.; Ochs, B.G.; Stacke, C.; Ronniger, M.; Sachtleben, J.; et al. Primary human osteoblasts with reduced alkaline phosphatase and matrix mineralization baseline capacity are responsive to extremely low frequency pulsed electromagnetic field exposure—Clinical implication possible. *Bone Rep.* **2015**, *3*, 48–56.
16. Ehnert, S.; van Griensven, M.; Unger, M.; Scheffler, H.; Falldorf, K.; Fentz, A.K.; Seeliger, C.; Schroter, S.; Nussler, A.K.; Balmayor, E.R. Co-Culture with Human Osteoblasts and Exposure to Extremely Low Frequency Pulsed Electromagnetic Fields Improve Osteogenic Differentiation of Human Adipose-Derived Mesenchymal Stem Cells. *Int. J. Mol. Sci.* **2018**, *19*, 994. doi.org/10.3390/ijms19040994.
17. Iwasa, K.; Reddi, A.H. Pulsed Electromagnetic Fields and Tissue Engineering of the Joints. *Tissue Eng. Part B Rev.* **2018**, *24*, 144–154.
18. Miller, S.L.; Coughlin, D.G.; Waldorff, E.I.; Ryaby, J.T.; Lotz, J.C. Pulsed electromagnetic field (PEMF) treatment reduces expression of genes associated with disc degeneration in human intervertebral disc cells. *Spine J.* **2016**, *16*, 770–776.
19. Simko, M.; Mattsson, M.O. Extremely low frequency electromagnetic fields as effectors of cellular responses in vitro: Possible immune cell activation. *J. Cell Biochem.* **2004**, *93*, 83–92.
20. Rollwitz, J.; Lupke, M.; Simko, M. Fifty-hertz magnetic fields induce free radical formation in mouse bone marrow-derived promonocytes and macrophages. *Biochim. Biophys Acta* **2004**, *1674*, 231–238.
21. Simko, M.; Droste, S.; Kriehuber, R.; Weiss, D.G. Stimulation of phagocytosis and free radical production in murine macrophages by 50 Hz electromagnetic fields. *Eur. J. Cell. Biol.* **2001**, *80*, 562–566.
22. Frahm, J.; Lantow, M.; Lupke, M.; Weiss, D.G.; Simko, M. Alteration in cellular functions in mouse macrophages after exposure to 50 Hz magnetic fields. *J. Cell Biochem.* **2006**, *99*, 168–177.

23. Patruno, A.; Costantini, E.; Ferrone, A.; Pesce, M.; Diomede, F.; Trubiani, O.; Reale, M. Short ELF-EMF Exposure Targets SIRT1/Nrf2/HO-1 Signaling in THP-1 Cells. *Int. J. Mol. Sci.* **2020**, *21*, 7284. doi.org/10.3390/ijms21197284.
24. Akan, Z.; Aksu, B.; Tulunay, A.; Bilsel, S.; Inhan-Garip, A. Extremely low-frequency electromagnetic fields affect the immune response of monocyte-derived macrophages to pathogens. *Bioelectromagnetics* **2010**, *31*, 603–612.
25. Chen, Y.; Aspera-Werz, R.H.; Menger, M.M.; Falldorf, K.; Ronniger, M.; Stacke, C.; Histing, T.; Nussler, A.K.; Ehnert, S. Exposure to 16 Hz Pulsed Electromagnetic Fields Protect the Structural Integrity of Primary Cilia and Associated TGF-beta Signaling in Osteoprogenitor Cells Harmed by Cigarette Smoke. *Int. J. Mol. Sci.* **2021**, *22*, 7036. doi.org/10.3390/ijms22137036.
26. Zhou, J.; Wang, J.Q.; Ge, B.F.; Ma, X.N.; Ma, H.P.; Xian, C.J.; Chen, K.M. Different electromagnetic field waveforms have different effects on proliferation, differentiation and mineralization of osteoblasts in vitro. *Bioelectromagnetics* **2014**, *35*, 30–38.
27. Zhang, X.; Zhang, J.; Qu, X.; Wen, J. Effects of different extremely low-frequency electromagnetic fields on osteoblasts. *Electromagn. Biol. Med.* **2007**, *26*, 167–177.
28. Linnemann, C.; Savini, L.; Rollmann, M.F.; Histing, T.; Nussler, A.K.; Ehnert, S. Altered Secretome of Diabetic Monocytes Could Negatively Influence Fracture Healing-An In Vitro Study. *Int. J. Mol. Sci.* **2021**, *22*, 9212. doi.org/10.3390/ijms22179212.
29. Ehnert, S.; Fentz, A.K.; Schreiner, A.; Birk, J.; Wilbrand, B.; Ziegler, P.; Reumann, M.K.; Wang, H.; Falldorf, K.; Nussler, A.K. Extremely low frequency pulsed electromagnetic fields cause antioxidative defense mechanisms in human osteoblasts via induction of *O2(-) and H2O2. *Sci. Rep.* **2017**, *7*, 14544, doi:10.1038/s41598-017-14983-9.
30. Bocker, W.; Yin, Z.; Drosse, I.; Haasters, F.; Rossmann, O.; Wierer, M.; Popov, C.; Locher, M.; Mutschler, W.; Docheva, D.; et al. Introducing a single-cell-derived human mesenchymal stem cell line expressing hTERT after lentiviral gene transfer. *J. Cell Mol. Med.* **2008**, *12*, 1347–1359.
31. Bedi, B.; Li, J.Y.; Grassi, F.; Tawfeek, H.; Weitzmann, M.N.; Pacifici, R. Inhibition of antigen presentation and T cell costimulation blocks PTH-induced bone loss. *Ann. N. Y. Acad. Sci.* **2010**, *1192*, 215–221.
32. Tsukasaki, M.; Takayanagi, H. Osteoimmunology: Evolving concepts in bone-immune interactions in health and disease. *Nat. Rev. Immunol.* **2019**, *19*, 626–642.
33. Julier, Z.; Park, A.J.; Briquez, P.S.; Martino, M.M. Promoting tissue regeneration by modulating the immune system. *Acta Biomater.* **2017**, *53*, 13–28.
34. Parihar, A.; Eubank, T.D.; Doseff, A.I. Monocytes and Macrophages Regulate Immunity through Dynamic Networks of Survival and Cell Death. *J. Innate Immun.* **2010**, *2*, 204–215.
35. Funk, R.H. Coupling of pulsed electromagnetic fields (PEMF) therapy to molecular grounds of the cell. *Am. J. Transl. Res.* **2018**, *10*, 1260–1272.
36. Ziegler, P.; Nussler, A.K.; Wilbrand, B.; Falldorf, K.; Springer, F.; Fentz, A.K.; Eschenburg, G.; Ziegler, A.; Stockle, U.; Maurer, E.; et al. Pulsed Electromagnetic Field Therapy Improves Osseous Consolidation after High Tibial Osteotomy in Elderly Patients-A Randomized, Placebo-Controlled, Double-Blind Trial. *J. Clin. Med.* **2019**, *8*, 2008.
37. Barros, M.H.M.; Hauck, F.; Dreyer, J.H.; Kempkes, B.; Niedobitek, G. Macrophage Polarisation: An Immunohistochemical Approach for Identifying M1 and M2 Macrophages. *PLoS ONE* **2013**, *8*, e80908, doi:10.1371/journal.pone.0080908.
38. Lo, H.M.; Chen, C.L.; Yang, C.M.; Wu, P.H.; Tsou, C.J.; Chiang, K.W.; Wu, W.B. The carotenoid lutein enhances matrix metalloproteinase-9 production and phagocytosis through intracellular ROS generation and ERK1/2, p38 MAPK, and RARbeta activation in murine macrophages. *J. Leukoc Biol.* **2013**, *93*, 723–735.
39. Tan, H.Y.; Wang, N.; Li, S.; Hong, M.; Wang, X.; Feng, Y. The Reactive Oxygen Species in Macrophage Polarization: Reflecting Its Dual Role in Progression and Treatment of Human Diseases. *Oxid. Med. Cell Longev.* **2016**, *2016*, 2795090, doi:10.1155/2016/2795090.
40. Huang, J.; Brumell, J.H. NADPH oxidases contribute to autophagy regulation. *Autophagy* **2009**, *5*, 887–889.
41. Sies, H. Oxidative eustress: On constant alert for redox homeostasis. *Redox Biol.* **2021**, *41*, 101867, doi:10.1016/j.redox.2021.101867.
42. Brune, B.; Dehne, N.; Grossmann, N.; Jung, M.; Namgaladze, D.; Schmid, T.; von Knethen, A.; Weigert, A. Redox control of inflammation in macrophages. *Antioxid. Redox Signal.* **2013**, *19*, 595–637.
43. Herb, M.; Gluschko, A.; Wiegmann, K.; Farid, A.; Wolf, A.; Utermohlen, O.; Krut, O.; Kronke, M.; Schramm, M. Mitochondrial reactive oxygen species enable proinflammatory signaling through disulfide linkage of NEMO. *Sci. Signal.* **2019**, *12*, doi:10.1126/scisignal.aar5926.
44. Zhou, R.; Tardivel, A.; Thorens, B.; Choi, I.; Tschopp, J. Thioredoxin-interacting protein links oxidative stress to inflammasome activation. *Nat. Immunol.* **2010**, *11*, 136–140.
45. Bulua, A.C.; Simon, A.; Maddipati, R.; Pelletier, M.; Park, H.; Kim, K.Y.; Sack, M.N.; Kastner, D.L.; Siegel, R.M. Mitochondrial reactive oxygen species promote production of proinflammatory cytokines and are elevated in TNFR1-associated periodic syndrome (TRAPS). *J. Exp. Med.* **2011**, *208*, 519–533.
46. Sies, H.; Jones, D.P. Reactive oxygen species (ROS) as pleiotropic physiological signalling agents. *Nat. Rev. Mol. Cell Biol.* **2020**, *21*, 363–383.
47. Herb, M.; Schramm, M. Functions of ROS in Macrophages and Antimicrobial Immunity. *Antioxidants* **2021**, *10*, 313, doi:10.3390/antiox10020313.
48. Dresner-Pollak, R.; Gelb, N.; Rachmilewitz, D.; Karmeli, F.; Weinreb, M. Interleukin 10-deficient mice develop osteopenia, decreased bone formation, and mechanical fragility of long bones. *Gastroenterology* **2004**, *127*, 792–801.
49. Henle, P.; Zimmermann, G.; Weiss, S. Matrix metalloproteinases and failed fracture healing. *Bone* **2005**, *37*, 791–798.

50. Colnot, C.; Thompson, Z.; Miclau, T.; Werb, Z.; Helms, J.A. Altered fracture repair in the absence of MMP9. *Development* **2003**, *130*, 4123–4133.
51. Boyce, B.F.; Xing, L. Functions of RANKL/RANK/OPG in bone modeling and remodeling. *Arch. Biochem. Biophys* **2008**, *473*, 139–146.
52. Sheng, J.; Xu, Z. Three decades of research on angiogenin: A review and perspective. *Acta Biochim. Biophys Sin.* **2016**, *48*, 399–410.
53. Weiss, S.; Zimmermann, G.; Pufe, T.; Varoga, D.; Henle, P. The systemic angiogenic response during bone healing. *Arch. Orthop. Trauma Surg.* **2009**, *129*, 989–997.
54. Zimmermann, G.; Henle, P.; Kusswetter, M.; Moghaddam, A.; Wentzensen, A.; Richter, W.; Weiss, S. TGF-beta1 as a marker of delayed fracture healing. *Bone* **2005**, *36*, 779–785.
55. Ehnert, S.; Sreekumar, V.; Aspera-Werz, R.H.; Sajadian, S.O.; Wintermeyer, E.; Sandmann, G.H.; Bahrs, C.; Hengstler, J.G.; Godoy, P.; Nussler, A.K. TGF-beta(1) impairs mechanosensation of human osteoblasts via HDAC6-mediated shortening and distortion of primary cilia. *J. Mol. Med.* **2017**, *95*, 653–663.
56. Moghaddam, A.; Weiss, S.; Wolfl, C.G.; Schmeckenbecher, K.; Wentzensen, A.; Grutzner, P.A.; Zimmermann, G. Cigarette smoking decreases TGF-b1 serum concentrations after long bone fracture. *Injury* **2010**, *41*, 1020–1025.
57. Meng, X.M.; Nikolic-Paterson, D.J.; Lan, H.Y. TGF-beta: The master regulator of fibrosis. *Nat. Rev. Nephrol* **2016**, *12*, 325–338.
58. Muszynska, M.; Ambrozewicz, E.; Gegotek, A.; Grynkiewicz, G.; Skrzydlewska, E. Protective Effects of Vitamin K Compounds on the Proteomic Profile of Osteoblasts under Oxidative Stress Conditions. *Molecules* **2020**, *25*, 1990.
59. Daley, W.P.; Peters, S.B.; Larsen, M. Extracellular matrix dynamics in development and regenerative medicine. *J. Cell Sci.* **2008**, *121*, 255–264.

2.2 Exposure to 16 Hz Pulsed Electromagnetic Fields Protect the Structural Integrity of Primary Cilia and Associated TGF-β Signaling in Osteoprogenitor Cells Harmed by Cigarette Smoke

(CHEN, Y., ASPERA-WERZ, R. H., MENGER, M. M., FALLDORF, K., RONNIGER, M., STACKE, C., HISTING, T., NUSSLER, A. K. & EHNERT, S. 2021. Exposure to 16 Hz Pulsed Electromagnetic Fields Protect the Structural Integrity of Primary Cilia and Associated TGF-beta Signaling in Osteoprogenitor Cells Harmed by Cigarette Smoke. Int J Mol Sci, 22.)

2.2.1 Summary and Major Findings

In the previous study, the focus was on the interaction between immune cells and osteoblasts, and how ELF-PEMF may modulate this interaction during fracture healing. The aim of the present study was to optimize ELF-PEMF exposure in osteogenic cells and provide deeper insights into the underlying molecular mechanisms. In the clinical routine, cigarette smoking is well-accepted as a risk factor leading to compromised bone strength, increased fracture risk, and delayed or impaired fracture healing. Therefore, exposure to cigarette smoke extract (CSE) served a pathologic model in the present study, as it has been shown before to affect the osteogenic differentiation of MSCs. In this cell type, 16 Hz ELF-PEMF showed beneficial effects on osteogenic differentiation; however, the exposure conditions (duration and timing) still required optimization. The results demonstrated that prolonging the daily ELF-PEMF (16 Hz) exposure from 7 min to 30 min significantly increased osteoprogenitor numbers, viability, migration, attachment, spreading, and osteogenic differentiation. However, further elongation of the exposure duration caused the opposite effect. ELF-PEMF treatment, under the optimized conditions, protected the structure of the primary cilia, and thus rescued canonical TGF-β signaling, which was effectively blocked in the presence of CSE. The data suggest that ELF-PEMF treatment may restore osteogenic function in CSE-exposed cells by rescuing primary cilia structure and associated TGF-β signaling.

Overall, this study partially achieved project **aims 1, 2, 4, and 5**. This work provides evidence that daily exposure to 16 Hz ELF-PEMF is a promising treatment to support new bone formation in the early stage of fracture healing, and thus could potentially prevent fracture non-unions in smokers.

Limitations and next steps: This study mainly focused on the protective effects of 16 Hz ELF-PEMF in terms of TGF-β signaling and primary cilia structure in osteogenic cells. However, there are many more receptors and ion channels located on primary cilia, which may be affected by ELF-PEMF treatment but were not considered in this study. Calcium channels regulating the influx of calcium ions, which are important secondary messengers, are also frequently located on primary cilia. Calcium channels may be regulated by voltage drops, thus their activity may be regulated by ELF-PEMF treatment. Therefore, our next steps will focus on exploring other potential molecular mechanisms as to how ELF-PEMF treatment affects osteogenic cells, *e.g.*, the activation of calcium ion channels.

2.2.2 Personal Contribution

I was the main person who performed the experiments and data analysis. I was also highly involved in the design of the experiments and preparation of the original manuscript draft.

International Journal of
Molecular Sciences

MDPI

Article

Exposure to 16 Hz Pulsed Electromagnetic Fields Protect the Structural Integrity of Primary Cilia and Associated TGF-β Signaling in Osteoprogenitor Cells Harmed by Cigarette Smoke

Yangmengfan Chen [1], Romina H. Aspera-Werz [1], Maximilian M. Menger [1], Karsten Falldorf [2], Michael Ronniger [2], Christina Stacke [2], Tina Histing [1], Andreas K. Nussler [1,*] and Sabrina Ehnert [1]

[1] Siegfried Weller Research Institute at the BG Trauma Center Tübingen, Department of Trauma and Reconstructive Surgery, University of Tübingen, Schnarrenbergstr. 95, D-72076 Tübingen, Germany; chenyangmengfantj@163.com (Y.C.); rominaaspera@hotmail.com (R.H.A.-W.); mmenger@bgu-tuebingen.de (M.M.M.); thisting@bgu-tuebingen.de (T.H.); andreas.nuessler@gmail.com (A.K.N.), sabrina.ehnert@med.uni-tuebingen.de (S.E.)

[2] Sachtleben GmbH, Haus Spectrum am UKE, Martinistraße 64, D-20251 Hamburg, Germany; falldorf@citresearch.de (K.F.), ronniger@citresearch.de (M.R.), stacke@citresearch.de (C.S.)

* Correspondence: andreas.nuessler@gmail.com; Tel.: +49-7071-606-1065

Abstract: Cigarette smoking (CS) is one of the main factors related to avoidable diseases and death across the world. Cigarette smoke consists of numerous toxic compounds that contribute to the development of osteoporosis and fracture nonunion. Exposure to pulsed electromagnetic fields (PEMF) was proven to be a safe and effective therapy to support bone fracture healing. The aims of this study were to investigate if extremely low frequency (ELF-) PEMFs may be beneficial to treat CS-related bone disease, and which effect the duration of the exposure has. In this study, immortalized human mesenchymal stem cells (SCP-1 cells) impaired by 5% cigarette smoke extract (CSE) were exposed to ELF-PEMFs (16 Hz) with daily exposure ranging from 7 min to 90 min. Cell viability, adhesion, and spreading were evaluated by Sulforhodamine B, Calcein-AM staining, and Phalloidin-TRITC/Hoechst 33342 staining. A migration assay kit was used to determine cell migration. Changes in TGF-β signaling were evaluated with an adenoviral Smad2/3 reporter assay, RT-PCR, and Western blot. The structure and distribution of primary cilia were analyzed with immunofluorescent staining. Our data indicate that 30 min daily exposure to a specific ELF-PEMF most effectively promoted cell viability, enhanced cell adhesion and spreading, accelerated migration, and protected TGF-β signaling from CSE-induced harm. In summary, the current results provide evidence that ELF-PEMF can be used to support early bone healing in patients who smoke.

Keywords: Extremely low frequency pulsed electromagnetic fields (ELF-PEMFs); mesenchymal stem cells; bone healing; cigarette smoke extract; TGF-β signaling; primary cilium

Citation: Chen, Y.; Aspera-Werz, R.H.; Menger, M.M.; Falldorf, K.; Ronniger, M.; Stacke, C.; Histing, T.; Nussler, A.K.; Ehnert, S. Exposure to 16 Hz Pulsed Electromagnetic Fields Protect the Structural Integrity of Primary Cilia and Associated TGF-β Signaling in Osteoprogenitor Cells Harmed by Cigarette Smoke. *Int. J. Mol. Sci.* **2021**, *22*, 7036. https://doi.org/10.3390/ijms22137036

Academic Editor: Francesca Paino

Received: 26 May 2021
Accepted: 28 June 2021
Published: 29 June 2021

Publisher's Note: MDPI stays neutral with regard to jurisdictional claims in published maps and institutional affiliations.

Copyright: © 2021 by the authors. Licensee MDPI, Basel, Switzerland. This article is an open access article distributed under the terms and conditions of the Creative Commons Attribution (CC BY) license (http://creativecommons.org/licenses/by/4.0/).

1. Introduction

Cigarette smoking (CS) is the principal cause of avoidable disease and death across the world in the 21st century. According to the project summary of Special Eurobarometer 458–Attitudes of Europeans towards tobacco and electronic cigarettes (https://ec.europa.eu/health/tobacco/eurobarometers_en accessed on 03 February 2021.), 23% of EU residents are defined as daily smokers. The percentage of daily smokers is especially high for southern European countries, e.g., Bulgaria (38%), Greece (42%), or Croatia (35%). Cigarette smoke extract (CSE) consists of more than 6,000 molecular species and toxic compounds. When applied to cells, CSE was proven to inhibit various signaling pathways, i.a., transform growth factor β (TGF-β) [1], insulin-like growth factor 1 [2], phosphoinositide 3-kinase (PI3K), and protein kinase B [3], as well as antioxidative

enzyme activities [4]. Moreover, CS severely affects the skeletal system, contributing to the development of osteoporosis [5], delayed fracture healing, and nonunion formation [6], the treatment of which adds a tremendous burden to the medical expenditure and socio-economy [7].

Along with the growing awareness of the negative effects of CS on the skeletal system, there is an increasing demand for effective therapies. In the recent decades, a variety of mechanical stimuli were used to treat skeletal diseases by maintaining the balance between osteoblastic bone formation and osteoclastic bone resorption [8]. Since 1978, pulsed electromagnetic fields (PEMFs) were recognized as a safe, non-invasive, and effective physical treatment for bone diseases, thus received substantial attention in the field of regenerative medicine [9]. Under physiological conditions, PEMFs will be generated in the human body due to piezoelectric phenomena [10]. For example, the frequency of mechanical strains caused by muscle activity is in the extremely low frequency (ELF) range between 5 Hz and 30 Hz [11]. Theoretically, this allows ELF-PEMFs to mimic the physiological stimulation, and thus to become a feasible treatment for the musculoskeletal system. Indeed, screening ELF-PEMFs with frequencies of up to 100 Hz revealed that osteoprogenitor cells respond well to the mentioned frequency range below 30 Hz [12]. Besides frequency, which has been investigated in earlier studies, there might be other parameters responsible for the type and magnitude of PEMF effects in cells and tissue such as intensity and exposure timing (duration and intervals). The latter was examined in this study. Nevertheless, research to date has not yet revealed the detailed mechanisms of how cells sense, translate, and transduce signals of ELF-PEMFs to regulate cellular activities.

To explore a potential mechanism, we focused on the primary cilium that is considered as the "mechanosensing antenna" in nearly all eukaryotic cells [13]. In bone tissue, the microtubule-based non-motile primary cilium protrudes from the membrane of osteoblasts. It touches the inner wall of the 'lacunae' to sense extracellular mechanical forces exerting on the bone tissue [14]. In response to mechanical signals, numerous receptors are recruited to the ciliary membrane to facilitate the activation of associated signaling pathways [15]. As a result, extracellular physical signals are sensed. For patients who smoke daily, the structural integrity of primary cilia, and thus the mechanosensory ability of bone cells, are damaged. This can be simulated in vitro by applying CSE to the cells [13]. The canonical TGF-β signaling, which plays a crucial role in early fracture healing [16], is strongly inter-dependent on the structural and functional integrity of the primary cilia [1,17–19]. TGF-β is known to promote bone regeneration, as it can enhance viability, proliferation, and migration of osteoprogenitor cells [20–22]. In smokers, not only do TGF-β levels fail to increase after trauma or orthopedic surgery [23,24], but also the primary cilia-mediated TGF-β signaling is inhibited [1]. This is proposed to impair the healing process. In this study, we intended to assess possible protective effects of ELF-PEMFs on cell viability, adhesion, and migration of immortalized human mesenchymal stem cells (SCP-1 cells) affected by CSE. Furthermore, we assessed whether the effects relate to the structure of the primary cilia and the associated TGF-β signaling.

2. Results

2.1. ELF-PEMFs Increased Viability and Alleviated the Negative Effects of CSE in SCP-1 Cells

Cell viability was determined in SCP-1 cells exposed to 16 Hz ELF-PEMFs for 0, 7, 30, and 90 min/day in the presence or absence of 5% CSE. As expected, CSE significantly impaired cell viability (Calcein-AM staining) and decreased cell numbers (total protein content). Exposure to ELF-PEMFs increased cell viability, both in the presence or absence of the CSE. The strongest effects were observed with 30 min daily exposure to the ELF-PEMF (Figure 1A, Figure 1B).

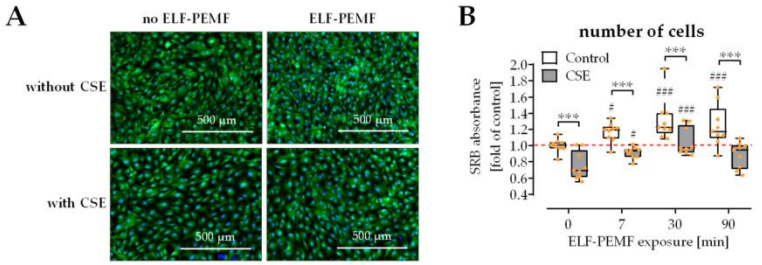

Figure 1. SCP-1 cell viability is affected by 16 Hz ELF-PEMFs (0, 7, 30, and 90 min) and 5% cigarette smoke extract (CSE). (**A**) Fluorescent Calcein-AM staining (2 µM, green) was used to visualize living cells, and Hoechst 33342 (2 µg/mL, blue) was used as nuclear counterstain. (**B**) Sulforhodamine B (SRB) staining was used to quantify cell numbers by total protein content after 3 days. N = 3, *n* = 3. Data are presented as a box plot (Min to Max with single data points). Data were compared by non-parametric two-way ANOVA followed by Tukey's multiple comparison test: *** $p < 0.001$ as indicated; # $p < 0.05$ ### $p < 0.001$ as compared to the respective control (no ELF-PEMF).

2.2. SCP-1 Cell Adhesion and Spreading Are Enhanced by ELF-PEMF Exposure

Cell adhesion and spreading are important for initiating the biological function of osteoprogenitor cells. In this study, microscopic visualization of the cytoskeleton and the nuclei was used to observe cell adhesion and spreading when exposed to 16 Hz ELF-PEMFs and/or 5% CSE (Figure 2A). Quantification of the number of adherent nuclei indicated that CSE impaired cell adhesion, but 7 min and 30 min daily exposure to 16 Hz ELF-PEMF favored cell adhesion (Figure 2B). Similarly, the mean cellular size indicated that 7 min and 30 min daily exposure to 16 Hz ELF-PEMF facilitated cell spreading, both in the presence or absence of 5% CSE (Figure 2C).

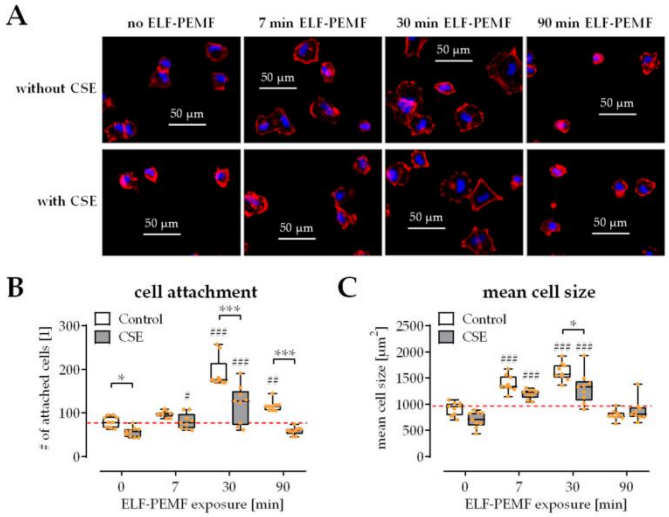

Figure 2. Influences of 16 Hz ELF-PEMFs (0, 7, 30, and 90 min) and 5% cigarette smoke extract (CSE) on SCP-1 cell adhesion and spreading after 4 h. (**A**) Representative images (400 x magnification) of the fluorescence staining for cytoskeleton (phalloidin-TRITC, 2 µg/mL, red) and nuclei (Hoechst 33342, 2 µg/mL, blue). (**B**) Automated quantification of adherent nuclei, and (**C**) the mean size of attached SCP-1 cells using the ImageJ software. N = 3, n = 3. Data are presented as box

plots (Min to Max with single data points). Data were compared by non-parametric two-way ANOVA followed by Tukey's multiple comparison test: * $p < 0.05$ and *** $p < 0.001$ as indicated; # $p < 0.05$, ## $p < 0.01$, and ### $p < 0.001$ as compared to the respective control (no ELF-PEMF).

2.3. Exposure to ELF-PEMFs Enhances Migration of SCP-1 Cells

Migration of osteoprogenitor cells plays a crucial role in early fracture healing. To evaluate the influences of 16 Hz ELF-PEMFs on SCP-1 cell migration, a cell migration assay kit was used to generate a cell-free circular area (migration zone) centrally in the cavities of 96-well plates (Figure 3A). Automated image evaluation demonstrated that 5% CSE strongly suppressed SCP-1 cell migration, while 16 Hz ELF-PEMFs accelerated SCP-1 cell migration both in the presence or absence of 5% CSE. The strongest effects of the 16 Hz ELF-PEMF were observed with 30 min daily exposure (Figure 3B).

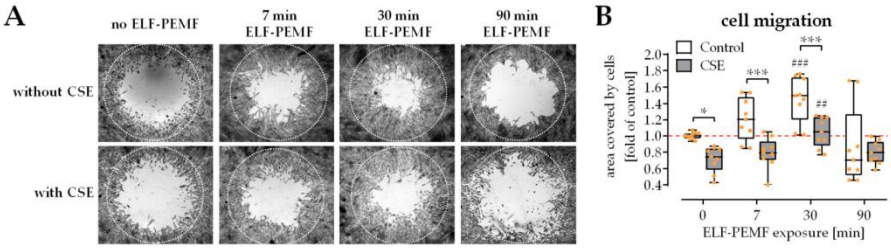

Figure 3. Migration of SCP-1 cells is affected by 16 Hz ELF-PEMFs (0, 7, 30, and 90 min) and 5% cigarette smoke extract (CSE). (**A**) Sulforhodamine B (SRB) staining was performed to better visualize cells invading into the migration zone (dotted circle) after 72 h. (**B**) SCP-1 cell migration was quantified using the ImageJ software. N = 4, *n* = 2. Data are presented as a box plot (Min to Max with single data points). Data were compared by non-parametric two-way ANOVA followed by Tukey's multiple comparison test: * $p < 0.05$ and *** $p < 0.001$ as indicated; ## $p < 0.01$ and ### $p < 0.001$ as compared to the respective control (no ELF-PEMF).

Overall the positive effect of the 16 Hz ELF-PEMF on SCP-1 cell viability, adhesion, spreading, and migration also displayed a positive effect on the osteogenic differentiation (Supplementary Figure 1). In line with earlier publications [12,25], daily exposure to 16 Hz ELF-PEMF induced alkaline phosphatase (ALP) activity and formation of mineralized matrix in SCP-1 cell. Prolonging the duration of the daily exposure from 7 min to 30 min, but not to 90 min, further enhanced the positive effect of the 16 Hz ELF-PEMF on the SCP-1 cells. The 30 min daily exposure to the 16 Hz ELF-PEMF was sufficient to reverse the well-known negative effect that continuous stimulation with 5% CSE has on SCP-1 cells [1,4,13].

2.4. ELF-PEMF Exposure Intensified TGF-β Signaling in SCP-1 Cells

TGF-β is a key factor favoring the migration of osteoprogenitor cells [22]. As exposure to 16 Hz ELF-PEMF induced SCP-1 cell migration, potential alterations in TGF-β signaling were investigated. Functional, canonical (Smad2/3) TGF-β signaling was quantified using an adenoviral reporter assay. As expected, medium supplementation with 5 ng/mL recombinant human TGF-β activated Smad2/3 signaling in SCP-1 cells. The presence of 5% CSE significantly reduced this effect. Exposure to the 16 Hz ELF-PEMFs intensified the TGF-β signaling by 50 to 60%, both in the presence or absence of 5% CSE. Significant results were observed again for 30 min daily exposure with the 16 Hz ELF-PEMF (Figure 4A); therefore, this condition was used for all further experiments.

Interestingly, a Western blot revealed that the amount of total Smad2 and Smad3 phosphorylated was only affected in the presence of 5% CSE and not by exposure to the 16 Hz ELF-PEMF. However, the basal levels of Smad2 and Smad3 were significantly re-

duced in the presence of 5% CSE. A period of 30 min exposure to 16 Hz ELF-PEMF significantly increased cellular levels of Smad2 and Smad3 (Figure 4B, Figure 4C)

As expected, SCP-1 cell migration was accelerated in presence of 5 ng/mL TGF-β. The addition of TGF-β alone was not able to restore the SCP-1 cell migration impaired by 5% CSE. However, an additional 30 min daily exposure to 16 Hz ELF-PEMF fortified the positive effect of TGF-β, to fully restore the SCP-1 cell migration suppressed by 5% CSE (Figure 4D).

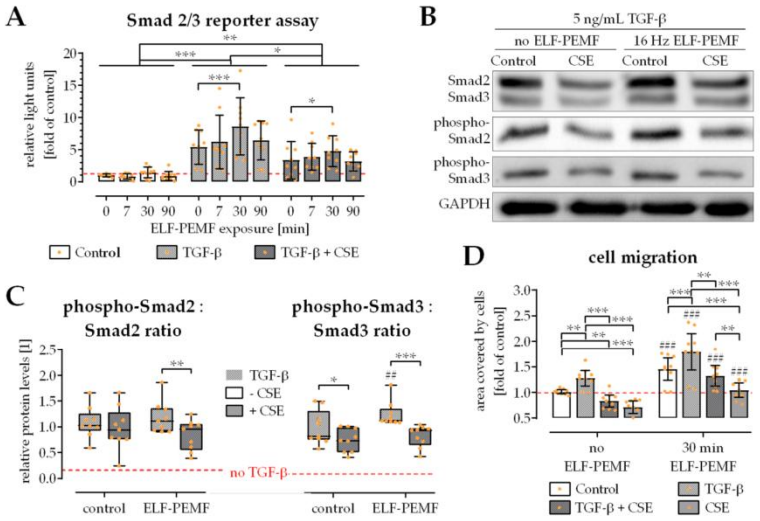

Figure 4. Canonical (Smad2/3) TGF-β signaling affected by 5% cigarette smoke extract (CSE) is fortified by exposure to the 16 Hz ELF-PEMFs. (**A**) An adenoviral reporter assay was used to quantify canonical (Smad2/3) TGF-β signaling in SCP-1 cells exposed to 5 ng/mL TGF-β, 5% CSE, and/or the 16 Hz ELF-PEMFs (0, 7, 30, 90 min daily exposure) for 72 h. Western blot was used to confirm phosphorylation of Smad2 and Smad3 in the cells with 30 min daily exposure to the 16 Hz ELF-PEMF. (**B**) Representative image of the Western blot. (**C**) Signal intensities were quantified with the ImageJ software and the ratio of phosphorylated-Smad2 to Smad2 and phosphorylated-Smad3 to Smad3 were determined. (**D**) SCP-1 cell migration was determined using the cell migration assay kit. Cells invading the migration zone were quantified using the ImageJ software. N = 3, *n* = 3. Data are presented as box plots (Min to Max with single data points). Data were compared by non-parametric two-way ANOVA followed by Tukey's multiple comparison test: * $p < 0.05$, ** $p < 0.01$, and *** $p < 0.001$ as indicated; $^{\#\#}$ $p < 0.01$ and $^{\#\#\#}$ $p < 0.001$ marking the ELF-PEMF effect.

2.5. ELF-PEMF Exposure Reversed CSE-Mediated Changes in Smad2, -3, and -7 Expression

In line with the Western blot results, gene expression of both *Smad2* and *Smad3* was significantly reduced in SCP-1 cells exposed to 5% CSE. The 30 min daily exposure to 16 Hz ELF-PEMF did not significantly affect the basal expression levels of *Smad2* and *Smad3*, but restored their expression in presence of 5% CSE (Figure 5A–C). As a regulator for TGF-β signaling, the expression levels of Smad7 were also determined. SCP-1 cells exposed to 5% CSE showed higher expression of the inhibitory *Smad7*. The 30 min daily exposure to 16 Hz ELF-PEMF did not alter the basal expression level of *Smad7*, but significantly reduced *Smad7* expression in presence of 5% CSE (Figure 5D).

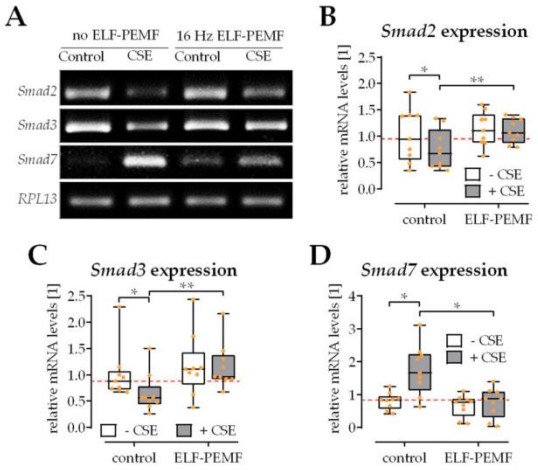

Figure 5. Gene expression of *Smads* is affected by exposure to 5% cigarette smoke extract (CSE) and 16 Hz ELF-PEMFs for 30 min daily for 3 days. (**A**) Representative RT-PCR images. Signal intensities were quantified with the ImageJ software. Expression of (**B**) *Smad2*, (**C**) *Smad3*, and (**D**) *Smad7* was normalized to *RPL13* (house-keeping gene). N = 3, *n* = 3. Data are presented as box plots (Min to Max with single data points). Data were compared by non-parametric two-way ANOVA followed by Tukey's multiple comparison test: * $p < 0.05$ and ** $p < 0.01$ as indicated.

2.6. The Structural Integrity of Primary Cilia Is Related to the Protective Effects of 16 Hz ELF-PEMFs

The primary cilium functions as the "antenna" in cells that can sense extracellular physical stimuli, e.g., ELF-PEMFs. During osteogenic differentiation, SCP-1 cells form primary cilia structures. The morphology and distribution of primary cilia were determined by the immunofluorescence staining (Figure 6A). Image analysis revealed that supplementing the differentiation medium with 5% CSE caused a significant drop in the amount of ciliated SCP-1 cells and a significant decrease in the average length of the primary cilia. A 30 min daily exposure for 5 days to 16 Hz ELF-PEMF significantly increased the number of ciliated cells and the length of the primary cilia, both in the presence or absence of the CSE (Figure 6B, Figure 6C).

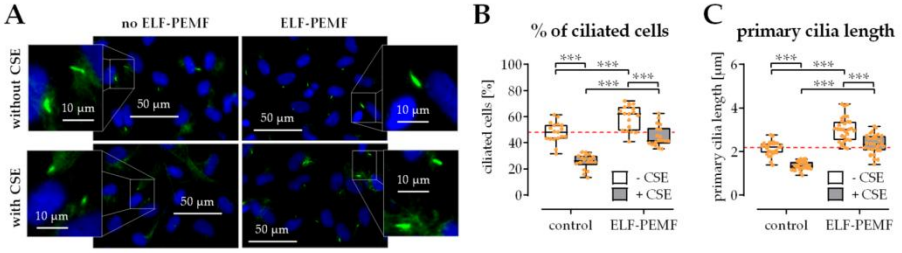

Figure 6. The structural integrity of primary cilia is affected by exposure to 5% cigarette smoke extract (CSE) and rescued by exposure to 16 Hz ELF-PEMFs for 5 days and 30 min daily. (**A**) Primary cilia were visualized by immunofluorescence staining for acetylated tubulin (green). Nuclei were counterstained with Hoechst 33342 (blue). Fluorescent images were analyzed with the ImageJ software, to determined (**B**) the amount of ciliated cells in percent and (**C**) the length of the primary cilia. N = 3, *n* = 3. Data are presented as box plots (Min to Max with single data points). Data were compared by non-parametric two-way ANOVA followed by Tukey's multiple comparison test: *** $p < 0.001$ as indicated.

3. Discussion

TGF-β is a key factor regulating the early phases of bone regeneration. The absence of the rise in TGF-β levels following a fracture is associated with a delayed or even impaired healing process [16]. It has been reported that smokers lack the rise in TGF-β levels expected following a fracture or orthopedic surgery [23,24]. Furthermore, CS was reported to harm the structural integrity of primary cilia by increasing oxidative stress [13], which in turn affects TGF-β signaling [1,18,19]. The data presented here provide evidence that exposure to 16 Hz ELF-PEMFs protects the structural integrity of the primary cilia and thus rescues TGF-β signaling in osteoprogenitor cells harmed by CSE. This way, 16 Hz ELF-PEMFs may support the early phases of bone regeneration. This is supported by a rodent study showing impaired fracture healing in mice with non-functional primary cilia [26]. In addition, a recent study showed that exposure to sinusoidal EMFs protected the rise in primary cilia structure and thus enhanced bone mineral density in rats, an effect attributed to the activation of BMP and Wnt signaling [27].

For almost half a decade, PEMFs were used in clinical settings to support bone regeneration. Addressing a complex repair process involving many components acting at different phases or time points, it has been a challenge to optimize PEMF exposure parameters (i.e., frequency of field, intensity of field, timing, and duration). Consequently, the physical parameters of the applied PEMFs varied on a large scale [9]. Despite being recognized as a safe and non-invasive physical treatment for bone diseases, the application of PEMFs could not yet be fully established in the clinical routine [28]. The present study utilized ELF-PEMFs with a fundamental frequency of 16 Hz (more details given in the Materials and Methods section). A screening approach identified ELF-PEMFs in this frequency range to best support the viability and differentiation of osteoprogenitor cells [12]. The effectiveness of the ELF-PEMF was confirmed in further studies, both in vitro and in vivo [25,29]. Comparing the effect on bone formation in this in vivo study [29] with other studies that used 4- to 200-times longer daily exposures revealed that increasing the exposure duration may enhance the observed effects [9]. Thus, in the present study, exposure duration was varied at first. Increasing the daily exposure from 7 min to 30 min could further improve viability, adhesion, spreading, and migration of SCP-1 cells. However, further elongation of the daily exposure duration reduced the observed positive effect of 16 Hz ELF-PEMF exposure on SCP-1 cells. It has been reported that repetitive exposure to this specific 16 Hz ELF-PEMF, induced anti-oxidative defense mechanisms in osteoprogenitor cells by formation of reactive oxygen species (ROS) [25]. It is possible that prolonged exposure to the 16 Hz ELF-PEMF causes an accumulation of ROS that becomes detrimental when reaching a certain level.

This is of special interest when this ELF-PEMF shall be used to support bone healing in patients with an already increased oxidative stress level, e.g., smokers. In vitro exposure to CSE significantly increases ROS levels in osteoprogenitor cells, affecting the cells' viability and function [4]. The viability, adhesion, spreading, and migration of osteoprogenitor cells are crucial for initiating bone regeneration after injury. Our data show that exposure to 5% CSE, which simulates smoking 10 cigarettes per day, significantly reduced the viability, adhesion, and migration of SCP-1 cells. Exposure to the 16 Hz ELF-PEMF improved the viability, adhesion, spreading, and migration of CSE-exposed SCP-1 cells. Daily exposure of 7 min (16 Hz ELF-PEMF) was sufficient to abrogate the damaging effects of the CSE exposure, when compared to control conditions. Daily exposure of 30 min (16 Hz ELF-PEMF) further ameliorated the effect, reaching levels above the control cells. Comparing the 16 Hz ELF-PEMF effects between the CSE and control group revealed that a longer duration of exposure was more effective in the control group. This might be another hint that prolonging the exposure time can cause accumulation of ROS, which more quickly reaches a threshold under stress conditions, e.g., with CSE.

As a possible regulatory mechanism, how CSE inhibits osteogenic function, CSE-dependent destruction of the cells' primary cilia was described [13], which impairs TGF-β signal transduction [1]. The importance of primary cilia for TGF-β signal transduction is highlighted with an in vivo study, which showed impaired fracture healing in mice lacking functional primary cilia in osteoprogenitor cells [30]. However, there are reports suggesting that PEMF therapy requires functional primary cilia on osteogenic cells to exert their effects [31,32]. The primary cilium is covered by many receptors required for initiating cell signaling [33,34]. PEMF exposure not only increases expression of such receptors, but also initiates their localization at the base of the primary cilium [31]. The pocket surrounding the base and proximal part of the primary cilium is a site for clathrin-dependent endocytosis, reported to regulate TGF-β signaling. The localization of the TGF-β receptors to the endocytotic vessels was reported to activate Smad2/3 and ERK1/2 (extracellular signal-regulated kinases 1 and 2) signaling at the ciliary base [18]. Our data show that SCP-1 cells with CSE-damaged primary cilia still respond to the 16 Hz ELF-PEMF exposure. It is described that primary cilia adapt their length in response to mechanical stimuli, which affects the mechanosensitivity of the cells. While the loss of primary cilia integrity is associated with reduced cell signaling [1,33], the lengthening of the microtubuli is reported to enhance cellular mechanosensitivity [35]. Our data revealed that exposure to 16 Hz ELF-PEMF elongated the primary cilia structures both in the presence or absence of the CSE. Therefore, enhanced cell signaling following the physical stimuli is expected.

TGF-β is robustly released from the bone matrix immediately after the bone fracture happens [36]. A temporal increase in TGF-β serum levels following a fracture is associated with successful fracture healing [16]. It has been reported that smokers lack this increase in TGF-β serum levels following a fracture or orthopedic surgery [23,24], which is thought to contribute to the delayed fracture healing in these patients. Thus, there is evidence that smokers with a fracture not only lack the required increase in TGF-β serum levels, but also that their osteoprogenitor cells may not adequately respond to the growth factor. In our experiment, exposure to CSE decreased the expression of *Smad2* and *Smad3*. Consequently, less Smad2 and Smad3 were phosphorylated. Exposure to CSE significantly lowered the ratio of phosphorylated Smad3 to Smad3, suggesting that CSE inhibits TGF-β signaling not only by inhibiting the expression of the regulator Smads, but also upstream before the phosphorylation of Smad3. The latter could be related to the structural integrity of the primary cilia, which regulate clathrin-dependent endocytosis reported to promote TGF-β-induced activation of Smads and transcriptional responses [37,38].

Several studies described that exposure to PEMFs significantly increases the expression of TGF-β in osteogenic cells both in vitro and in vivo [39]. However, little is known about the underlying mechanisms. One study proposed that increased expression of TGF-β in PEMF-treated MSCs is facilitated by an increase in miRNA-21, which suppresses the expression of the inhibitory *Smad7* [40]. This could explain our findings, which show decreased expression of *Smad7* in SCP-1 cells exposed to 16 Hz ELF-PEMFs. Other well-reported target genes of miRNA-21 include *TGFβR*, the PI3K inhibitor *PTEN*, and the ERK1/2 inhibitor *Spry* [41]. The latter is in accordance with our finding that the positive effect of 16 Hz ELF-PEMF stimulation on osteoprogenitor cells requires activation of ERK1/2 signaling [12].

4. Materials and Methods

If not cited differently, chemicals, media and medium supplements were purchased from Sigma-Aldrich, which is now part of Merck (Darmstadt, GER).

4.1. Cell Culture

The human-immortalized mesenchymal stem cell line SCP-1 was used in this study. SCP-1 cells were provided by Professor Matthias Schieker. SCP-1 cells were cultured in

α-MEM medium (Gibco, Darmstadt, Germany) supplemented with 5% fetal bovine serum (FBS) in a water-saturated atmosphere of 5% CO_2 at 37 °C. For osteogenic differentiation, SCP-1 cells at a confluence of 90% were cultured in an osteogenic differentiation medium (α-MEM medium supplemented with 1% FBS, 200 µM L-ascorbate-2-phosphate, 5 mM β-glycerol-phosphate, 25 mM HEPES, 1.5 mM $CaCl_2$, and 100 nM dexamethasone). The culture medium was changed twice a week.

4.2. ELF-PEMF Device and Exposure

The ELF-PEMF devices (Somagen®), provided by the Sachtleben GmbH (Hamburg, Germany), are medical devices certified according to European law (CE 0482, compliant with EN ISO 13485:2016 + EN ISO 14971:2012). The ELF-PEMFs applied in this study have a fundamental frequency of 16 Hz and an intensity of 6-282 µT (B field amplitude 6 mm above the applicator), which is emitted as groups of pulses (bursts) in sending–pause intervals [12]. The daily ELF-PEMF exposure was 7, 30, or 90 min.

The device applicators distort the local earth magnetic field due to a magnetic foil in the panels. This leads to an inhomogeneous local earth magnetic field (DC), which superpositions with the alternating magnetic field (AC) of the applicator coil. The AC field corresponds here to the ELF-PEMF. The magnetic field is defined by

$$\vec{B}_{DC} = \left(B_{DC,x}, B_{DC,y}, B_{DC,z}\right)^{\tau} \quad (1)$$

$$\vec{B}_{AC}(\vec{r},t) = \left(B_{AC,x}(\vec{r},t), B_{AC,y}(\vec{r},t), B_{AC,z}(\vec{r},t)\right)^{\tau} \quad (2)$$

which leads to the total magnetic field

$$\vec{B}_{total}(\vec{r},t) = \vec{B}_{DC} + \vec{B}_{AC}(\vec{r},t), \quad (3)$$

which is finally exposed to the cells.

The AC magnetic field of the applicator coil shows a common dipole characteristic and vanishes very fast with distance (Figure 7).

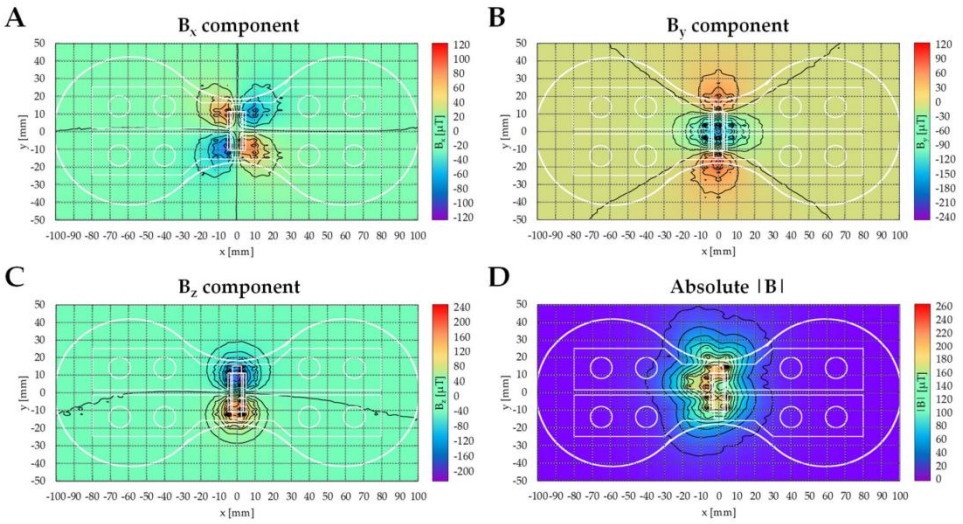

Figure 7. The AC magnetic field distribution of the applicator coil for all 3 directions and the absolute field approximately 4 mm above the coil. Heat maps summarize the distribution of the magnetic flux density: (**A**) B_x component, (**B**) B_y

component, (**C**) B_z component, and (**D**) absolute |B|. The measurement was taken with the recalibrated 3 axes PNI RM3100 sensor for a constant current (I = 0.1A) after subtracting the local earth magnetic field (I = 0A).

4.3. Cigarette Smoke Extract (CSE) Preparation

To generate the CSE, the smoke of cigarettes (Marlboro, Philip Morris, New York, NY, USA) was bubbled through a plain α-MEM culture medium at a speed of 100 bubbles/min. The concentration of the CSE solution was evaluated photometrically at 320 nm. An optical density (OD) of 0.7 was considered as 100% CSE. After being filtered and mixed with the culture medium, 5% CSE (which is considered as smoking 10 cigarettes per day) was used in this study [42].

4.4. Cell Viability

Cell viability was quantified by sulforhodamine B (SRB) staining, which was used to determine the total protein content. In detail, SCP-1 cells were fixed with ice-cold 99% ethanol (–20 °C) for 1 h. Subsequently, cells were washed 3 times with PBS and stained with SRB staining solution (0.4% SRB in 1% acetic acid, Sigma-Aldrich, Germany) for 30 min at room temperature. Then, cells were washed 4 to 5 times with 1% acetic acid to remove unbound SRB. For quantification, the bound SRB was resolved with 10 mM unbuffered TRIS solution (pH ~ 10.5). The OD was measured with a microplate reader at 565 nm–690 nm[4].

4.5. Live Staining and Cytoskeleton Staining

Calcein-AM staining was performed to determine cell viability. Briefly, cells were washed 3 times with PBS and subsequently incubated with Calcein-AM (2 µM) and Hoechst 33342 (2 µg/mL) in plain medium at 37 °C for 30 min. Images of cells were taken with a fluorescence microscope (EVOS FL, life technologies, Darmstadt, Germany). To explore cell adhesion and morphological changes, the cytoskeleton of the SCP-1 cells was stained with phalloidin-TRITC. Cells were fixed with 4% formaldehyde at room temperature for 10 min, actin cytoskeleton was stained with phalloidin-TRITC (2 ng/mL), and nuclei were counter-stained with Hoechst 33342 (2 ng/mL) for 30 min at room temperature. After washing with PBS, images were taken with a fluorescence microscope and quantified with the ImageJ software [13].

4.6. Cell Migration Assay

Cell migration was evaluated by using the cell migration assay kit (Tebu-bio, Offenbach, Germany). Sterilized stoppers were placed in 96-well plates. Then, SCP-1 cells were seeded around the inserts at a concentration of 4×10^4 cells/well in a growth medium. After 24 h, the stoppers were removed from the wells, and the cells were washed 3 times with PBS. Then, the growth medium was replaced by an osteogenic differentiation medium with or without stimuli (ELF-PEMF, CSE, and TGF-β). Immediately, an image was taken with the microscope to document time point 0. After 72 h, SCP-1 cells were stained with SRB for better visualization. Microscopic images were analyzed with the ImageJ software and the "gap closure" was calculated.

4.7. Immunofluorescent (IF) Staining for Primary Cilia

SCP-1 cells were fixed with a 4% formaldehyde solution for 10 min at room temperature, then incubated with 0.2% Triton-X-100 for 10 min, and subsequently with 2% formaldehyde for 10 min. After that, cells were blocked with 5% bovine serum albumin (BSA, Carl Roth, Darmstadt, Germany) for 1 h. Then, cells were incubated with primary antibody solution (acetylated α-tubulin, 1:100, Santa Cruz, Heidelberg, Germany) overnight at 4 °C. The next day, cells were washed with PBS and incubated with Alexa-488 labeled secondary antibody (1:2000, Invitrogen, Karlsruhe, Germany) and Hoechst 33342

(2 ng/mL) for 2 h. Fluorescent images were taken with a fluorescence microscope (200- or 400-fold magnification) and analyzed with the ImageJ software [13].

4.8. Transient Cells Infection and Reporter Assay

Adenoviral reporter constructs (Smad2/3 reporter, Ad5-CAGA9-MLP-Luc, 1:10 v/v) [1] were used to infect SCP-1 cells. After 24 h, cells were washed with PBS, and treated with or without 5% CSE (in the osteogenic differentiation medium) for 72 h. After 24 h, cells were additionally stimulated with 10 ng/mL recombinant human TGF-β1 for 48 h. Finally, cells were lysed with a lysis buffer (Luciferase substrate kit, Promega, Madison, USA); 20 µl cell lysate was mixed with 20 µl luciferase substrate, and the luminescent signal was detected immediately with the microplate reader. The luminescence was normalized to the total protein content, determined by micro Lowry [43].

4.9. Conventional RT-PCR

Reverse transcription polymerase chain reaction (RT-PCR) was used to evaluate the expression of genes involved in the TGF-β signaling pathway. In brief, RNA was isolated by Phenol–Chloroform extraction. The cDNA synthesis kit (Fermentas, St. Leo-Rot, Germany) was used to synthesize the first-strand cDNA. Primer sequences and PCR parameters are summarized in Table 1. The products of RT-PCR were subjected to a 2% (w/v) agarose gel electrophoresis with ethidium bromide, and the results were analyzed by using ImageJ software.

Table 1. Primer information.

target gene	Gene Bank accession number	Forward Primer (5′–3′)	Reverse Primer (5′–3′)	amplicon size [bp]	Ta [°C]	number of cycles
Smad2	NM_001003652.3	CAAACCAGGTCTCTTGATGG	GAGGCGGAAGTTCTGTTAGG	259	60	35
Smad3	NM_005902.2	GGAGAAATGGTGCGAGAAGG	GAAGGCGAACTCACACAGC	259	60	35
Smad7	NM_005904.1	TTCGGACAACAAGAGTCAGC	AAGCCTTGATGGAGAAACC	200	60	35
RPL13	NM_012423.3	AAGTACCAGGCAGTGACAG	CCTGTTTCCGTAGCCTCATG	100	56	30

4.10. Western Blot

To harvest total protein, cells were lysed in ice-cold RIPA buffer (50 mM TRIS, 250 mM NaCl, 2% NP40, 2.5 mM EDTA, 0.1% SDS, 0.5% DOC, and protease/phosphatase inhibitors: 1 µg/mL pepstatin, 5 µg/mL leupeptin, 1 mM PMSF, 5 mM NaF, and 1 mM Na_3VO_4) and the lysate was centrifuged (3000×g, 10 min) to remove cell debris. The protein concentration was measured by micro Lowry [43]; 25 µg of total protein were separated by SDS-PAGE (10% acrylamide-bisacrylamide gels, 100 V, 180 min) and subsequently transferred to nitrocellulose membranes (100 mA, 180 min). Protein separation and transfer were checked by Ponceau staining; 5% BSA was used to block the unspecific binding sites. Membranes were incubated with primary antibodies against p-Smad2, p-Smad3, Smad2/3 (all 1:1,000, sc-133098, sc-517575 from Santa Cruz Biotechnology, Heidelberg, Germany and 3108 from Cell Signaling Technologies, Danvers, MA, USA), and GAPDH (1:5,000, G9545 from Sigma-Aldrich, Munich, Germany) diluted in TBST, overnight at 4 °C. Subsequently, membranes were incubated with the corresponding HRP-labeled secondary antibodies (1:10,000 in TBST) for 2 h at room temperature. Membranes were covered with enhanced chemiluminescent substrate solution (1.25 mM luminol, 0.2 mM p-coumaric acid, 0.03% H_2O_2 in 100 mM TRIS, pH=8.5) and a CCD camera was used to detect the chemiluminescent signals. Signal intensities were determined with the ImageJ software.

4.11. Statistical Analysis

Results are displayed as mean ± SEM. Data were analyzed with two-way ANOVA followed by Tukey's multiple comparison test using the GraphPad Prism software (El Camino Real, USA); $p < 0.05$ was considered as statistically significant.

5. Conclusions

In line with the literature, our data show that 5% CSE, which is equivalent to smoking 10 cigarettes per day, negatively affects the viability, adhesion, spreading, migration, and differentiation of SCP-1 cells. Daily exposure to 16 Hz ELF-PEMFs partly reversed the negative effect of the CSE, especially when the duration of the daily exposure was increased from 7 min to 30 min, but not longer. As a possible regulatory mechanism, an ELF-PEMF-mediated rescue of the primary cilia structure and the amount of ciliated cells was identified. This, in turn, was associated with a fortification of the canonical (Smad2/3) TGF-β signaling and a decreased expression of *Smad7*. In summary, our data suggest that 30 min daily exposure to the 16 Hz ELF-PEMF can be used as an adjunct therapy to support early fracture healing in smokers, who frequently have to struggle with delayed or impaired fracture healing.

Supplementary Materials: The following are available online at www.mdpi.com/article/10.3390/ijms22137036/s1, Figure S1: title, Table S1: title, Video S1: title

Author Contributions: Conceptualization, S.E.; methodology, Y.C., R.H.A.-W., and S.E.; software, M.R., A.K.N., and T.H.; validation, S.E.; formal analyses, Y.C.; investigation, Y.C.; resources, M.M.M., K.F., A.K.N., and T.H.; data curation, C.S. and S.E.; writing—original draft preparation, Y.C. and S.E.; writing—review and editing, all authors; visualization, M.R. and S.E.; supervision, S.E. and A.K.N.; project administration, A.K.N.; funding acquisition, A.K.N. and S.E.; All authors have read and agreed to the published version of the manuscript.

Funding: S.E. received funding from the German Research Foundation (DFG EH 471/2). Y.C. received support from the China Scholarship Council to cover his living expenses.

Institutional Review Board Statement: Not required for work with cell lines.

Informed Consent Statement: Not applicable.

Data Availability Statement: The datasets generated during and/or analyzed during the current study are available from the corresponding author on reasonable request.

Acknowledgments: We would like to thank Sachtleben GmbH which provided the ELF-PEMF devices (Somagen®) and the background on the physical parameters. We would like to thank M. Schieker, who provided us the SCP-1 cells. The data presented in this manuscript were obtained during the Ph.D. work of Y.C. and R.H.A.-W. We would like to thank Bianca Braun and Regina Breinbauer for their excellent technical assistance.

Conflicts of Interest: The authors declare no conflict of interest. Sachtleben GmbH provided the ELF-PEMF devices (Somagen®) and the background on the physical parameters, but were not involved in the study design or the data evaluation.

Abbreviations:

CS	cigarette smoking
CSE	cigarette smoke extract
ELF-PEMF	extremely low frequency pulsed electromagnetic field
EtOH	ethanol
ERK1/2	extracellular signal-regulated kinases 1 and 2
MSCs	mesenchymal stem cells
PI3K	phosphoinositide 3-kinase
ROS	reactive oxygen species
SRB	Sulforhodamine B
TRITC	tetramethylrhodamine

References

1. Aspera-Werz, R.H.; Chen, T.; Ehnert, S.; Zhu, S.; Frohlich, T.; Nussler, A.K. Cigarette Smoke Induces the Risk of Metabolic Bone Diseases: Transforming Growth Factor Beta Signaling Impairment via Dysfunctional Primary Cilia Affects Migration, Proliferation, and Differentiation of Human Mesenchymal Stem Cells. *Int. J. Mol. Sci.* **2019**, *20*, 2915.
2. Deng, Y.; Cao, H.; Cu, F.; Xu, D.; Lei, Y.; Tan, Y.; Magdalou, J.; Wang, H.; Chen, L. Nicotine-induced retardation of chondrogenesis through down-regulation of IGF-1 signaling pathway to inhibit matrix synthesis of growth plate chondrocytes in fetal rats. *Toxicol. Appl. Pharmacol.* **2013**, *269*, 25–33.
3. Cheng, Y.; Gu, W.; Zhang, G.; Li, X.; Guo, X. Activation of Notch1 signaling alleviates dysfunction of bone marrow-derived mesenchymal stem cells induced by cigarette smoke extract. *Int. J. Chronic Obstr. Pulm. Dis.* **2017**, *12*, 3133–3147.
4. Aspera-Werz, R.H.; Ehnert, S.; Heid, D.; Zhu, S.; Chen, T.; Braun, B.; Sreekumar, V.; Arnscheidt, C.; Nussler, A.K. Nicotine and Cotinine Inhibit Catalase and Glutathione Reductase Activity Contributing to the Impaired Osteogenesis of SCP-1 Cells Exposed to Cigarette Smoke. *Oxid. Med. Cell Longev.* **2018**, *2018*, 3172480.
5. Li, H.Q.; Wallin, M.; Barregard, L.; Sallsten, G.; Lundh, T.; Ohlsson, C.; Mellstrom, D.; Andersson, E.M. Smoking-Induced Risk of Osteoporosis Is Partly Mediated by Cadmium From Tobacco Smoke: TheMrOSSweden Study. *J. Bone Miner. Res.* **2020**, *35*, 1424–1429.
6. Tamaki, J.; Iki, M.; Fujita, Y.; Kouda, K.; Yura, A.; Kadowaki, E.; Sato, Y.; Moon, J.S.; Tomioka, K.; Okamoto, N.; et al. Impact of smoking on bone mineral density and bone metabolism in elderly men: The Fujiwara-kyo Osteoporosis Risk in Men (FORMEN) study. *Osteoporos. Int.* **2011**, *22*, 133–141.
7. Scolaro, J.A.; Schenker, M.L.; Yannascoli, S.; Baldwin, K.; Mehta, S.; Ahn, J. Cigarette smoking increases complications following fracture: A systematic review. *J. Bone Joint Surg. Am.* **2014**, *96*, 674–681.
8. Kaku, M.; Komatsu, Y. Functional Diversity of Ciliary Proteins in Bone Development and Disease. *Curr. Osteoporos. Rep.* **2017**, *15*, 96–102.
9. Ehnert, S.; Schroter, S.; Aspera-Werz, R.H.; Eisler, W.; Falldorf, K.; Ronniger, M.; Nussler, A.K. Translational Insights into Extremely Low Frequency Pulsed Electromagnetic Fields (ELF-PEMFs) for Bone Regeneration after Trauma and Orthopedic Surgery. *J. Clin. Med.* **2019**, *8*, 2028.
10. Yasuda, I. Classic Fundamental Aspects of Fracture Treatment. *Clin. Orthop. Relat. Res.* **1977**, *124*, 5–8.
11. Bhandari, M.; Fong, K.; Sprague, S.; Williams, D.; Petrisor, B. Variability in the definition and perceived causes of delayed unions and nonunions: A cross-sectional, multinational survey of orthopaedic surgeons. *J. Bone Joint Surg. Am.* **2012**, *94*, e1091–e1096.
12. Ehnert, S.; Falldorf, K.; Fentz, A.K.; Ziegler, P.; Schroter, S.; Freude, T.; Ochs, B.G.; Stacke, C.; Ronniger, M.; Sachtleben, J.; et al. Primary human osteoblasts with reduced alkaline phosphatase and matrix mineralization baseline capacity are responsive to extremely low frequency pulsed electromagnetic field exposure—Clinical implication possible. *Bone Rep.* **2015**, *3*, 48–56.
13. Sreekumar, V.; Aspera-Werz, R.; Ehnert, S.; Strobel, J.; Tendulkar, G.; Heid, D.; Schreiner, A.; Arnscheidt, C.; Nussler, A.K. Resveratrol protects primary cilia integrity of human mesenchymal stem cells from cigarette smoke to improve osteogenic differentiation in vitro. *Arch. Toxicol.* **2018**, *92*, 1525–1538.
14. Jacobs, C.R.; Temiyasathit, S.; Castillo, A.B. Osteocyte mechanobiology and pericellular mechanics. *Annu. Rev. Biomed. Eng.* **2010**, *12*, 369–400.
15. Seeger-Nukpezah, T.; Golemis, E.A. The extracellular matrix and ciliary signaling. *Curr. Opin. Cell Biol.* **2012**, *24*, 652–661.
16. Zimmermann, G.; Moghaddam, A.; Reumann, M.; Wangler, B.; Breier, L.; Wentzensen, A.; Henle, P.; Weiss, S. TGF-beta1 as a pathophysiological factor in fracture healing. *Unfallchirurg* **2007**, *110*, 130–136.
17. Ehnert, S.; Sreekumar, V.; Aspera-Werz, R.H.; Sajadian, S.O.; Wintermeyer, E.; Sandmann, G.H.; Bahrs, C.; Hengstler, J.G.; Godoy, P.; Nussler, A.K. TGF-beta(1) impairs mechanosensation of human osteoblasts via HDAC6-mediated shortening and distortion of primary cilia. *J. Mol. Med.* **2017**, *95*, 653–663.
18. Clement, C.A.; Ajbro, K.D.; Koefoed, K.; Vestergaard, M.L.; Veland, I.R.; Henriques de Jesus, M.P.; Pedersen, L.B.; Benmerah, A.; Andersen, C.Y.; Larsen, L.A.; et al. TGF-beta signaling is associated with endocytosis at the pocket region of the primary cilium. *Cell Rep.* **2013**, *3*, 1806–1814.
19. Alvarez-Satta, M.; Lago-Docampo, M.; Bea-Mascato, B.; Solarat, C.; Castro-Sanchez, S.; Christensen, S.T.; Valverde, D. ALMS1 Regulates TGF-beta Signaling and Morphology of Primary Cilia. *Front. Cell Dev. Biol.* **2021**, *9*, 623829.
20. Crane, J.L.; Cao, X. Bone marrow mesenchymal stem cells and TGF-beta signaling in bone remodeling. *J. Clin. Investig.* **2014**, *124*, 466–472.
21. Majidinia, M.; Sadeghpour, A.; Yousefi, B. The roles of signaling pathways in bone repair and regeneration. *J. Cell Physiol.* **2018**, *233*, 2937–2948.
22. Ehnert, S.; Linnemann, C.; Aspera-Werz, R.H.; Bykova, D.; Biermann, S.; Fecht, L.; De Zwart, P.M.; Nussler, A.K.; Stuby, F. Immune Cell Induced Migration of Osteoprogenitor Cells Is Mediated by TGF-beta Dependent Upregulation of NOX4 and Activation of Focal Adhesion Kinase. *Int. J. Mol. Sci.* **2018**, *19*, 2239.
23. Ehnert, S.; Aspera-Werz, R.H.; Ihle, C.; Trost, M.; Zirn, B.; Flesch, I.; Schroter, S.; Relja, B.; Nussler, A.K. Smoking Dependent Alterations in Bone Formation and Inflammation Represent Major Risk Factors for Complications Following Total Joint Arthroplasty. *J. Clin. Med.* **2019**, *8*, 406.
24. Moghaddam, A.; Weiss, S.; Wolfl, C.G.; Schmeckenbecher, K.; Wentzensen, A.; Grutzner, P.A.; Zimmermann, G. Cigarette smoking decreases TGF-b1 serum concentrations after long bone fracture. *Injury* **2010**, *41*, 1020–1025.

25. Ehnert, S.; Fentz, A.-K.; Schreiner, A.; Birk, J.; Wilbrand, B.; Ziegler, P.; Reumann, M.K.; Wang, H.; Falldorf, K.; Nussler, A.K. Extremely low frequency pulsed electromagnetic fields cause antioxidative defense mechanisms in human osteoblasts via induction of *O2(-) and H2O2. *Sci. Rep.* **2017**, *7*, 14544.
26. Qiu, N.; Xiao, Z.; Cao, L.; Buechel, M.M.; David, V.; Roan, E.; Quarles, L.D. Disruption of Kif3a in osteoblasts results in defective bone formation and osteopenia. *J. Cell Sci.* **2012**, *125*, 1945–1957.
27. Zhou, J.; Gao, Y.H.; Zhu, B.Y.; Shao, J.L.; Ma, H.P.; Xian, C.J.; Chen, K.M. Sinusoidal Electromagnetic Fields Increase Peak Bone Mass in Rats by Activating Wnt10b/beta-Catenin in Primary Cilia of Osteoblasts. *J. Bone Miner. Res.* **2019**, *34*, 1336–1351.
28. Daish, C.; Blanchard, R.; Fox, K.; Pivonka, P.; Pirogova, E. The Application of Pulsed Electromagnetic Fields (PEMFs) for Bone Fracture Repair: Past and Perspective Findings. *Ann. Biomed. Eng.* **2018**, *46*, 525–542.
29. Ziegler, P.; Nussler, A.K.; Wilbrand, B.; Falldorf, K.; Springer, F.; Fentz, A.K.; Eschenburg, G.; Ziegler, A.; Stockle, U.; Maurer, E.; et al. Pulsed Electromagnetic Field Therapy Improves Osseous Consolidation after High Tibial Osteotomy in Elderly Patients-A Randomized, Placebo-Controlled, Double-Blind Trial. *J. Clin. Med.* **2019**, *8*, 2008.
30. Liu, M.; Alharbi, M.; Graves, D.; Yang, S. IFT80 Is Required for Fracture Healing Through Controlling the Regulation of TGF-beta Signaling in Chondrocyte Differentiation and Function. *J. Bone Miner. Res.* **2020**, *35*, 571–582.
31. Xie, Y.-F.; Shi, W.G.; Zhou, J.; Gao, Y.-H.; Li, S.-F.; Fang, Q.-Q.; Wang, M.-G.; Ma, H.-P.; Wang, J.-F.; Xian, C.J.; et al. Pulsed electromagnetic fields stimulate osteogenic differentiation and maturation of osteoblasts by upregulating the expression of BMPRII localized at the base of primary cilium. *Bone* **2016**, *93*, 22–32.
32. Yan, J.-L.; Zhou, J.; Ma, H.-P.; Ma, X.-N.; Gao, Y.-H.; Shi, W.-G.; Fang, Q.-Q.; Ren, Q.; Xian, C.J.; Chen, K.-M. Pulsed electromagnetic fields promote osteoblast mineralization and maturation needing the existence of primary cilia. *Mol. Cell Endocrinol.* **2015**, *404*, 132–140.
33. Pala, R.; Alomari, N.; Nauli, S.M. Primary Cilium-Dependent Signaling Mechanisms. *Int. J. Mol. Sci.* **2017**, *18*, 2272.
34. Hua, K.; Ferland, R.J. Primary cilia proteins: Ciliary and extraciliary sites and functions. *Cell Mol. Life Sci.* **2018**, *75*, 1521–1540.
35. Spasic, M.; Jacobs, C.R. Lengthening primary cilia enhances cellular mechanosensitivity. *Eur. Cell Mater.* **2017**, *33*, 158–168.
36. Horiguchi, M.; Ota, M.; Rifkin, D.B. Matrix control of transforming growth factor-beta function. *J. Biochem.* **2012**, *152*, 321–329.
37. Chen, Y.G. Endocytic regulation of TGF-beta signaling. *Cell Res.* **2009**, *19*, 58–70.
38. Pedersen, L.B.; Mogensen, J.B.; Christensen, S.T. Endocytic Control of Cellular Signaling at the Primary Cilium. *Trends Biochem. Sci.* **2016**, *41*, 784–797.
39. Yuan, J.; Xin, F.; Jiang, W. Underlying Signaling Pathways and Therapeutic Applications of Pulsed Electromagnetic Fields in Bone Repair. *Cell Physiol. Biochem.* **2018**, *46*, 1581–1594.
40. Selvamurugan, N.; He, Z.; Rifkin, D.; Dabovic, B.; Partridge, N.C. Pulsed Electromagnetic Field Regulates MicroRNA 21 Expression to Activate TGF-beta Signaling in Human Bone Marrow Stromal Cells to Enhance Osteoblast Differentiation. *Stem Cells Int.* **2017**, *2017*, 2450327.
41. Liu, R.H.; Ning, B.; Ma, X.E.; Gong, W.M.; Jia, T.H. Regulatory roles of microRNA-21 in fibrosis through interaction with diverse pathways (Review). *Mol. Med. Rep.* **2016**, *13*, 2359–2366.
42. Su, Y.; Han, W.; Giraldo, C.; De Li, Y.; Block, E.R. Effect of cigarette smoke extract on nitric oxide synthase in pulmonary artery endothelial cells. *Am. J. Respir. Cell Mol. Biol.* **1998**, *19*, 819–825.
43. Lowry, O.H.; Rosebrough, N.J.; Farr, A.L.; Randall, R.J. Protein measurement with the Folin phenol reagent. *J. Biol. Chem.* **1951**, *193*, 265–275.

2.3 Intermittent Exposure to 16 Hz ELF-PEMF Improves Osteogenesis Through Activating Piezo1-induced Ca^{2+} Influx

(Chen, Y.; Menger, MM.; Braun, BJ.; Falldorf, K.; Ronniger, M.; Histing, T.; Nussler, AK.; Ehnert, S.; in preparation)

2.3.1 Summary and Major Findings

The use of ELF-PEMF is recognized as a promising adjuvant treatment to stabilize bone metabolism and support bone healing. Our previous study proved that exposure to 16 Hz ELF-PEMF effectively promoted new bone formation and that prolonging the exposure time from 7 min to 30 min enhanced this effect. The aim of this study was to further optimize the exposure strategy to improve the therapeutic effects while exploring the underlying molecular mechanisms. Therefore, we divided the daily continuous exposure (30 min/day) into intermittent exposure (10 min every 8 h) and compared the influence of these treatments on SCP-1 cells. The results showed that intermittent exposure exhibited stronger effects than continuous exposure in improving the cell viability and osteogenesis of SCP-1 cells. To explore the molecular mechanism responsible for this effect, we investigated the expression and function of the mechanosensitive and voltage gated calcium channel piezo1. Intermittent exposure to ELF-PEMF not only upregulated the expression of *piezo1*, but also activated piezo1 to induce greater calcium ion influx into SCP-1 cells. In summary, intermittent exposure is a promising exposure strategy for ELF-PEMF to promote new bone formation.

This study further achieved project **aims 1, 2, 4, and 5**. Our work illustrated that intermittent exposure to 16 Hz ELF-PEMF is a better strategy to promote new bone formation than longer duration, continuous exposure to 16 Hz ELF-PEMF. Our data further showed that exposure to 16 Hz ELF-PEMF induced the expression and activation of piezo1 and consequently stimulated Ca^{2+} influx. Therefore, the application of ELF-PEMF as an adjuvant treatment may provide patients with a convenient, low cost, and home implemented option to improve their bone state.

Limitations and next steps: In addition to some well-known parameters, *e.g.*, frequency and intensity, this study clarified that the exposure strategy, *i.e.*, intermittent exposure *versus* continuous exposure, is also an important factor that can influence the therapeutic effects of ELF-PEMF treatment. Although the data on piezo1 expression and activation could be clearly confirmed by using agonists and

antagonists, it cannot be excluded that other ion channels may be activated by ELF-PEMF exposure. Thus, more potential mechanisms as to how ELF-PEMF exposure affects osteogenic cells shall be investigated in the future.

2.3.2 Personal Contribution

I was the main person who designed the experiments, and performed most of the assays and experiments in this study. I also performed the data analysis and visualization, and I prepared the original draft of the manuscript.

2.3.3 Introduction

Bone homeostasis is a dynamic process strongly affected by external mechanical stimuli. The lack of proper mechanical stimuli caused by prolonged bed rest, immobility, or microgravity, usually leads to skeletal fragility, osteopenia, or osteoporosis. For example, patients with disuse osteoporosis lack proper external stimuli, thus inhibiting osteoblastic differentiation and disrupting bone homeostasis (Sasaki *et al.*, 2020). To improve bone mineral density (BMD) in these patients, it is necessary to restore suitable stimuli. *e.g.*, by applying ELF-PEMF (Chen *et al*., 2021).

In the last century, the German anatomist and surgeon Julius Wolff reported the association between bone remolding and mechanical stimuli, known as “Wolff’s law”. In the meantime, Antonsson *et al.* determined that normal walking induced mechanical forces with a frequency of approximately 15 Hz on the human skeletal system (Antonsson and Mann, 1985). In a previous study screening different ELF-PEMF in a frequency range from 10 Hz to 90.6 Hz , it was found that exposure to 16 Hz ELF-PEMF strongly promoted mineral deposition *in vitro* (Ehnert *et al.*, 2015), and enhanced osseous consolidation *in vivo* (Ziegler *et al.*, 2019). Therefore, applying 16 Hz ELF-PEMF to restore mechanical stimuli on the skeleton could be an effective, non-invasive, and convenient therapy for patients with (disuse) osteoporosis. However, application of ELF-PEMF is currently limited by, *i.e.*, 1) the short exposure duration, which may not reach desirable therapeutic effects *i.e.*, 30 min daily exposure is better than 7 min daily exposure (Chen *et al*., 2021); 2) the immobilization caused by prolonged exposure might lead to other complications, *e.g.*, bedsores, deep venous thrombosis (DVT), or pendant pneumonia (Tu *et al.*, 2020). To solve this challenge, this study aimed at optimizing the exposure strategy for ELF-PEMF treatment along with an improved therapeutic effect for osteoporosis patients.

In our previous study, we found that 7 min daily exposure to 16 Hz ELF-PEMF induced anti-oxidative defense mechanisms (Ehnert *et al.*, 2017) and mineral deposition in exposed cells (Ehnert *et al*., 2015). Furthermore, it was demonstrated that prolonging the daily ELF-PEMF exposure from 7 min to 30 min had a protective effect on osteoprogenitor cells *in vitro* (Chen *et al.*, 2021). However, considering that prolonged daily exposure might reduce patient compliance to this therapy, we intended to define a compromise strategy, which could be the division of 30 min of continuous exposure per day into shorter phases, referred to here as intermittent exposure (10 min every 8 h).

Apparently, as far as we observed the exposure strategy is essential, but its influences on the therapeutic effects of ELF-PEMF have often been neglected. To contribute to our understanding of the mechanism and optimization of the exposure strategy, this study aimed to investigate the influences of intermittent 16 Hz ELF-PEMF exposure on piezo1 expression and activity. Piezo1, which was originally defined as a mechanosensitive Ca^{2+} channel (Yoneda *et al.*, 2019), also shows voltage sensitivity (Kaestner *et al.*, 2020). Piezo1 is located on the plasma membrane of osteoblasts to transfer mechanical stimuli from the environment to osteoblasts by regulating Ca^{2+} influx. A recent study reported that piezo1 is highly expressed in the presence of mechanical stimuli, *e.g.,* low-intensity pulsed ultrasound (Zhang *et al.*, 2021) and fluid shear stress (Li *et al.*, 2019). Upregulation of piezo1 has been reported to promote fracture healing, while piezo1 deficiency is highly correlated with osteoporosis (Sun *et al.*, 2019). These studies emphasize the importance of piezo1 expression and activity in regulating bone regeneration.

Therefore, this study aimed at exploring if intermittent ELF-PEMF exposure could further improve cell viability and mineral deposition in SCP-1 cells as compared with continuous ELF-PEMF exposure. Furthermore, it was analyzed whether piezo1-induced Ca^{2+} influx is involved in this process.

2.3.4 Materials and Methods

Most of the materials and methods of this work, which is currently in preparation for submission, were used in the other manuscripts included in this cumulative thesis:

Materials and Methods	Refer to
Culture and differentiation of SCP-1 cells	4.1 cell culture; page 55
Sulforhodamine B (SRB) viability	4.4 cell viability; page 57
Calcein-AM staining	4.5 live staining and cytoskeletal staining; page 57

Only those methods newly established for this study are provided separately:

2.3.4.1 ELF-PEMF Device and Exposure

The 16 Hz ELF-PEMF generator (Somagen®) and ELF-PEMF incubator system were kindly provided by Sachtleben GmbH (Hamburg, Germany). The application and

maintenance strictly followed the manufacturer's instructions. Two ELF-PEMF exposure strategies were used in this study: (1) continuous exposure: 30 min of daily exposure without break; (2) intermittent exposure: 10 min of exposure every 8 h.

2.3.4.2 qRT-PCR

The total RNA of SCP-1 cells was isolated in the fume hood by phenol-chloroform extraction. The resulting RNA pellets were resuspended in DEPC water. The concentration and purity of the RNAs were determined photometrically, and the integrity of the RNAs was checked by performing agarose gel electrophoresis. Intact RNA was converted into cDNA with a commercial cDNA synthesis kit (Thermo Fisher Scientific, Sindelfingen, Germany) (Chen *et al*., 2021). qRT-PCR was performed using a Green Master Mix (Cat# M3052, Ulm, Germany). The relative gene expression of *piezo1* was calculated by using the $2^{-\Delta\Delta CT}$ method (Rao *et al.*, 2013). Information on the primers used in this study is shown in Table 1.

Table 1. Primer information

Gene	*GenBank ID*	*Forward primer*	*Reverse primer*	*T_a [°C]*
Piezo1	NM_001142864.4	ACCAACCTCATCAGCGACTT	AACAGGTATCGGAAGACGGC	*56*
EF1α	NM_001402.5	CCCCGACACAGTAGCATTTG	TGACTTTCCATCCCTTGAACC	*56*

2.3.4.3 Measurement of Intracellular Calcium Ions

SCP-1 cells were loaded with 4 µM Fluo-8 AM (ab142773, Abcam, Berlin, GER) at 37°C for 1.5 h in the dark. Then, SCP-1 cells were gently washed with PBS and incubated in a medium containing 1.5 mM $CaCl_2$. For each group, time-lapse fluorescence serial (every 30 seconds) images of intracellular calcium $[Ca^{2+}]_i$ were recorded with a fluorescence microscope (EVOS FL, Life Technologies, Darmstadt, Germany). The fluorescence intensity was also quantified with a microplate reader at Ex/Em = 490/525 nm. Yoda1 (SML1558, Sigma-Aldrich, Munich, Germany), Jedi2 (SML2532, Sigma-Aldrich, Munich, Germany), and Dooku1 (SML2397, Sigma-Aldrich, Munich, Germany) were used in this study as piezo1 agonists or antagonists. Images were analyzed with the time series analyzer V3 plugin for ImageJ software.

2.3.4.4 Evaluation of the Osteogenic Differentiation

After 2 weeks or 4 weeks of osteogenic differentiation, the AP activity in SCP-1 cells was measured with a plate reader. SCP-1 cells were gently washed with PBS

buffer, and incubated with the AP reaction buffer (50 mM glycine, 100 mM TRIS buffer with pH 10.5, 1 mM $MgCl_2$, and 2% 4-nitrophenyl-phosphate) in a 37°C incubator for 30 min. Afterward, the AP activity was measured photometrically with a plate reader at λ = 405 nm.

To evaluate mineralization, SCP-1 cells were first fixed with ethanol (99% v/v) at -20°C for at least 1 h. Afterward, the fixed SCP-1 cells were gently washed with tap water. Subsequently, the cells were incubated with 0.5% alizarin red solution (pH 4.0) for 30 min at RT. To quantify mineralization, the labeled alizarin red was resolved in cetylpyridinium chloride (10% w/v) and assayed photometrically at λ = 562 nm. For von Kossa staining, SCP-1 cells were gently washed with tap water, then the cells were incubated with 3% silver nitrate for 30 min at RT, then gently washed with tap water, and incubated with a mixture of 0.5 M sodium carbonate and 10% formaldehyde for 2 min, then incubated with 5% sodium thiosulfate buffer for 5 min.

2.3.4.5 Statistical Analysis

The results of this study are displayed as box plots. Because a Gaussian distribution could not be assumed due to the small sample size, conditions were compared using the non-parametric Kruskal-Wallis test and Dunn's multiple comparison test, or non-parametric two-way ANOVA followed by Tukey's multiple comparison test, using GraphPad Prism software version 9.0 (El Camino Real, USA); $p < 0.05$ was considered statistically significant.

2.3.5 Results

2.3.5.1 16 Hz ELF-PEMF Exposure Strategies Affected SCP-1 Cell Number and Viability

The number of SCP-1 cells was determined after exposure to 16 Hz ELF-PEMF. First, we investigated the influence of different intensities of 16 Hz ELF-PEMF on SCP-1 cell numbers. The results indicated that exposure to16 Hz ELF-PEMF with intensities ranging from 38.85 μT to 275.45 μT showed no significant difference in the number of SCP-1 cells (Fig. 9A). Secondly, the effects of different exposure strategies on cell activity were explored. The results showed that continuous exposure (30 min per day) significantly increased cell numbers (1.2-fold with $p = 0.0117$) compared with the control (unstimulated group). Interestingly, intermittent exposure had a stronger effect on increasing cell numbers (1.5-fold with $p < 0.0001$) compared with the control (Fig. 9B). Similarly, the fluorescence intensity of calcein-AM staining verified that

intermittent exposure was more effective in increasing the cell viability of SCP-1 cells than simply prolonging exposure time in a continuous way (Fig. 9C)

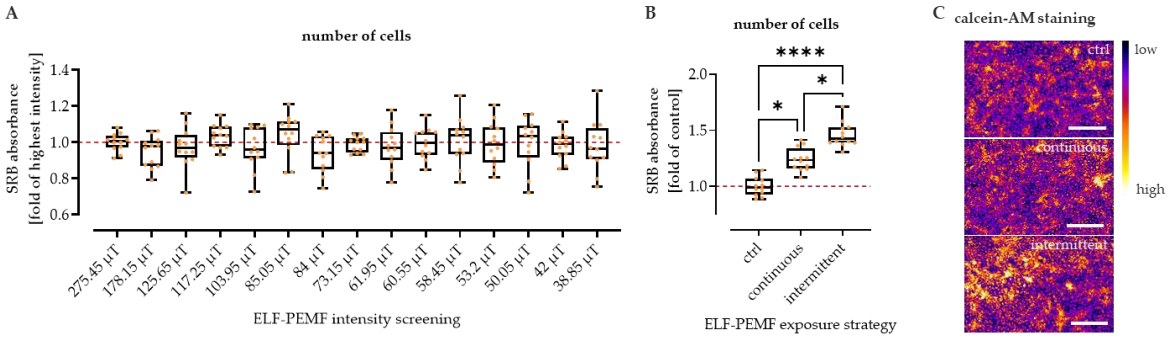

Figure 9: Number and viability of SCP-1 cells were strongly influenced by 16 Hz ELF-PEMF with different exposure strategies (continuous or intermittent exposure), rather than intensities (38.85 µT to 275.45 µT). (A&B) Sulforhodamine B (SRB) staining was performed to evaluate cell numbers after 3 days of exposure. (C) Calcein-AM staining was used to evaluate cell viability; the images were overlaid with pseudo-color (fire) using ImageJ software, and the bar on the right indicates cell viability. N = 3, n = 4. Data are presented as a box plot. Because a Gaussian distribution could not be assumed due to the small sample size, conditions were compared using the non-parametric Kruskal-Wallis test and Dunn's multiple comparison test, * $p < 0.05$, and **** $p < 0.0001$.

2.3.5.2 Intermittent ELF-PEMF Promoted Alkaline Phosphatase (AP) Activity and Mineralization of SCP-1 Cells

To investigate the influence of intermittent 16 Hz ELF-PEMF exposure on osteogenic differentiation, SCP-1 cells were cultured in osteogenic differentiation medium with daily continuous or intermittent ELF-PEMF exposure for up to 28 days. The early osteogenesis marker AP activity was enhanced after 14 days of culture for both ELF-PEMF exposures (Fig. 10A). Similarly, mineralization of the ECM (late osteogenic marker) also significantly increased after 14 days of exposure to both ELF-PEMF strategies (Fig. 10B). The representative images of alizarin red staining (Fig. 10C) and von Kossa staining (Fig. 10D) confirmed that intermittent ELF-PEMF exposure promoted more mineralization compared with the control group or continuous exposure.

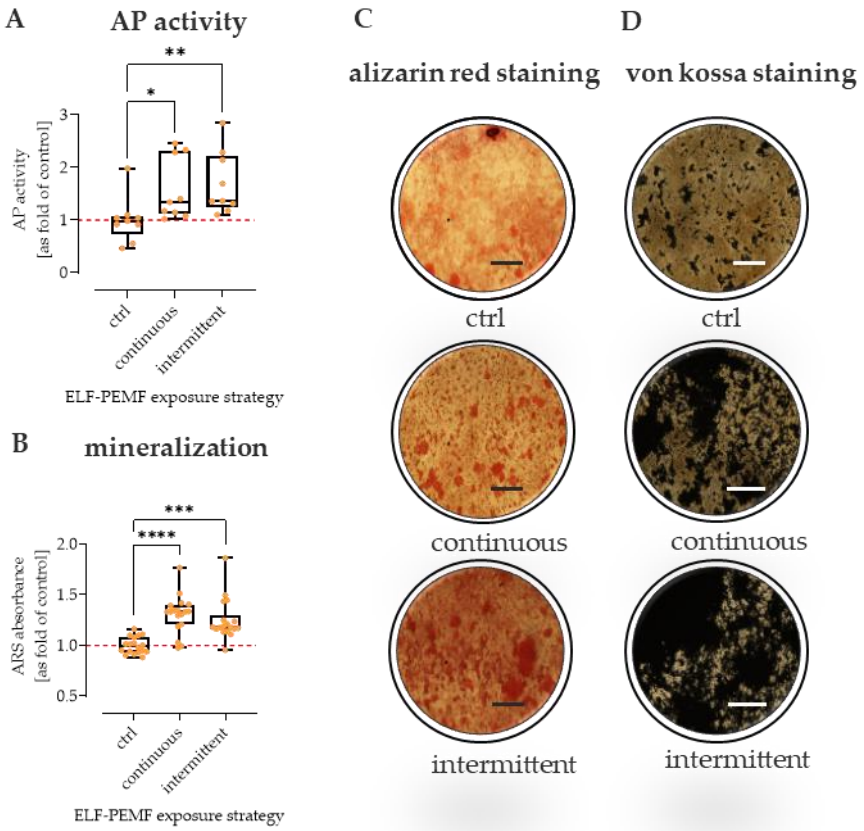

Figure 10: AP activity and mineral deposition of SCP-1 cells affected by continuous or intermittent exposure to 16 Hz ELF-PEMF. (A) AP activity on day 14 of culture. (B) Mineralization indicated by alizarin red staining on day 14 of culture. Representative images of (C) alizarin red staining and (D) von Kossa staining on day 28 of culture. Scale bar equals 500 µm, N = 4, n ≥ 2. Data are presented as a box plot. Because a Gaussian distribution could not be assumed due to the small sample size, conditions were compared using the non-parametric Kruskal-Wallis test and Dunn's multiple comparison test, * $p < 0.05$, ** $p < 0.01$, *** $p < 0.001$, and **** $p < 0.0001$.

2.3.5.3 Intermittent ELF-PEMF Upregulated Expression of Piezo1

After continuous or intermittent exposure to 16 Hz ELF-PEMF, gene expression of *piezo1* was evaluated. On day 7 of culture, continuous exposure of ELF-PEMF showed no effect on the expression of *piezo1*, while intermittent ELF-PEMF exposure upregulated expression of *piezo1* (1.5-fold with $p = 0.0198$) compared with continuous exposure (Fig. 11A). On day 14 of culture, intermittent ELF-PEMF exposure significantly increased the expression of *piezo1* (2.0-fold with $p = 0.0269$) compared with control (Fig. 11B). Taken together, intermittent ELF-PEMF exposure upregulated the expression of *piezo1* in SCP-1 cells on day 7 and day 14 of culture.

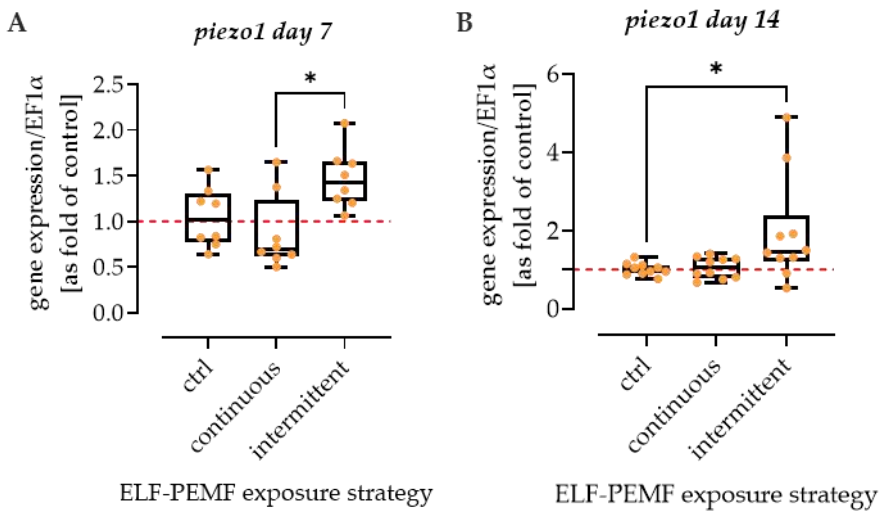

Figure 11: Changes in gene expression of the mechanosensitive Ca^{2+} channel *piezo1* after continuous or intermittent ELF-PEMF exposure (A) on day 7 and (B) on day 14 of culture. N ≥ 2, n = 2. Data are presented as a box plot. Because a Gaussian distribution could not be assumed due to the small sample size, conditions were compared using the non-parametric Kruskal-Wallis test and Dunn's multiple comparison test, * $p < 0.05$.

2.3.5.4 Yoda1 and Jedi2 pharmacologically increased $[Ca^{2+}]_i$, while Dooku1 inhibited ELF-PEMF induced Ca^{2+} influx

As an essential step before determining if the piezo1-induced Ca^{2+} influx could be affected by ELF-PEMF, it was necessary to find a suitable concentration of Yoda1, Jedi2 (both agonists of piezo1), and Dooku1 (an antagonist of piezo1). Our data indicated that 1 µM and 2 µM Yoda1 immediately increased and stably maintained intracellular Ca^{2+} ($[Ca^{2+}]_i$). With a concentration of 4 µM, Yoda1 $[Ca^{2+}]_i$ was no longer proportionally increased and reduced with time (Fig. 12A). Jedi2, another piezo1 agonist, had a similar effect to that of Yoda1. 2.5 µM and 5 µM Jedi2 rapidly induced and maintained $[Ca^{2+}]_I$, which could not be further improved by increasing the Jedi2 concentration. However, overall, 5 µM Jedi2 showed weaker efficiency and less stability than 2 µM Yoda1 (Fig. 12B). Therefore, 2 µM Yoda1 was used in further experiments as the control condition for piezo1 activity. To identify a suitable concentration of the piezo1 antagonist Dooku1, SCP-1 cells were pre-incubated with 0, 5, 20, and 40 µM Dooku1 for 5 min (baseline). Our data showed that 5 µM Dooku1 delayed the effects of Yoda1. 20 µM Dooku1 was required to not only delay but also block the effects of Yoda1, while 40 µM Dooku1 completely diminished the effects of Yoda1 (Fig. 12C).

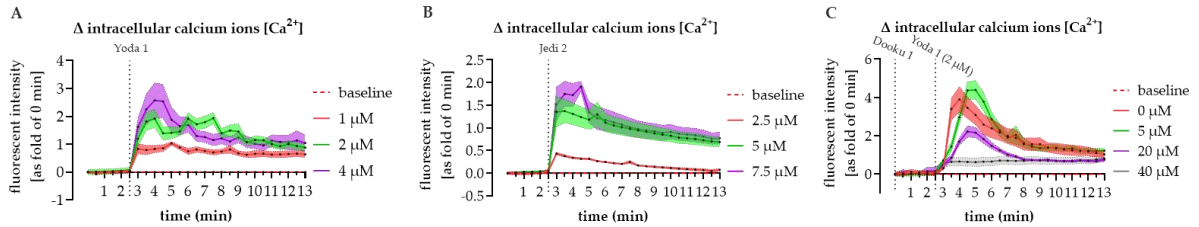

Figure 12: The efficiency of different concentrations of Yoda1, Jedi2, and Dooku1 on Ca^{2+} influx in SCP-1 cells. Ca^{2+} influx was determined by fluorescent intensity. (A) Ca^{2+} influx in SCP-1 cells after treatment with 1, 2, and 4 μM Yoda1. (B) Ca^{2+} influx in SCP-1 cells after treatment with 2.5, 5, and 7.5 μM Jedi2. (C) Ca^{2+} influx in SCP-1 cells after pre-incubation with 0, 5, 20, and 40 μM Dooku1, then treatment with 2 μM Yoda1. Dash line indicates baseline without any treatment. Data are presented as mean ± SEM. N = 3, n = 3 cells for each image.

2.3.5.5 Intermittent ELF-PEMF Exposure Maintained and Accumulated $[Ca^{2+}]_i$ in SCP-1 Cells

To investigate the $[Ca^{2+}]_i$ changes in SCP-1 cells, both continuous and intermittent exposure of ELF-PEMF were performed SCP-1 cells and Ca^{2+} influx was assessed. Our data indicated that $[Ca^{2+}]_i$ of SCP-1 cells immediately increased during a continuous 30 min exposure to 16 Hz ELF-PEMF, while $[Ca^{2+}]_i$ slowly decreased towards the baseline after ELF-PEMF was turned off (Fig. 13A). Interestingly, $[Ca^{2+}]_i$ of SCP-1 cells increased most during the first phase of intermittent ELF-PEMF exposure. The accumulated $[Ca^{2+}]_i$ was maintained during the second phase, and further increased during the third phase of exposure to 16 Hz ELF-PEMF (Fig. 13B). Then, SCP-1 cells were exposed to 16 Hz ELF-PEMF for 7 min. Dooku1 treatment strongly inhibited the effects of 16 Hz ELF-PEMF. In detail, 10 μM Dooku1 obviously reduced the effects of ELF-PEMF on $[Ca^{2+}]_i$, while 20 μM and 40 μM Dooku1 completely diminished the effects of ELF-PEMF exposure (Fig. 13C). Therefore, 10 μM Dooku1 was used in the following experiments to block the effect of ELF-PEMF exposure on piezo1-dependent Ca^{2+} influx. In summary, intermittent exposure of 16 Hz ELF-PEMF maintained and further increased $[Ca^{2+}]_i$ through activating piezo1 in SCP-1 cells compared with continuous exposure.

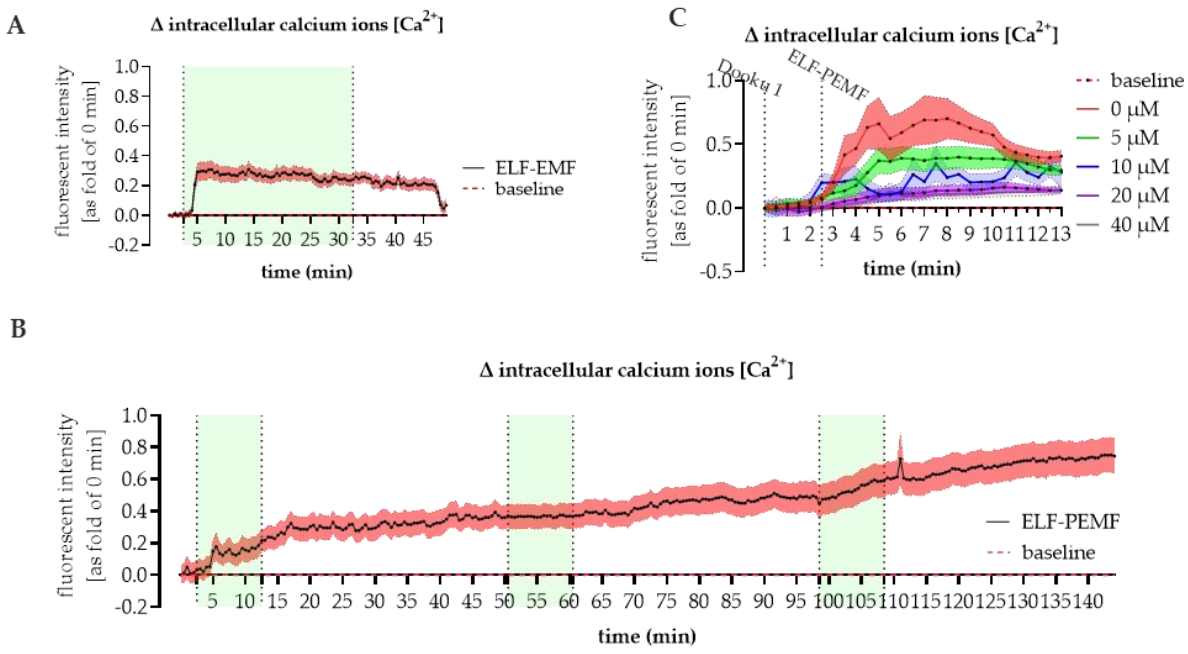

Figure 13: Effects of short-term continuous and intermittent exposure of 16 Hz ELF-PEMF on Ca^{2+} influx into SCP-1 cells. (A) $[Ca^{2+}]_i$ increased during continuous exposure to 16 Hz ELF-PEMF ; (B) $[Ca^{2+}]_i$ increased during intermittent exposure to 16 Hz ELF-PEMF. (C) Ca^{2+} influx of SCP-1 cells after pre-incubation with 0, 5, 10, 20, and 40 μM Dooku1; cells then were exposed to 16 Hz ELF-PEMF. Dash line indicates baseline without any treatment. Data are presented as mean ± SEM. N = 3, n ≥ 8 cells for each image.

2.3.5.6 Intermittent Exposure Increased the Sensitivity of SCP-1 Cells to ELF-PEMF-induced Calcium Influx

Since the gene expression of *piezo1* was upregulated on day 7 and day 14 after daily intermittent ELF-PEMF exposure, we next explored if the upregulated expression of piezo1 also resulted in an increased $[Ca^{2+}]_i$ on day 7 and day 14 after daily intermittent ELF-PEMF exposure. To support this hypothesis, SCP-1 cells were cultured in differentiation medium and exposed to ELF-PEMF every day. On day 7 or day 14, $[Ca^{2+}]_i$ was quantified with a microplate reader. The result indicated that, on day 7, $[Ca^{2+}]_i$ was significantly increased after intermittent exposure (1.8-fold with p = 0.0449) compared with the control (Fig. 14A). On day 14, no significant increase in $[Ca^{2+}]_i$ was observed (Fig. 14B).

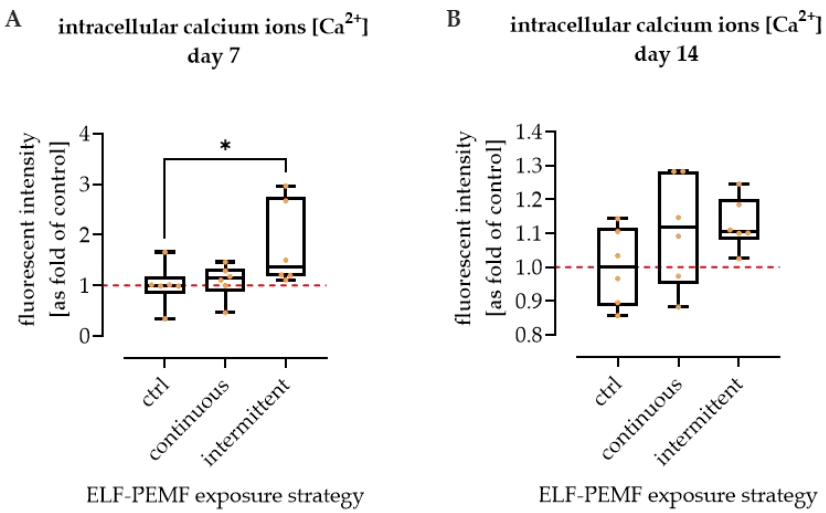

Figure 14: Daily exposure to continuous or intermittent ELF-PEMF increased the sensitivity of SCP-1 cells to ELF-PEMF-induced Ca^{2+} influx. $[Ca^{2+}]_i$ was evaluated after 2 min of ELF-PEMF stimulation (peak calcium influx) on (A) day 7 and (B) day 14 of culture. N = 3, n = 2. Data are presented as a box plot. Because a Gaussian distribution could not be assumed due to the small sample size, conditions were compared using the non-parametric Kruskal-Wallis test and Dunn's multiple comparison test, * $p < 0.05$.

2.3.5.7 Antagonizing Piezo1 with Dooku1 Impaired Cell Viability and Osteogenesis Induced by 16 Hz ELF-PEMF Exposure

To evaluate the influence of ELF-PEMF exposure on cell viability and osteogenesis, SCP-1 cells were cultured for up to 28 days with daily ELF-PEMF exposure. In our study, 10 µM Dooku1 was used to block the Ca^{2+} influx induced by piezo1. As expected, ELF-PEMF exposure (especially intermittent exposure) significantly increased cell viability (Fig. 15A&D) and AP activity (Fig. 15B&E), and promoted mineral deposition (Fig. 15C&F). Additional Dooku1 treatment, which blocks the function of piezo1, neutralized the positive effect of 16 viability and osteogenesis in SCP-1 cells. The representative images of alizarin red staining (Figure 15G) and von Kossa staining (Fig. 15H) showed that intermittent exposure strongly increased the mineralization of SCP-1 cells. In summary, antagonizing piezo1 decreased cell viability and impaired osteogenesis in SCP-1 cells. Intermittent exposure to 16 Hz ELF-PEMF was more effective than continuous exposure in reversing the inhibition caused by piezo1 dysfunction.

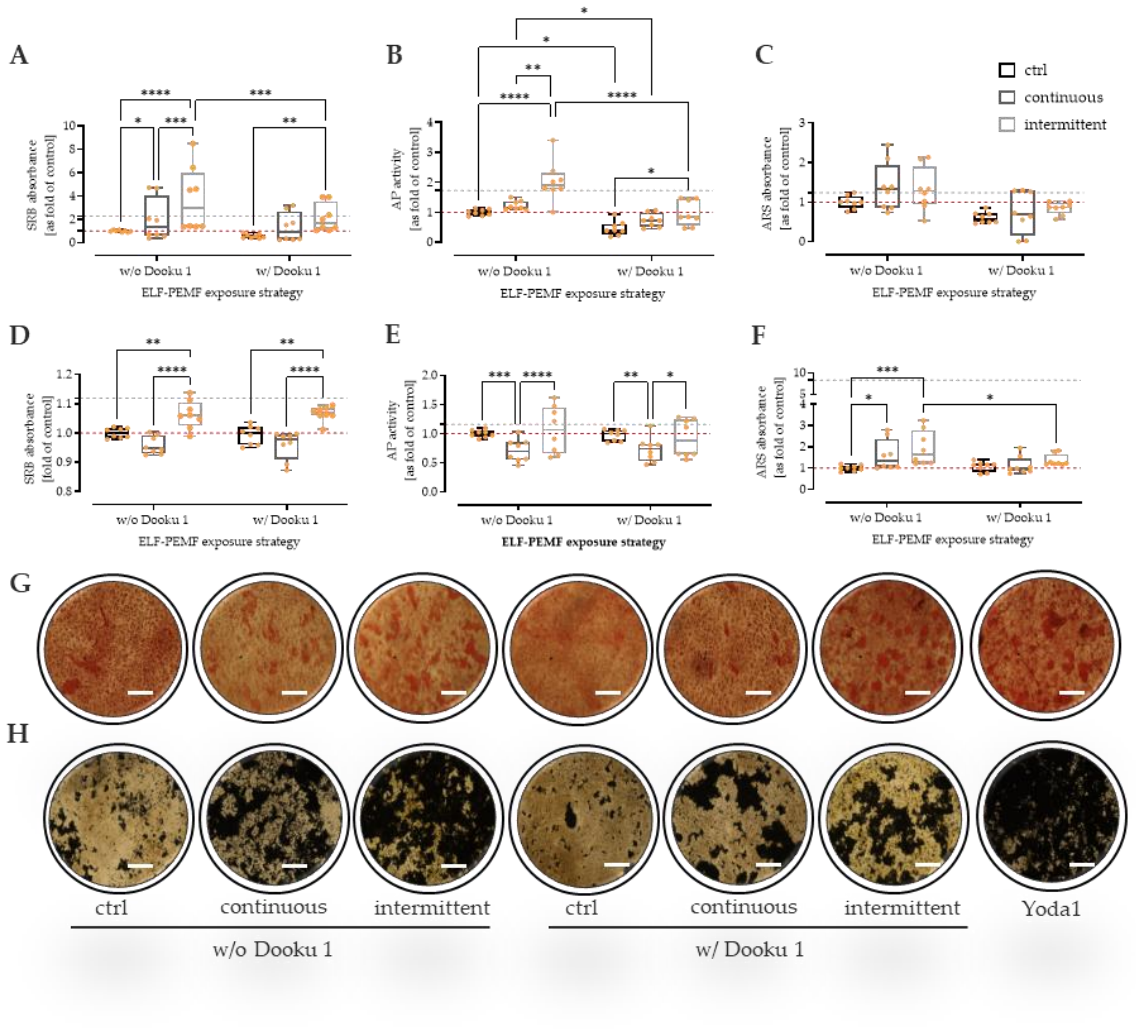

Figure 15: Antagonizing piezo1 with Dooku1 strongly decreased cell viability and osteogenesis induced by intermittent exposure of ELF-PEMF. On day 14, (A) SRB staining was performed to evaluate cell numbers; (B) AP activity; (C) mineralization indicated by alizarin red staining. On day 28, (D) SRB staining was performed to evaluate cell numbers by total protein content; (E) AP activity; (F) mineralization indicated by alizarin red staining. Representative images of (G) alizarin red staining and (H) von Kossa staining. The grey dashed line represents Yoda1 treatment as a positive control. Scale bar equals 500 µm. N = 4, n = 2. Data are presented as a box plot. Because a Gaussian distribution could not be assumed due to the small sample size, conditions were compared using the non-parametric two-way ANOVA followed by Tukey's multiple comparison test, * $p < 0.05$, ** $p < 0.01$, *** $p < 0.001$, and **** $p < 0.0001$.

2.3.6 Discussion

The etiology and progression of osteoporosis is multifactorial and still not fully understood. With the development of evidence-based medicine and pathophysiology, the treatment for promoting the new bone formation and restoring the health of bone has gradually developed into a multidisciplinary and comprehensive treatment (Calori *et al.*, 2013). In recent decades, a variety of physical therapies have been developed to support fracture healing, *e.g.*, mechanical stretching (Grier *et al.*, 2017), dynamic

compression (Pelaez *et al.*, 2012), vibration (Uzer *et al.*, 2018), and low intensity pulsed ultrasound (Hui *et al.*, 2011). However, few studies have been conducted to investigate the therapeutic effects and molecular mechanism of a novel physical therapy, *i.e.*, ELF-PEMF exposure(Ehnert *et al*., 2015).

In this study, we evaluated the influence of continuous and intermittent exposure of 16 Hz ELF-PEMF on piezo1 expression and activity, cell viability, and osteogenesis in SCP-1 cells. Interestingly, our qRT-PCR data indicated that intermittent exposure significantly increased the expression of *piezo1* after 7 days of daily exposure compared with the control group. The observed increase in *piezo1* on day 7 and day 14 indicates that late osteogenic differentiation was initiated, accompanied by changes in $[Ca^{2+}]_i$. To support this hypothesis, we performed a real-time evaluation of $[Ca^{2+}]_i$ after exposure to 16 Hz ELF-PEMF. 2 μM Yoda1 was used as a piezo1 agonist in this study due to its better efficiency and stability than Jedi2. Dooku1 functions as an antagonist of piezo1, and 10 μM Dooku1 was found to be sufficient to completely inhibit piezo1 activation. Moreover, we showed that continuous ELF-PEMF exposure can increase Ca^{2+} influx during exposure, but intermittent exposure was found to maintain and further accumulate $[Ca^{2+}]_i$. Completely blocking piezo1 with 10 μM or 20 μM Dooku1 abolished the agonistic effects of ELF-PEMF on piezo1. These results not only indicate that piezo1 plays an important role in modulating Ca^{2+} influx in SCP-1 cells, but also show that ELF-PEMF modulates $[Ca^{2+}]_i$, at least partly by activating piezo1. It is well-accepted that Ca^{2+} and its related signaling pathways are highly involved in the formation and degradation of bone. Ca^{2+} not only functions as the mediator of many hormones and cytokines, but also mediates communication between adjacent cells and tissue through gap junctions (Henriksen *et al.*, 2006). However, it was reported that the Ca^{2+} influx in MSCs is a “double-edged sword”, in that the induction of Ca^{2+} influx may exhibit an anabolic effect or lead to apoptosis (Blair *et al.*, 2007). The positive or negative effects of Ca^{2+} influx on fracture healing is mainly based on the stimulation pattern or the involved channel (Blair *et al*., 2007). For instance, Ca^{2+} influx can activate the PI3K/Akt signaling pathway to enhance anabolic and survival pathways in MSCs (Danciu *et al.*, 2003). Alternatively, Ca^{2+} influx may also lead to nicotinamide adenine dinucleotide / ryanodine receptors (NAD+/RyR)-related apoptosis (Romanello *et al.*, 2001). To further determine the influence of ELF-PEMF on Ca^{2+} influx and the activity of SCP-1 cells, we investigated the details of $[Ca^{2+}]_i$ changes during exposure to 16 Hz ELF-PEMF, by applying either

continuous exposure or intermittent exposure. The results show that $[Ca^{2+}]_i$ immediately increased under 30 min of continuous ELF-PEMF exposure, then slightly decreased to baseline. In contrast, during three phases of intermittent exposure, the first phase of intermittent exposure increased $[Ca^{2+}]_i$, while $[Ca^{2+}]_i$ did not show a tendency to decrease due to the subsequent intermittent exposure. Calcium influx determines various signaling pathways, including the TGF-β signaling pathway (Mukherjee *et al.*, 2012). Thus, the current study seems to verify our previous study showing that 16 Hz ELF-PEMF promotes cell viability and matrix formation in osteoprogenitors through initialing the TGF-β-Smad2/3 signaling pathway (Chen *et al.*, 2021). In addition, the current study shows that the impact of ELF-PEMF exposure on piezo1 and Ca^{2+} influx may eventually increase new bone formation.

Taken together, even though the sum of daily exposure duration was the same, the current data indicate that intermittent exposure has stronger effects on cell viability and osteogenesis in SCP-1 cells, compared with continuous exposure (30 min per 24 h period). Therefore, a different exposure strategy, *i.e.*, intermittent exposure, is a promising way to further optimize the therapeutic potential regarding fracture healing or to treat osteoporosis. Intermittent ELF-PEMF exposure had stronger effects in activating piezo1-induced Ca^{2+} influx, and further enhanced the positive effects of ELF-PEMF exposure in terms of cell viability and osteogenesis in MSCs as compared to simply prolonging ELF-PEMF exposure in a continuous way.

3 General Discussion

3.1 The Influence of ELF-PEMF on Cell Viability and Proliferation

In the early phase of fracture healing, cell viability and proliferation of MSCs and osteoblasts at the fracture site are extremely important, because the cell number is a major factor that directly affects subsequent matrix synthesis, mineral deposition, and fracture healing (Wang *et al.*, 2013).

It is widely recognized that specific ELF-PEMF can increase cell viability and proliferation. For example, continuous exposure to ELF-PEMF (14.9 Hz, 0.4 mT) for 72 h significantly enhanced the proliferation of osteoblasts (Barnaba *et al.*, 2013); daily exposure to ELF-PEMF (15 Hz, 4 mT) for 30 min strongly promoted cell proliferation (Esmail *et al.*, 2012); a continuous 9 h exposure to ELF-PEMF (75 Hz, 1.5 mT) also increased cell proliferation (Lin and Lin, 2011). Our results are similar, in that daily exposure to ELF-PEMF strongly increased cell viability and the number of MSCs (Chen *et al*., 2021). Of note, with a competitive and comprehensive analysis of our publications and preliminary results (Chen *et al.*, In preparation), we have some hypotheses to explain unexpected results such as: 1) the amplitudes of ELF-PEMF in our project (38.85 μT - 275.45 μT) did not show significant differences in their positive effects on cell proliferation. This phenomenon might be explained by amplitudes that were higher than the threshold, or the amplitude parameters in our project were extremely low, so the amplitude interval between groups was too small to show biological differences. 2) The exposure timeframe, *e.g.*, duration and strategy, are an important but underestimated factor. Our published work indicated that continuous 30 min daily exposure showed stronger effects on cell viability than 7 min or 90 min daily exposure (Chen *et al*., 2021). In addition, our results indicated that intermittent exposure may further enhance the viability of MSCs compared with continuous exposure (Chen *et al*., In preparation). Taken together, our data suggest that ELF-PEMF exposure with an extremely low frequency, amplitude, and short-term exposure may provide an effective and safe treatment option for patients.

In contrast to our findings, it has been reported that 45 min of ELF-PEMF (4 Hz, 0.65 mT) exposure does not influence the proliferation of MG-63 cells (Noriega-Luna *et al.*, 2011). This phenomenon could be explained by the nature of the osteoblast-like osteosarcoma-derived cell line used in this study, which are known to be more mature bone cells (Pautke *et al.*, 2004) than the MSC-like SCP-1 cells used in our experiments. Also, it is interesting to note that the work by Safari *et al.* demonstrating

that EMF (50 Hz, 400 μT) with a waveform of alternating current (AC) and rectified half-wave (RHW) significantly reduced the viability and proliferation of MSCs (Safari *et al.*, 2016). One possible explanation for this observation might be the fact that the authors tried to differentiate cells towards neurons (Safari *et al.*, 2016). Therefore, the therapeutic effects of ELF-PEMF not only depend on the intrinsic property and differentiation stage of the cell, but also depend on the culture environment and the state of the host.

3.2 ELF-PEMF Exposure Promoted Cell Attachment and Spreading

The attachment and spreading ability of cells are important in the early fracture healing stage. It has been reported that attachment and spreading are associated with osteogenic differentiation, because osteoblasts express more ezrin, radixin, and myosin (ERM) proteins, *i.e.*, than undifferentiated MSCs (Titushkin and Cho, 2009). As a result, more crosslinks between actin filaments and the plasma membrane will be subsequently formed (Titushkin and Cho, 2009). The knockout of ERM proteins (Titushkin and Cho, 2011) or focal adhesion kinase (FAK) (Salasznyk *et al.*, 2007) strongly decreased AP and osteogenic ability, thus reducing or slowing down fracture healing. Moreover, the spreading actin cytoskeleton is essential for osteogenesis, and insufficient spread and attachment within the first 48 h may abolish the osteogenic potential of MSCs (Mathieu and Loboa, 2012).

To promote adhesion and improve osseointegration in the early-stage post-operative period, various methods have been established, *e.g.*, modifying the implant surface wettability (Wang *et al.*, 2010), surface charge density (Rebl *et al.*, 2010), and decoration (Man *et al.*, 2016). However, these research findings are far from satisfying because of their high cost, low safety, and lack of long-term stability (To *et al.*, 2020). Instead, ELF-PEMF exposure is an excellent adjuvant pre-treatment option to increase adhesion and osseointegration of MSCs on the implant after modern orthopedic surgery. In this project, we found that 30 min and 90 min of 16 Hz ELF-PEMF exposure strongly enhanced cell attachment, while 7 min of exposure to ELF-PEMF and 30 min of exposure to ELF-PEMF significantly increased cell spreading (Chen *et al.*, 2021). Moreover, our data indicate that ELF-PEMF exposure also promotes the attachment of immune cells by differentiating monocytes into Mφ (Chen *et al.*, 2021). The immunomodulatory ability of ELF-PEMF may also confer effects on the actin cytoskeleton. It was reported that a change in actin polymerization

and organization is accompanied by the activation of monocytic cells (Ravetto *et al.*, 2014). Therefore, the use of ELF-PEMF may directly and/or indirectly affect the process of fracture healing by promoting attachment and spreading of MSCs and immune cells in the very early stage (Chen *et al.*, 2021).

It has been reported that adhesion and spreading of osteoblasts are mainly regulated by three signaling pathways: the canonical and the noncanonical Src-FAK dependent pathway, as well as the E-cadherin/β-catenin pathway (Chen *et al.*, 2018). Although the influence of ELF-PEMF exposure on promoting MSC adhesion and spreading were observed, the molecular mechanisms and signaling pathways behind these events are still unclear. Based on our own previous work (Ehnert *et al.*, 2015), we hypothesized that phosphorylation of the Src-FAK complex caused by ELF-PEMF exposure activates the downstream Ras-MAPK-ERK1/2 signaling pathway to enhance osteogenesis and mineralization in MSCs (Fig. 16). To support this hypothesis and the important role of cell adhesion, research is needed in the future.

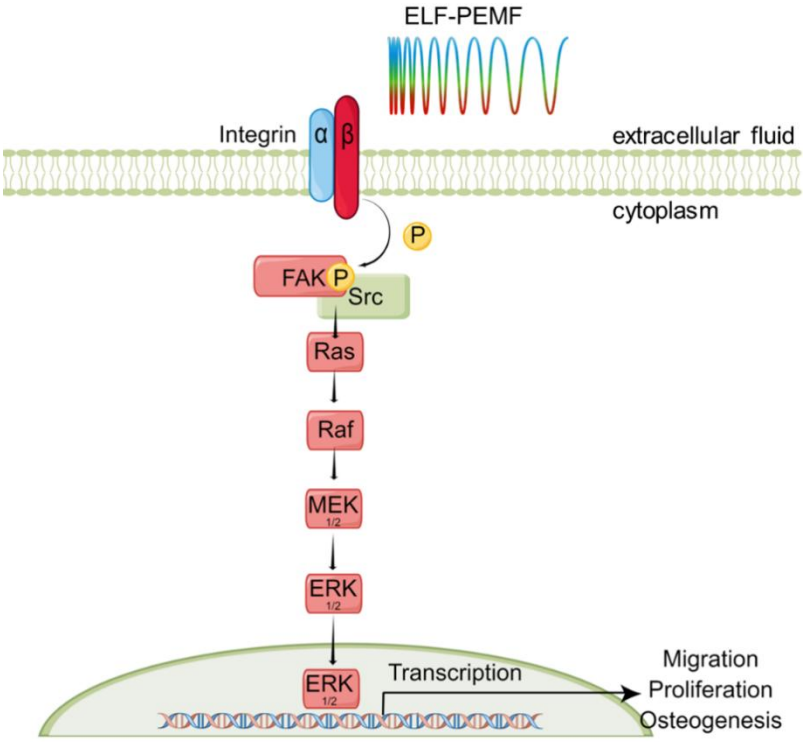

Figure 16: ELF-PEMF exposure may promote cell adhesion and spread via activating integrins and the integrin-linked tyrosine kinase Src. Afterward, Src mediates the phosphorylation of FAK, which involves activation of the downstream Ras-MAPK/ERK1/2 signaling pathway and promotes cell migration, proliferation, and osteogenesis. Graphic elements were provided by Servier (smart.servier.com). This schematic diagram was graphically processed based on a previous study (Hsu *et al.*, 2020).

3.3 The Multidimensional Promoting Effects of ELF-PEMF on MSC Migration

To achieve a quick and efficient healing process, the migration of MSCs to the site of injury is a critical step to initiate wound or bone healing. It has been reported that MSCs from osteoporosis patients exhibit impaired migration capacity. To promote fracture healing, considerable effort has been devoted to rescuing or enhancing the migration capacity of MSCs. For example, the transplantation of CXCR4-expressing MSCs (MSC^{CX4}) to stimulate MSC homing (Lien *et al.*, 2009) and use of the bone-seeking peptide LLP2A to attract MSCs to bone (Guan *et al.*, 2012) have been reported to significantly increase new bone formation. In our study, daily exposure to ELF-PEMF for 7 min or 30 min significantly increased the migration of SCP-1 cells (Chen *et al.*, 2021). MSC migration is also affected by the surrounding microenvironment, *e.g.*, the ECM, chemokines, and adjacent cells. During the inflammation phase of fracture healing, MSCs are recruited by the inflammatory stimulus, which is secreted by infiltrating immune cells, *i.e.*, Mφ (Peng *et al.*, 2005). Our data indicate that different ELF-PEMF can diversely modulate the inflammatory activity or anti-inflammatory activity of Mφ (Chen *et al.*, 2021). The cytokine array in our study suggested that exposure to specific ELF-PEMF altered Mφ secretion of cytokines and chemokines, and thus indirectly enhanced MSC migration. For instance, tumor necrosis factor-alpha (TNF-α) has been reported to direct the migration of BMSCs to promote new bone formation at the target site (Wang *et al.*, 2017). Increased levels of matrix metalloproteinases (MMPs) (Kim *et al.*, 2013) or BMPs (Chen *et al.*, 2016) may also contribute to MSC homing to the fracture ends of bone.

Taken together, the use of ELF-PEMF at a non-union site can directly increase MSC migration or modulate the activity of Mφ to indirectly recruit MSCs, thus providing a suitable environment for bone healing.

3.4 The Multidimensional Promoting Effects of ELF-PEMF on Osteogenesis

Osteogenic differentiation is a coordinated and complex process during fracture healing. In the first few days, MSCs exhibit strong proliferative capacity and initiate the synthesis of ECM components, *e.g.*, collagen I (Quarles *et al.*, 1992) and versican (Hoshiba *et al.*, 2009). From day 5 to day 14, MSCs differentiate into pre-osteoblasts, and their proliferation gradually decreases while AP activity increases to its peak (Carluccio *et al.*, 2020). From day 14 to day 28, pre-osteoblasts become mature osteoblasts, and AP activity gradually decreases, but the levels of osteocalcin,

osteopontin, and mineralization increase (Hoemann *et al.*, 2009). Afterward, mineral is deposited in the ECM, and osteoblasts eventually become osteocytes (Schaffler *et al.*, 2014). The different phases of osteogenesis overlap in time and space and the progression of differentiation is influenced by various internal and external factors. Therefore, the proper regulation of signaling molecules is an important factor to accelerate osteogenesis and promote bone healing.

As part of this project, we found that ELF-PEMF can directly activate canonical TGF-β signaling pathways to initial osteogenesis (Chen *et al*., 2021). Intermittent ELF-PEMF exposure directly promoted Ca^{2+} influx into SCP-1 cells and significantly increased mineral deposition at later stages. In addition, specific ELF-PEMF modulated the activity of Mφ to indirectly increase the gene expression of *ECM* components, *e.g.*, *Col1A1*, *FN1*, *BGN*, and *VCAN* in MSCs (Chen *et al*., 2021). In our preliminary results, we explored the influences of intermittent exposure on osteogenic differentiation, early differentiation marker AP activity, and late differentiation marker mineralization (Chen *et al*., In preparation). Intermittent exposure increased AP activity in SCP-1 cells more than continuous exposure after 2 weeks, although no obvious differences in mineralization were found between the two exposure strategies. After 4 weeks, intermittent exposure strongly reduced the AP activity of SCP-1 cells, along with strongly increased mineralization. The change in differentiation markers demonstrated that intermittent exposure reduced the time required for the transition from the early differentiation stage into the late differentiation stage (Chen *et al*., In preparation). Our study indicates that intermittent exposure might further accelerate new bone formation.

3.5 The Effects of ELF-PEMF on Other Innate Immune Cells

During the course of my thesis, we realized that exposure to ELF-PEMF has considerable effects on the majority of innate immune cells. Comprehensive research on the influences of ELF-PEMF on different types of immune cells can not only ameliorate potential side-effects of ELF-PEMF, but also provide an integrated and multidimensional approach to modulate the osteoimmune microenvironment.

Our study mainly focused on the Mφ-dominated osteoimmune microenvironment and ignored the fact that neutrophils are also an important innate immune cell during fracture healing. Neutrophils are the first immune cell type that arrives at the fracture site and affect the local microenvironment (Baht *et al*., 2018). Dysfunction of

neutrophils may lead to infection and osteomyelitis (Wagner *et al.*, 2004), and "overactive" neutrophils may lead to non-union or implant failure (Wozniak *et al.*, 2004). Therefore, exploring the influence of ELF-PEMF on neutrophils may provide clinicians with more options for fracture healing and may even prevent infection. Neutrophils have a well-known antimicrobial function; for instance, neutrophils can remove pathogens and bacteria through phagocytosis (Kobayashi *et al.*, 2018). In a concomitant study performed by another lab member, we investigated another bactericidal pathway, *i.e.*, neutrophil extracellular traps (NETs) (Linnemann *et al.*, 2020). During the process of NET formation, the neutrophil releases its DNA, histones, and a variety of antimicrobial proteases; this plays a key role in capturing and killing microbes (Reeves *et al.*, 2002). Of note, the process of NETosis has been recognized as a double-edged sword, *i.e.*, NETs exhibit strong bactericidal and bacteriostatic activity (Kaplan and Radic, 2012), but the overactivation of NETs may also lead to inflammatory disease, *e.g.*, rheumatoid arthritis (Hidalgo *et al.*, 2019) or type 1 diabetes mellitus (Mutua and Gershwin, 2021). Similar to monocytes/macrophages, neutrophils exhibit high susceptibility and reactivity during fracture healing; therefore, neutrophils might also represent a target cell type to be modulated by ELF-PEMF and support fracture healing. It has been reported that 300 μT ELF-PEMF exposure increased NETosis in phorbol myristate acetate (PMA)-pretreated neutrophils (Mutua and Gershwin, 2021). In our preliminary work, we observed that ELF-PEMF exposure decreased DNA release from PMA-pretreated neutrophils, and this phenomenon was dependent on the frequency of ELF-PEMF (data not shown). Moreover, we also investigated the molecular mechanism by detecting Ca^{2+} influx in neutrophils. Our preliminary results indicated that a single 7 min exposure to ELF-PEMF increased Ca^{2+} influx into neutrophils. Interestingly, the waveform of Ca^{2+} influx in neutrophils was different from that of SCP-1 cells, which may indicate that the effects of ELF-PEMF on Ca^{2+} influx are dependent on the cell type (Chen *et al*., In preparation). However, in-depth research to illustrate the importance of neutrophils is still needed in the future.

In addition to monocytes/macrophages and neutrophils, natural killer (NK) cells are another important immune cell type that influences the osteoimmune microenvironment (Orru *et al.*, 2013). NK cells participate in the scavenging of pathogens, detecting transformed cells, and communicating with other immune cells, *e.g.*, Mφ or neutrophils. However, studies on the effects of EMF on NK cells are

limited, and their findings are controversial. For example, it has been reported that exposure to 50 Hz sinusoidal EMF decreased the number of NK cells (Boscolo *et al.*, 2001, Di Giampaolo *et al.*, 2006), while other researchers reported that exposure to EMF showed either positive effects (Tuschl *et al.*, 2000) or had no effect on the number of NK cells (House *et al.*, 1996). Therefore, a comprehensive and systemic study is needed in the future to define the exact role of NK cells in fracture healing and explore the influences of ELF-PEMF on the activity of NK cells.

In summary, the crosstalk and interaction between the skeletal system and the immune system during fracture healing results in a highly sophisticated microenvironment. This immune microenvironment is critical for the initiation, regeneration, and outcome of fracture healing. Regarding the application of ELF-PEMF in preventing fracture non-union, further research should not only focus on the activity of bone cells, but also devote efforts to exploring complex interactions in the osteoimmune microenvironment.

3.6 Other Potential Mechanisms Behind the Therapeutic Effects of ELF-PEMF

Despite the importance of ELF-PEMF on bone healing being widely recognized, there has been little clear and conclusive evidence about the molecular mechanisms behind it.

To explore the mechanism, in this project, we investigated mechanically activated (MA) ion channels. As recently described MA ion channels, we investigated the so-called piezo ion channel family (Coste *et al.*, 2010). Piezo1 is located on the plasma membrane of non-excitable cells, *e.g.,* osteoblasts, and functions as a sensor of extracellular mechanical stimuli (Zhang *et al.*, 2021), including membrane potential (Kaestner *et al.*, 2020) and magnetic forces (Wu *et al.*, 2016). After activation, piezo1-induced calcium influx leads to the phosphorylation of Erk1/2 and p38 (Halloran *et al.*, 2020), Akt and GSK-3β (Song *et al.*, 2020), NF-κB (Hu *et al.*, 2002), and the activation of the Nfat-Yap1-β-catenin (Zhou *et al.*, 2020) signaling pathway, and might be important in osteogenesis and other healing processes.

As an important mechanosensitive organelle, the assembly and disassembly of the primary cilium itself has been ignored. Immediately after ciliary receptors receive stimuli from ELF-PEMF, an efficient biological process should be initiated to translate and transfer this physical signal into biological activity. This essential biological process requires a special metabolic and transport system of primary cilia, *i.e.*, the

intraflagellar transport (IFT) system. Upon ciliogenesis, a complex and highly regulated transport process is initiated (Taschner *et al.*, 2012). During transport, a wide range of IFT proteins and motors allow the orderly bidirectional movement of molecules in the space between the flagellar membrane and the doublet microtubules (Kozminski *et al.*, 1993). Therefore, the IFT train plays a critical role in the structure and mechanosensitivity of the primary cilium. The mutation of IFT genes impairs ciliogenesis and results in more than 30 ciliopathies (Reiter and Leroux, 2017). For example, bone dysplasia is present in many diseases such as Jeune syndrome, Ellis-van Creveld syndrome, and orofacial digital syndrome (Yuan and Yang, 2015). The Jeune syndrome mouse model, established by IFT140 knockout, presents as a dwarf phenotype with decreased bone length and density, growth retardation, and disappearance of the growth plate (Tao *et al.*, 2019). The mutation of IFT88 results in attenuated mandibular development and damaged osteogenesis by inhibiting Hedgehog signaling (Kitamura *et al.*, 2020). Considering the positive effects of ELF-EMF on primary cilia, it is theoretically plausible that ELF-EMF could be an effective therapy for ciliopathy disorders in the future.

3.7 Limitations in the Research Area

Since 1974, when non-invasive, convenient, and effective PEMF were reported with therapeutic effects on fracture healing by Bassett *et al.,* it has triggered a surge of investigations into ELF-PEMF as a treatment option for bone diseases (Bassett *et al.*, 1974). For example, ELF-PEMF has been shown to effectively promote acute fracture healing (Martinez-Rondanelli *et al.*, 2014), healing of osteotomies (Eyres *et al.*, 1996), osteoporosis (Li *et al*., 2018), and spinal fusion (Jenis *et al.*, 2000, Ziegler *et al*., 2019). However, different laboratories used different methods, *e.g.*, amplitude (Yan *et al*., 2015), frequency (Zhang *et al.*, 2018), exposure duration (Adie *et al.*, 2011), or waveform (Yong *et al*., 2016). These inconsistencies make it difficult to screen for a reproducible protocol for a specific bone disease. Even though many studies have demonstrated that ELF-PEMF can effectively promote new bone formation (Ehnert *et al*., 2015, Ziegler *et al*., 2019), there is still a long way to go to achieve proper clinical translation, because of the many inconsistencies in this research area. These inconsistencies can be subclassified as follows:

1) EMF generating devices vary across laboratories/companies, *e.g.*, size, composition, the structure of the compartment, and types of coils (a single solenoid

coil or a pair of Helmholtz coils) (Daish *et al*., 2018). All of these factors may directly or indirectly affect the direction of magnetic lines, as well as the intensity and distribution of the EMF, thus leading to inconsistencies.

2) The EMF parameters that presumably exert positive effects vary across laboratories/companies, *e.g.*, frequency, amplitude, and exposure time. Without a proper explanation or even better a comparison of different devices, the definition of the positive parameters seems to be somewhat arbitrary. This phenomenon makes it difficult for subsequent investigators to summarize and compare results as well as to further optimize the therapeutic effects of ELF-PEMF (Ross *et al.*, 2015).

3) Considering that fracture healing is a continuous process without a cut-off point, and the differences in time interval, clinical criteria, and radiographic criteria (Wittauer *et al.*, 2021), the definitions of fracture non-union are not unified (Bhandari *et al.*, 2012). Therefore, it is necessary to have uniform evaluation criteria in order to systematically identify the healing stages and define the union states of fractured bone (Wittauer *et al*., 2021).

4) One of the merits of ELF-PEMF treatment is the socioeconomic advantages; however, we still lack a systematic and exhaustive study to analyze this aspect (Button *et al.*, 2009).

3.8 Future Outlook

With the deepening of relevant research, the safety of clinical EMF has gradually raised concerns. EMF exposure has been reported to affect the activity of stem cells during embryonic development, reduce the success rate of assisted reproductive technology, and lead to congenital malformations, *e.g.*, Wiedemann syndrome or Angelman syndrome (Maher *et al.*, 2003). To avoid these safety issues, an extremely low frequency or intensity should be widely adopted, because it not only effectively regulates cellular activities but also prevents DNA damage caused by energetic radiofrequencies or ionizing frequencies (Blank and Goodman, 2009). In addition, the high penetrating capacity of ELF-PEMF exposure may affect organs adjacent to the bone, *e.g.*, the heart (Elmas, 2016), liver (Lin *et al.*, 2018), and ovaries (Burcu *et al.*, 2020). Therefore, a combination of a precise method and a personalized strategy will be a good way to avoid additional and unnecessary side effects. In turn, a precise method may allow ELF-PEMF exposure to modulate the local immune microenvironment to kill tumor cells or eliminate infections. Recently, many

cross-discipline studies have explored the synergistic effects of biomaterials and an EMF on fracture healing, resulting in encouraging therapeutic effects (Ho-Shui-Ling *et al.*, 2018, Paun *et al.*, 2018).

In summary, using ELF-PEMF to promote new bone formation is a promising therapeutic approach. ELF-PEMF is recognized as an effective, safe, and convenient treatment for fracture non-union. However, there is still a long way to go in improving the therapeutic efficiency and developing the application of ELF-PEMF treatment.

4 Summary

In this project, we proved that the use of ELF-PEMF as a treatment for promoting new bone formation and preventing fracture non-union is effective and feasible. Our data indicated that the daily exposure of specific ELF-PEMF was able to directly increase the cell viability, migration, spreading, and adhesion of SCP-1 cells. The molecular mechanism is that ELF-PEMF activated the TGF-β signaling pathway, and protected the structure and function of the primary cilia of SCP-1 cells. Moreover, we found that the daily intermittent exposure (10 min every 8 h) is even better than the daily continuous exposure (30 min every 24 h) in improving cell viability. Interestingly, we found that piezo1 played an important role in the ELF-PEMF treatment. The gene expression of piezo1 increased after the intermittent exposure, and the function of piezo1 was activated thus leading to calcium influx into SCP-1 cells. In contrast, treating cells with piezo1 inhibitor Dooku1 blocked the function of piezo1 and impaired the mineral deposition. Therefore, ELF-PEMF can directly promote fracture healing. Nevertheless, we also found that ELF-PEMF with specific parameters can modulate the activity of macrophages to indirectly affect the osteogenesis of SCP-1 cells, *e.g.*, field A induced the pro-inflammatory activity of macrophages, and field B induced the anti-inflammatory activity of macrophages, and enhanced the ECM formation of SCP-1 cells on the early stage. Taken together, ELF-PEMF exposure can, directly and indirectly, promote the healing process and might be a useful tool in critical bone healing such as Pseudarthrosis.

5 German Summary

In diesem Projekt haben wir bewiesen, dass die Verwendung von ELF-PEMF als Behandlung zur Förderung der Knochenneubildung und zur Verhinderung von Pseudarthrosen effektiv und durchführbar ist. Unsere Daten zeigten eindeutig, dass eine Exposition von 16 Hz ELF-PEMF die Viabilität, Migration, Proliferation und Adhäsion von SCP-1-Zellen direkt erhöhen konnte. Der molekulare Mechanismus besteht zum Teil darin, dass ELF-PEMF den TGF-β-Signalweg aktiviert und die Struktur und Funktion primärer Zilien von SCP-1-Zellen z.B. gegenüber Zigarettenrauch schützt. Darüber hinaus haben wir festgestellt, dass eine tägliche intermittierende Exposition (10 min alle 8 h) sogar besser ist als die tägliche kontinuierliche Exposition (30 min jede 24 h), um die Viabilität der Zellen zu verbessern. Interessanterweise fanden wir heraus, dass piezo1 eine wichtige Rolle bei der ELF-PEMF-Behandlung spielte. Die Genexpression und Aktivität von piezo1 nahm nach der intermittierenden Exposition zu, was zu einem Kalziumeinstrom in SCP-1-Zellen führte. Im Gegensatz dazu blockierte die Behandlung von Zellen mit dem piezo1-Inhibitor Dooku1 die Funktion von piezo1 und beeinträchtigte die Mineralisierung der Matrix. Daher kann die ELF-PEMF Exposition die Frakturheilung direkt fördern. Darüber hinaus zeigte sich, dass ELF-PEMF mit spezifischen Parametern die Aktivität von Makrophagen modulieren kann, um indirekt die Osteogenese von SCP-1-Zellen zu beeinflussen, z. B. induzierte Feld A die entzündungsfördernde Aktivität von Makrophagen während Feld B die entzündungshemmende Aktivität von Makrophagen förderte, was zu einer verstärkten ECM-Bildung durch SCP-1-Zellen im Frühstadium führte. Zusammengenommen kann die ELF-PEMF-Exposition den Heilungsprozess direkt und indirekt fördern und könnte bei kritischen Heilungsverläufen wie bei der Pseudarthrose von Nutzen sein.

6 References

ADIE, S., HARRIS, I. A., NAYLOR, J. M., RAE, H., DAO, A., YONG, S. & YING, V. 2011. Pulsed electromagnetic field stimulation for acute tibial shaft fractures: a multicenter, double-blind, randomized trial. *J Bone Joint Surg Am,* 93**,** 1569-76.

ALPER, S. L. 2017. Genetic Diseases of PIEZO1 and PIEZO2 Dysfunction. *Piezo Channels,* 79**,** 97-134.

ANNAMALAI, R. T., TURNER, P. A., CARSON, W. F. T., LEVI, B., KUNKEL, S. & STEGEMANN, J. P. 2018. Harnessing macrophage-mediated degradation of gelatin microspheres for spatiotemporal control of BMP2 release. *Biomaterials,* 161**,** 216-227.

ANTONSSON, E. K. & MANN, R. W. 1985. The frequency content of gait. *J Biomech,* 18**,** 39-47.

ANVARIAN, Z., MYKYTYN, K., MUKHOPADHYAY, S., PEDERSEN, L. B. & CHRISTENSEN, S. T. 2019. Cellular signalling by primary cilia in development, organ function and disease. *Nature Reviews Nephrology,* 15**,** 199-219.

ARINGER, M., HOUSSIAU, F., GORDON, C., GRANINGER, W. B., VOLL, R. E., RATH, E., STEINER, G. & SMOLE, J. S. 2009. Adverse events and efficacy of TNF-alpha blockade with infliximab in patients with systemic lupus erythematosus: long-term follow-up of 13 patients. *Rheumatology,* 48**,** 1451-1454.

ASPARUHOVA, M. B., CABALLE-SERRANO, J., BUSER, D. & CHAPPUIS, V. 2018. Bone-conditioned medium contributes to initiation and progression of osteogenesis by exhibiting synergistic TGF-beta1/BMP-2 activity. *Int J Oral Sci,* 10**,** 20.

ASPERA-WERZ, R. H., CHEN, T., EHNERT, S., ZHU, S., FROHLICH, T. & NUSSLER, A. K. 2019. Cigarette Smoke Induces the Risk of Metabolic Bone Diseases: Transforming Growth Factor Beta Signaling Impairment via Dysfunctional Primary Cilia Affects Migration, Proliferation, and Differentiation of Human Mesenchymal Stem Cells. *International Journal of Molecular Sciences,* 20.

AVIDOR-REISS, T. & GOPALAKRISHNAN, J. 2013. Cell Cycle Regulation of the Centrosome and Cilium. *Drug Discov Today Dis Mech,* 10**,** e119-e124.

BAGHERI, L., PELLATI, A., RIZZO, P., AQUILA, G., MASSARI, L., DE MATTEI, M. & ONGARO, A. 2018. Notch pathway is active during osteogenic differentiation of human bone marrow mesenchymal stem cells induced by pulsed electromagnetic fields. *Journal of Tissue Engineering and Regenerative Medicine,* 12**,** 304-315.

BAHT, G. S., VI, L. & ALMAN, B. A. 2018. The Role of the Immune Cells in Fracture Healing. *Current Osteoporosis Reports,* 16**,** 138-145.

BARNABA, S., PAPALIA, R., RUZZINI, L., SGAMBATO, A., MAFFULLI, N. & DENARO, V. 2013. Effect of pulsed electromagnetic fields on human osteoblast cultures. *Physiother Res Int,* 18**,** 109-14.

BASCONES-MARTINEZ, A., MATTILA, R., GOMEZ-FONT, R. & MEURMAN, J. H. 2014. Immunomodulatory drugs: Oral and systemic adverse effects. *Medicina Oral Patologia Oral Y Cirugia Bucal,* 19**,** E24-E31.

BASSETT, C. A., MITCHELL, S. N., NORTON, L. & PILLA, A. 1978. Repair of non-unions by pulsing electromagnetic fields. *Acta Orthop Belg,* 44**,** 706-24.

BASSETT, C. A., PAWLUK, R. J. & PILLA, A. A. 1974. Augmentation of bone repair by inductively coupled electromagnetic fields. *Science,* 184**,** 575-7.
BASSETT, C. A. L. 1993. Beneficial-Effects of Electromagnetic-Fields. *Journal of Cellular Biochemistry,* 51**,** 387-393.
BEAVER, R., BRINKER, M. R. & BARRACK, R. L. 1997. An analysis of the actual cost of tibial nonunions. *J La State Med Soc,* 149**,** 200-6.
BECKER, R. O., BACHMAN, C. H. & FRIEDMAN, H. 1962. The direct current control system. A link between environment and organism. *N Y State J Med,* 62**,** 1169-76.
BELSUE, J., CALVO, S., JIMENEZ-SANCHEZ, C., PEREZ-PALOMARES, S., HERRERO, P. & BELLOSTA-LOPEZ, P. 2021. Osteoarthrosis Is It Just a Local Disease? *Topics in Geriatric Rehabilitation,* 37**,** 209-213.
BHANDARI, M., FONG, K., SPRAGUE, S., WILLIAMS, D. & PETRISOR, B. 2012. Variability in the definition and perceived causes of delayed unions and nonunions: a cross-sectional, multinational survey of orthopaedic surgeons. *J Bone Joint Surg Am,* 94**,** e1091-6.
BIGHAM-SADEGH, A. & ORYAN, A. 2015. Basic concepts regarding fracture healing and the current options and future directions in managing bone fractures. *International Wound Journal,* 12**,** 238-247.
BIZ, C., REFOLO, M., ZINNARELLO, F. D., CRIMI, A., DANTE, F. & RUGGIERI, P. 2022. A historical review of calcaneal fractures: from the crucifixion of Jesus Christ and Don Juan injuries to the current plate osteosynthesis. *International Orthopaedics*.
BLAIR, H. C., SCHLESINGER, P. H., HUANG, C. L. & ZAIDI, M. 2007. Calcium signalling and calcium transport in bone disease. *Subcell Biochem,* 45**,** 539-62.
BLANK, M. & GOODMAN, R. 2009. Electromagnetic fields stress living cells. *Pathophysiology,* 16**,** 71-8.
BODAMYALI, T., BHATT, B., HUGHES, F. J., WINROW, V. R., KANCZLER, J. M., SIMON, B., ABBOTT, J., BLAKE, D. R. & STEVENS, C. R. 1998. Pulsed electromagnetic fields simultaneously induce osteogenesis and upregulate transcription of bone morphogenetic proteins 2 and 4 in rat osteoblasts in vitro. *Biochem Biophys Res Commun,* 250**,** 458-61.
BOSCOLO, P., BERGAMASCHI, A., DI SCIASCIO, M. B., BENVENUTI, F., REALE, M., DI STEFANO, F., CONTI, P. & DI GIOACCHINO, M. 2001. Effects of low frequency electromagnetic fields on expression of lymphocyte subsets and production of cytokines of men and women employed in a museum. *Sci Total Environ,* 270**,** 13-20.
BRASINIKA, D., KOUMOULOS, E. P., KYRIAKIDOU, K., GKARTZOU, E., KRITIKOU, M., KAROUSSIS, I. K. & CHARITIDIS, C. A. 2020. Mechanical Enhancement of Cytocompatible 3D Scaffolds, Consisting of Hydroxyapatite Nanocrystals and Natural Biomolecules, Through Physical Cross-Linking. *Bioengineering (Basel),* 7.
BURCU, A., NEVIN, E., ILKAY, A., AMAC, K., ALPER, B. H. & MUGE, K. 2020. The effects of prenatal and postnatal exposure to electromagnetic field on rat ovarian tissue. *Toxicol Ind Health,* 36**,** 1010-1018.
BUSSE, J. W., BHANDARI, M., SPRAGUE, S., JOHNSON-MASOTTI, A. P. & GAFNI, A. 2005. An economic analysis of management strategies for closed and open grade I tibial shaft fractures. *Acta Orthop,* 76**,** 705-12.
BUTTON, M. L., SPRAGUE, S., GHARSAA, O., LATOUCHE, S. & BHANDARI, M. 2009. Economic evaluation of bone stimulation modalities: A systematic review of the literature. *Indian J Orthop,* 43**,** 168-74.

CAI, J., SHAO, X., YANG, Q. J., YANG, Y. Q., YAN, Z. D., LUO, E. P., FENG, X. & JING, D. 2020. Pulsed electromagnetic fields modify the adverse effects of glucocorticoids on bone architecture, bone strength and porous implant osseointegration by rescuing bone-anabolic actions. *Bone,* 133.

CALORI, G. M., COLOMBO, M., MAZZA, E., RIPAMONTI, C., MAZZOLA, S., MARELLI, N. & MINEO, G. V. 2013. Monotherapy vs. polytherapy in the treatment of forearm non-unions and bone defects. *Injury,* 44 Suppl 1**,** S63-9.

CARANO, R. A. & FILVAROFF, E. H. 2003. Angiogenesis and bone repair. *Drug Discov Today,* 8**,** 980-9.

CARLUCCIO, M., ZIBERI, S., ZUCCARINI, M., GIULIANI, P., CACIAGLI, F., DI IORIO, P. & CICCARELLI, R. 2020. Adult mesenchymal stem cells: is there a role for purine receptors in their osteogenic differentiation? *Purinergic Signalling,* 16**,** 263-287.

CATALANO, A., LODDO, S., BELLONE, F., PECORA, C., LASCO, A. & MORABITO, N. 2018. Pulsed electromagnetic fields modulate bone metabolism via RANKL/OPG and Wnt/beta-catenin pathways in women with postmenopausal osteoporosis: A pilot study. *Bone,* 116**,** 42-46.

CHEN, G. N., FANG, T. T., QI, Y. Y., YIN, X. F., DI, T. Y., FENG, G., LEI, Z., ZHANG, Y. X. & HUANG, Z. M. 2016. Combined Use of Mesenchymal Stromal Cell Sheet Transplantation and Local Injection of SDF-1 for Bone Repair in a Rat Nonunion Model. *Cell Transplantation,* 25**,** 1801-1817.

CHEN, S. C., GUO, Y. L., LIU, R. H., WU, S. Y., FANG, J. H., HUANG, B. X., LI, Z. P., CHEN, Z. F. & CHEN, Z. T. 2018. Tuning surface properties of bone biomaterials to manipulate osteoblastic cell adhesion and the signaling pathways for the enhancement of early osseointegration. *Colloids and Surfaces B-Biointerfaces,* 164**,** 58-69.

CHEN, S. F., LIANG, H., JI, Y. H., KOU, H. W., ZHANG, C., SHANG, G. W., SHANG, C. F., SONG, Z. M., YANG, L., LIU, L., WANG, Y. K. & LIU, H. J. 2021. Curcumin Modulates the Crosstalk Between Macrophages and Bone Mesenchymal Stem Cells to Ameliorate Osteogenesis. *Frontiers in Cell and Developmental Biology,* 9.

CHEN, Y., ASPERA-WERZ, R. H., MENGER, M. M., FALLDORF, K., RONNIGER, M., STACKE, C., HISTING, T., NUSSLER, A. K. & EHNERT, S. 2021. Exposure to 16 Hz Pulsed Electromagnetic Fields Protect the Structural Integrity of Primary Cilia and Associated TGF-beta Signaling in Osteoprogenitor Cells Harmed by Cigarette Smoke. *Int J Mol Sci,* 22.

CHEN, Y., GUAN, M., REN, R., GAO, C., CHENG, H., LI, Y., GAO, B., WEI, Y., FU, J., SUN, J. & XIONG, W. 2020. Improved Immunoregulation of Ultra-Low-Dose Silver Nanoparticle-Loaded TiO2 Nanotubes via M2 Macrophage Polarization by Regulating GLUT1 and Autophagy. *Int J Nanomedicine,* 15**,** 2011-2026.

CHEN, Y., MENGER, M., BRAUN, B., LINNEMANN, C., FALLDORF, K., RONNIGER, M., HISTING, T., NUSSLER, A. & EHNERT, S. In preparation. Intermittent ELF-PEMFs improve osteoporosis through activating piezo1-induced Ca2+ influx.

CHEN, Y., MENGER, M. M., BRAUN, B. J., SCHWEIZER, S., LINNEMANN, C., FALLDORF, K., RONNIGER, M., WANG, H., HISTING, T., NUSSLER, A. K. & EHNERT, S. 2021. Modulation of Macrophage Activity by Pulsed Electromagnetic Fields in the Context of Fracture Healing. *Bioengineering (Basel),* 8.

CHEN, Z. T., KLEIN, T., MURRAY, R. Z., CRAWFORD, R., CHANG, J., WU, C. T. & XIAO, Y. 2016. Osteoimmunomodulation for the development of advanced bone biomaterials. *Materials Today,* 19**,** 304-321.

CLAES, L., RECKNAGEL, S. & IGNATIUS, A. 2012. Fracture healing under healthy and inflammatory conditions. *Nat Rev Rheumatol,* 8**,** 133-43.

CLEMENT, C. A., AJBRO, K. D., KOEFOED, K., VESTERGAARD, M. L., VELAND, I. R., HENRIQUES DE JESUS, M. P., PEDERSEN, L. B., BENMERAH, A., ANDERSEN, C. Y., LARSEN, L. A. & CHRISTENSEN, S. T. 2013. TGF-beta signaling is associated with endocytosis at the pocket region of the primary cilium. *Cell Rep,* 3**,** 1806-14.

COSTE, B., MATHUR, J., SCHMIDT, M., EARLEY, T. J., RANADE, S., PETRUS, M. J., DUBIN, A. E. & PATAPOUTIAN, A. 2010. Piezo1 and Piezo2 are essential components of distinct mechanically activated cation channels. *Science,* 330**,** 55-60.

COTTRELL, J. A., TURNER, J. C., ARINZEH, T. L. & O'CONNOR, J. P. 2016. The Biology of Bone and Ligament Healing. *Foot and Ankle Clinics,* 21**,** 739-761.

COX, C. D., BAE, C., ZIEGLER, L., HARTLEY, S., NIKOLOVA-KRSTEVSKI, V., ROHDE, P. R., NG, C. A., SACHS, F., GOTTLIEB, P. A. & MARTINAC, B. 2016. Removal of the mechanoprotective influence of the cytoskeleton reveals PIEZO1 is gated by bilayer tension. *Nature Communications,* 7.

DAISH, C., BLANCHARD, R., FOX, K., PIVONKA, P. & PIROGOVA, E. 2018. The Application of Pulsed Electromagnetic Fields (PEMFs) for Bone Fracture Repair: Past and Perspective Findings. *Annals of Biomedical Engineering,* 46**,** 525-542.

DANCIU, T. E., ADAM, R. M., NARUSE, K., FREEMAN, M. R. & HAUSCHKA, P. V. 2003. Calcium regulates the PI3K-Akt pathway in stretched osteoblasts. *FEBS Lett,* 536**,** 193-7.

DE MATTOS, C. B. R., BINITIE, O. & DORMANS, J. P. 2012. Pathological fractures in children. *Bone & Joint Research,* 1**,** 272-280.

DELANY, A. M. & HANKENSON, K. D. 2009. Thrombospondin-2 and SPARC/osteonectin are critical regulators of bone remodeling. *J Cell Commun Signal,* 3**,** 227-38.

DI GIAMPAOLO, L., DI DONATO, A., ANTONUCCI, A., PAIARDINI, G., TRAVAGLINI, P., SPAGNOLI, G., MAGRINI, A., REALE, M., DADORANTE, V., IANNACCONE, U., DI SCIASCIO, M. B., DI GIOACCHINO, M. & BOSCOLO, P. 2006. Follow up study on the immune response to low frequency electromagnetic fields in men and women working in a museum. *Int J Immunopathol Pharmacol,* 19**,** 37-42.

DITURI, F., COSSU, C., MANCARELLA, S. & GIANNELLI, G. 2019. The Interactivity between TGFbeta and BMP Signaling in Organogenesis, Fibrosis, and Cancer. *Cells,* 8.

DOUGUET, D., PATEL, A., XU, A. M., VANHOUTTE, P. M. & HONORE, E. 2019. Piezo Ion Channels in Cardiovascular Mechanobiology. *Trends in Pharmacological Sciences,* 40**,** 956-970.

DUNDAR, U., ASIK, G., ULASLI, A. M., SINICI, S., YAMAN, F., SOLAK, O., TOKTAS, H. & EROGLU, S. 2016. Assessment of pulsed electromagnetic field therapy with Serum YKL-40 and ultrasonography in patients with knee osteoarthritis. *International Journal of Rheumatic Diseases,* 19**,** 287-293.

EBLE, J. A. & DE REZENDE, F. F. 2014. Redox-Relevant Aspects of the Extracellular Matrix and Its Cellular Contacts via Integrins. *Antioxidants & Redox Signaling,* 20**,** 1977-1993.

EHNERT, S., FALLDORF, K., FENTZ, A. K., ZIEGLER, P., SCHROTER, S., FREUDE, T., OCHS, B. G., STACKE, C., RONNIGER, M., SACHTLEBEN, J. & NUSSLER, A. K. 2015. Primary human osteoblasts with reduced alkaline phosphatase and matrix mineralization baseline capacity are responsive to extremely low frequency pulsed electromagnetic field exposure - Clinical implication possible. *Bone Rep,* 3**,** 48-56.

EHNERT, S., FENTZ, A. K., SCHREINER, A., BIRK, J., WILBRAND, B., ZIEGLER, P., REUMANN, M. K., WANG, H., FALLDORF, K. & NUSSLER, A. K. 2017. Extremely low frequency pulsed electromagnetic fields cause antioxidative defense mechanisms in human osteoblasts via induction of *O2(-) and H2O2. *Sci Rep,* 7**,** 14544.

EHNERT, S., RELJA, B., SCHMIDT-BLEEK, K., FISCHER, V., IGNATIUS, A., LINNEMANN, C., RINDERKNECHT, H., HUBER-LANG, M., KALBITZ, M., HISTING, T. & NUSSLER, A. K. 2021. Effects of immune cells on mesenchymal stem cells during fracture healing. *World J Stem Cells,* 13**,** 1667-1695.

EHNERT, S., SCHROTER, S., ASPERA-WERZ, R. H., EISLER, W., FALLDORF, K., RONNIGER, M. & NUSSLER, A. K. 2019. Translational Insights into Extremely Low Frequency Pulsed Electromagnetic Fields (ELF-PEMFs) for Bone Regeneration after Trauma and Orthopedic Surgery. *Journal of Clinical Medicine,* 8.

EHNERT, S., SREEKUMAR, V., ASPERA-WERZ, R. H., SAJADIAN, S. O., WINTERMEYER, E., SANDMANN, G. H., BAHRS, C., HENGSTLER, J. G., GODOY, P. & NUSSLER, A. K. 2017. TGF-beta(1) impairs mechanosensation of human osteoblasts via HDAC6-mediated shortening and distortion of primary cilia. *Journal of Molecular Medicine-Jmm,* 95**,** 653-663.

EHNERT, S., ZHAO, J., PSCHERER, S., FREUDE, T., DOOLEY, S., KOLK, A., STOCKLE, U., NUSSLER, A. K. & HUBE, R. 2012. Transforming growth factor beta(1) inhibits bone morphogenic protein (BMP)-2 and BMP-7 signaling via upregulation of Ski-related novel protein N (SnoN): possible mechanism for the failure of BMP therapy? *Bmc Medicine,* 10.

EINHORN, T. A. & GERSTENFELD, L. C. 2015. Fracture healing: mechanisms and interventions. *Nature Reviews Rheumatology,* 11**,** 45-54.

ELMAS, O. 2016. Effects of electromagnetic field exposure on the heart: a systematic review. *Toxicol Ind Health,* 32**,** 76-82.

ESMAIL, M. Y., SUN, L., YU, L., XU, H., SHI, L. & ZHANG, J. 2012. Effects of PEMF and glucocorticoids on proliferation and differentiation of osteoblasts. *Electromagn Biol Med,* 31**,** 375-81.

EYRES, K. S., SALEH, M. & KANIS, J. A. 1996. Effect of pulsed electromagnetic fields on bone formation and bone loss during limb lengthening. *Bone,* 18**,** 505-509.

FINKELSTEIN, E., CHANG, W., CHAO, P. H., GRUBER, D., MINDEN, A., HUNG, C. T. & BULINSKI, J. C. 2004. Roles of microtubules, cell polarity and adhesion in electric-field-mediated motility of 3T3 fibroblasts. *J Cell Sci,* 117**,** 1533-45.

FOLEY, K. T., MROZ, T. E., ARNOLD, P. M., CHANDLER, H. C., DIXON, R. A., GIRASOLE, G. J., RENKENS, K. L., RIEW, K. D., SASSO, R. C., SMITH, R. C., TUNG, H., WECHT, D. A. & WHITING, D. M. 2008. Randomized, prospective, and controlled clinical trial of pulsed electromagnetic field stimulation for cervical fusion. *Spine Journal,* 8**,** 436-442.

FORD, M. J., YEYATI, P. L., MALI, G. R., KEIGHREN, M. A., WADDELL, S. H., MJOSENG, H. K., DOUGLAS, A. T., HALL, E. A., SAKAUE-SAWANO, A.,

MIYAWAKI, A., MEEHAN, R. R., BOULTER, L., JACKSON, I. J., MILL, P. & MORT, R. L. 2018. A Cell/Cilia Cycle Biosensor for Single-Cell Kinetics Reveals Persistence of Cilia after G1/S Transition Is a General Property in Cells and Mice. *Dev Cell,* 47**,** 509-523 e5.

FOTIOU, E., MARTIN-ALMEDINA, S., SIMPSON, M. A., LIN, S., GORDON, K., BRICE, G., ATTON, G., JEFFERY, I., REES, D. C., MIGNOT, C., VOGT, J., HOMFRAY, T., SNYDER, M. P., ROCKSON, S. G., JEFFERY, S., MORTIMER, P. S., MANSOUR, S. & OSTERGAARD, P. 2015. Novel mutations in PIEZO1 cause an autosomal recessive generalized lymphatic dysplasia with non-immune hydrops fetalis. *Nature Communications,* 6.

FRACCHIOLLA, N. S., FATTIZZO, B. & CORTELEZZI, A. 2017. Mesenchymal Stem Cells in Myeloid Malignancies: A Focus on Immune Escaping and Therapeutic Implications. *Stem Cells Int,* 2017**,** 6720594.

FUNK, R. H. W., MONSEES, T. & OZKUCUR, N. 2009. Electromagnetic effects - From cell biology to medicine. *Progress in Histochemistry and Cytochemistry,* 43**,** 177-264.

FURST, A., MEIER, D., MICHEL, S., SCHMIDLIN, A., HELD, L. & LAIB, A. 2008. Effect of age on bone mineral density and micro architecture in the radius and tibia of horses: an Xtreme computed tomographic study. *BMC Vet Res,* 4**,** 3.

GERSTENFELD, L. C., ALKHIARY, Y. M., KRALL, E. A., NICHOLLS, F. H., STAPLETON, S. N., FITCH, J. L., BAUER, M., KAYAL, R., GRAVES, D. T., JEPSEN, K. J. & EINHORN, T. A. 2006. Three-dimensional reconstruction of fracture callus morphogenesis. *J Histochem Cytochem,* 54**,** 1215-28.

GERSTENFELD, L. C., CULLINANE, D. M., BARNES, G. L., GRAVES, D. T. & EINHORN, T. A. 2003. Fracture healing as a post-natal developmental process: Molecular, spatial, and temporal aspects of its regulation. *Journal of Cellular Biochemistry,* 88**,** 873-884.

GIBON, E., LOI, F., CORDOVA, L. A., PAJARINEN, J., LIN, T., LU, L., NABESHIMA, A., YAO, Z. & GOODMAN, S. B. 2016. Aging Affects Bone Marrow Macrophage Polarization: Relevance to Bone Healing. *Regen Eng Transl Med,* 2**,** 98-104.

GLIM, J. E., NIESSEN, F. B., EVERTS, V., VAN EGMOND, M. & BEELEN, R. H. J. 2013. Platelet derived growth factor-CC secreted by M2 macrophages induces alpha-smooth muscle actin expression by dermal and gingival fibroblasts. *Immunobiology,* 218**,** 924-929.

GREENBAUM, A., HSU, Y. M. S., DAY, R. B., SCHUETTPELZ, L. G., CHRISTOPHER, M. J., BORGERDING, J. N., NAGASAWA, T. & LINK, D. C. 2013. CXCL12 in early mesenchymal progenitors is. required for haematopoietic stem-cell maintenance. *Nature,* 495**,** 227-230.

GRIER, W. G., MOY, A. S. & HARLEY, B. A. 2017. Cyclic tensile strain enhances human mesenchymal stem cell Smad 2/3 activation and tenogenic differentiation in anisotropic collagen-glycosaminoglycan scaffolds. *Eur Cell Mater,* 33**,** 227-239.

GUAN, M., YAO, W., LIU, R. W., LAM, K. S., NOLTA, J., JIA, J. J., PANGANIBAN, B., MENG, L. P., ZHOU, P., SHAHNAZARI, M., RITCHIE, R. O. & LANE, N. E. 2012. Directing mesenchymal stem cells to bone to augment bone formation and increase bone mass. *Nature Medicine,* 18**,** 456-U159.

HAK, D. J., FITZPATRICK, D., BISHOP, J. A., MARSH, J. L., TILP, S., SCHNETTLER, R., SIMPSON, H. & ALT, V. 2014. Delayed union and nonunions: epidemiology, clinical issues, and financial aspects. *Injury,* 45 Suppl 2**,** S3-7.

HALLORAN, D., DURBANO, H. W. & NOHE, A. 2020. Bone Morphogenetic Protein-2 in Development and Bone Homeostasis. *J Dev Biol,* 8.
HAO, Z., LI, J., LI, B., ALDER, K. D., CAHILL, S. V., MUNGER, A. M., LEE, I., KWON, H. K., BACK, J., XU, S., KANG, M. J. & LEE, F. Y. 2021. Smoking Alters Inflammation and Skeletal Stem and Progenitor Cell Activity During Fracture Healing in Different Murine Strains. *J Bone Miner Res,* 36**,** 186-198.
HARTMANN, K., KOENEN, M., SCHAUER, S., WITTIG-BLAICH, S., AHMAD, M., BASCHANT, U. & TUCKERMANN, J. P. 2016. Molecular Actions of Glucocorticoids in Cartilage and Bone during Health, Disease, and Steroid Therapy. *Physiological Reviews,* 96**,** 409-447.
HE, M., SUBRAMANIAN, R., BANGS, F., OMELCHENKO, T., LIEM, K. F., KAPOOR, T. M. & ANDERSON, K. V. 2014. The kinesin-4 protein Kif7 regulates mammalian Hedgehog signalling by organizing the cilium tip compartment. *Nature Cell Biology,* 16**,** 663-+.
HE, R. T., TU, M. G., HUANG, H. L., TSAI, M. T., WU, J. & HSU, J. T. 2019. Improving the prediction of the trabecular bone microarchitectural parameters using dental cone-beam computed tomography. *BMC Med Imaging,* 19**,** 10.
HE, Y., GAO, Y., ZHANG, Q., ZHOU, G. Y., CAO, F. & YAO, S. T. 2020. IL-4 Switches Microglia/macrophage M1/M2 Polarization and Alleviates Neurological Damage by Modulating the JAK1/STAT6 Pathway Following ICH. *Neuroscience,* 437**,** 161-171.
HELDIN, C. H. & MOUSTAKAS, A. 2016. Signaling Receptors for TGF-beta Family Members. *Cold Spring Harbor Perspectives in Biology,* 8.
HENDRICKX, G., FISCHER, V., LIEDERT, A., VON KROGE, S., HAFFNER-LUNTZER, M., BRYLKA, L., PAWLUS, E., SCHWEIZER, M., YORGAN, T., BARANOWSKY, A., ROLVIEN, T., NEVEN, M., SCHUMACHER, U., BEECH, D. J., AMLING, M., IGNATIUS, A. & SCHINKE, T. 2021. Piezo1 Inactivation in Chondrocytes Impairs Trabecular Bone Formation. *Journal of Bone and Mineral Research,* 36**,** 369-384.
HENRIKSEN, Z., HIKEN, J. F., STEINBERG, T. H. & JORGENSEN, N. R. 2006. The predominant mechanism of intercellular calcium wave propagation changes during long-term culture of human osteoblast-like cells. *Cell Calcium,* 39**,** 435-44.
HERNANDEZ, R. K., DO, T. P., CRITCHLOW, C. W., DENT, R. E. & JICK, S. S. 2012. Patient-related risk factors for fracture-healing complications in the United Kingdom General Practice Research Database. *Acta Orthop,* 83**,** 653-60.
HERNIGOU, J. & SCHUIND, F. 2019. Tobacco and bone fractures: A review of the facts and issues that every orthopaedic surgeon should know. *Bone Joint Res,* 8**,** 255-265.
HIDALGO, A. I., CARRETTA, M. D., ALARCON, P., MANOSALVA, C., MULLER, A., NAVARRO, M., HIDALGO, M. A., KAEHNE, T., TAUBERT, A., HERMOSILLA, C. R. & BURGOS, R. A. 2019. Pro-inflammatory mediators and neutrophils are increased in synovial fluid from heifers with acute ruminal acidosis. *BMC Vet Res,* 15**,** 225.
HIEPEN, C., MENDEZ, P. L. & KNAUS, P. 2020. It Takes Two to Tango: Endothelial TGFbeta/BMP Signaling Crosstalk with Mechanobiology. *Cells,* 9.
HIGGINS, M., OBAIDI, I. & MCMORROW, T. 2019. Primary cilia and their role in cancer. *Oncology Letters,* 17**,** 3041-3047.
HO-SHUI-LING, A., BOLANDER, J., RUSTOM, L. E., JOHNSON, A. W., LUYTEN, F. P. & PICART, C. 2018. Bone regeneration strategies: Engineered scaffolds,

bioactive molecules and stem cells current stage and future perspectives. *Biomaterials,* 180**,** 143-162.
HOEMANN, C. D., EL-GABALAWY, H. & MCKEE, M. D. 2009. In vitro osteogenesis assays: Influence of the primary cell source on alkaline phosphatase activity and mineralization. *Pathologie Biologie,* 57**,** 318-323.
HONG, J. H., LEE, G. T., LEE, J. H., KWON, S. J., PARK, S. H., KIM, S. J. & KIM, I. Y. 2009. Effect of bone morphogenetic protein-6 on macrophages. *Immunology,* 128**,** e442-50.
HORIGUCHI, M., OTA, M. & RIFKIN, D. B. 2012. Matrix control of transforming growth factor-beta function. *Journal of Biochemistry,* 152**,** 321-329.
HOSHIBA, T., KAWAZOE, N., TATEISHI, T. & CHEN, G. P. 2009. Development of Stepwise Osteogenesis-mimicking Matrices for the Regulation of Mesenchymal Stem Cell Functions. *Journal of Biological Chemistry,* 284**,** 31164-31173.
HOUSE, R. V., RATAJCZAK, H. V., GAUGER, J. R., JOHNSON, T. R., THOMAS, P. T. & MCCORMICK, D. L. 1996. Immune function and host defense in rodents exposed to 60-Hz magnetic fields. *Fundam Appl Toxicol,* 34**,** 228-39.
HSU, P. C., YANG, C. T., JABLONS, D. M. & YOU, L. 2020. The Crosstalk between Src and Hippo/YAP Signaling Pathways in Non-Small Cell Lung Cancer (NSCLC). *Cancers,* 12.
HU, Q., NATARAJAN, V. & ZIEGELSTEIN, R. C. 2002. Phospholipase D regulates calcium oscillation frequency and nuclear factor-kappaB activity in histamine-stimulated human endothelial cells. *Biochem Biophys Res Commun,* 292**,** 325-32.
HUANG, Y. F., WANG, X. Y., ZHOU, D. X., ZHOU, W. W., DAI, F. Y. & LIN, H. 2021. Macrophages in heterotopic ossification: from mechanisms to therapy. *Npj Regenerative Medicine,* 6.
HUI, C. F., CHAN, C. W., YEUNG, H. Y., LEE, K. M., QIN, L., LI, G., LEUNG, K. S., HU, Y. Y. & CHENG, J. C. 2011. Low-intensity pulsed ultrasound enhances posterior spinal fusion implanted with mesenchymal stem cells-calcium phosphate composite without bone grafting. *Spine (Phila Pa 1976),* 36**,** 1010-6.
ISHIKAWA, M., ITO, H., KITAORI, T., MURATA, K., SHIBUYA, H., FURU, M., YOSHITOMI, H., FUJII, T., YAMAMOTO, K. & MATSUDA, S. 2014. MCP/CCR2 Signaling Is Essential for Recruitment of Mesenchymal Progenitor Cells during the Early Phase of Fracture Healing. *Plos One,* 9.
JACOBS, C. R., TEMIYASATHIT, S. & CASTILLO, A. B. 2010. Osteocyte mechanobiology and pericellular mechanics. *Annu Rev Biomed Eng,* 12**,** 369-400.
JENIS, L. G., AN, H. S., STEIN, R. & YOUNG, B. 2000. Prospective comparison of the effect of direct current electrical stimulation and pulsed electromagnetic fields on instrumented posterolateral lumbar arthrodesis. *J Spinal Disord,* 13**,** 290-6.
JIANG, Y., YANG, X. Z., JIANG, J. H. & XIAO, B. L. 2021. Structural Designs and Mechanogating Mechanisms of the Mechanosensitive Piezo Channels. *Trends in Biochemical Sciences,* 46**,** 472-488.
KAESTNER, L., BOGDANOVA, A. & EGEE, S. 2020. Calcium Channels and Calcium-Regulated Channels in Human Red Blood Cells. *Adv Exp Med Biol,* 1131**,** 625-648.
KAKU, M. & KOMATSU, Y. 2017. Functional Diversity of Ciliary Proteins in Bone Development and Disease. *Current Osteoporosis Reports,* 15**,** 96-102.

KANIS, J. A., NORTON, N., HARVEY, N. C., JACOBSON, T., JOHANSSON, H., LORENTZON, M., MCCLOSKEY, E. V., WILLERS, C. & BORGSTROM, F. 2021. SCOPE 2021: a new scorecard for osteoporosis in Europe. *Archives of Osteoporosis,* 16.

KAPLAN, M. J. & RADIC, M. 2012. Neutrophil extracellular traps: double-edged swords of innate immunity. *J Immunol,* 189**,** 2689-95.

KEATING, J. F., SIMPSON, A. H. & ROBINSON, C. M. 2005. The management of fractures with bone loss. *J Bone Joint Surg Br,* 87**,** 142-50.

KIM, Y. S., NOH, M. Y., KIM, J. Y., YU, H. J., KIM, K. S., KIM, S. H. & KOH, S. H. 2013. Direct GSK-3 beta Inhibition Enhances Mesenchymal Stromal Cell Migration by Increasing Expression of Beta-PIX and CXCR4. *Molecular Neurobiology,* 47**,** 811-820.

KITAMURA, A., KAWASAKI, M., KAWASAKI, K., MEGURO, F., YAMADA, A., NAGAI, T., KODAMA, Y., TRAKANANT, S., SHARPE, P. T., MAEDA, T., TAKAGI, R. & OHAZAMA, A. 2020. Ift88 is involved in mandibular development. *Journal of Anatomy,* 236**,** 317-324.

KOBAYASHI, S. D., MALACHOWA, N. & DELEO, F. R. 2018. Neutrophils and Bacterial Immune Evasion. *J Innate Immun,* 10**,** 432-441.

KOBAYASHI, T. & DYNLACHT, B. D. 2011. Regulating the transition from centriole to basal body. *Journal of Cell Biology,* 193**,** 435-444.

KOZMINSKI, K. G., JOHNSON, K. A., FORSCHER, P. & ROSENBAUM, J. L. 1993. A Motility in the Eukaryotic Flagellum Unrelated to Flagellar Beating. *Proceedings of the National Academy of Sciences of the United States of America,* 90**,** 5519-5523.

LABUSCA, L., ZUGUN-ELOAE, F. & MASHAYEKHI, K. 2015. Stem cells for the treatment of musculoskeletal pain. *World J Stem Cells,* 7**,** 96-105.

LAFUENTE-GRACIA, L., BORGIANI, E., NASELLO, G. & GERIS, L. 2021. Towards in silico Models of the Inflammatory Response in Bone Fracture Healing. *Front Bioeng Biotechnol,* 9**,** 703725.

LAI, J. C., LI, L., WANG, D. P., ZHANG, M. H., MO, S. R., WANG, X., ZENG, K. Y., LI, C. H., JIANG, Q., YOU, X. Z. & ZUO, J. L. 2018. A rigid and healable polymer cross-linked by weak but abundant Zn(II)-carboxylate interactions. *Nature Communications,* 9.

LAI, Y. S., WAHYUNINGTYAS, R., AUI, S. P. & CHANG, K. T. 2019. Autocrine VEGF signalling on M2 macrophages regulates PD-L1 expression for immunomodulation of T cells. *Journal of Cellular and Molecular Medicine,* 23**,** 1257-1267.

LEE, H. Y., CHO, K. M., KIM, M. K., LEE, M., KIM, H., CHOI, C. Y., KIM, K. K., PARK, J. S., KIM, H. H. & BAE, Y. S. 2021. Sphingosylphosphorylcholine blocks ovariectomy-induced bone loss by suppressing Ca(2+) /calmodulin-mediated osteoclast differentiation. *J Cell Mol Med,* 25**,** 473-483.

LEMMON, M. A. & SCHLESSINGER, J. 2010. Cell Signaling by Receptor Tyrosine Kinases. *Cell,* 141**,** 1117-1134.

LI, C., XING, Q., YU, B., XIE, H., WANG, W., SHI, C., CRANE, J. L., CAO, X. & WAN, M. 2013. Disruption of LRP6 in osteoblasts blunts the bone anabolic activity of PTH. *J Bone Miner Res,* 28**,** 2094-108.

LI, R. D., DENG, Z. L., HU, N., LIANG, X., LIU, B., LUO, J. Y., CHEN, L., YIN, L. J., LUO, X. J., SHUI, W., HE, T. C. & HUANG, W. 2012. Biphasic effects of TGF beta 1 on BMP9-induced osteogenic differentiation of mesenchymal stem cells. *Bmb Reports,* 45**,** 509-514.

LI, S., JIANG, H., WANG, B., GU, M., BI, X., YIN, Y. & WANG, Y. 2018. Magnetic Resonance Spectroscopy for Evaluating the Effect of Pulsed Electromagnetic Fields on Marrow Adiposity in Postmenopausal Women With Osteopenia. *J Comput Assist Tomogr,* 42**,** 792-797.
LI, X., HAN, L., NOOKAEW, I., MANNEN, E., SILVA, M. J., ALMEIDA, M. & XIONG, J. 2019. Stimulation of Piezo1 by mechanical signals promotes bone anabolism. *Elife,* 8.
LIAO, C. S., ZHANG, C. F., JIN, L. J. & YANG, Y. Q. 2020. IL-17 alters the mesenchymal stem cell niche towards osteogenesis in cooperation with osteocytes. *Journal of Cellular Physiology,* 235**,** 4466-4480.
LIEN, C. Y., HO, K. C. Y., LEE, O. K., BLUNN, G. W. & SU, Y. 2009. Restoration of Bone Mass and Strength in Glucocorticoid-Treated Mice by Systemic Transplantation of CXCR4 and Cbfa-1 Co-Expressing Mesenchymal Stem Cells. *Journal of Bone and Mineral Research,* 24**,** 837-848.
LIN, H. Y. & LIN, Y. J. 2011. In vitro effects of low frequency electromagnetic fields on osteoblast proliferation and maturation in an inflammatory environment. *Bioelectromagnetics,* 32**,** 552-60.
LIN, Q., DONG, L., XU, Y. & DI, G. 2018. Studies on effects of static electric field exposure on liver in mice. *Sci Rep,* 8**,** 15507.
LINNEMANN, C., VENTURELLI, S., KONRAD, F., NUSSLER, A. K. & EHNERT, S. 2020. Bio-impedance measurement allows displaying the early stages of neutrophil extracellular traps. *EXCLI J,* 19**,** 1481-1495.
LIU, H. L., HU, J. L., ZHENG, Q. C., FENG, X. J., ZHAN, F. F., WANG, X. F., XU, G. H. & HUA, F. Z. 2022. Piezo1 Channels as Force Sensors in Mechanical Force-Related Chronic Inflammation. *Frontiers in Immunology,* 13.
LIU, Q., LI, M., WANG, S. Y., XIAO, Z. S., XIONG, Y. Y. & WANG, G. W. 2020. Recent Advances of Osterix Transcription Factor in Osteoblast Differentiation and Bone Formation. *Frontiers in Cell and Developmental Biology,* 8.
LIU, Z. Z., KUANG, W. L., ZHOU, Q. & ZHANG, Y. Y. 2018. TGF-beta 1 secreted by M2 phenotype macrophages enhances the stemness and migration of glioma cells via the SMAD2/3 signalling pathway. *International Journal of Molecular Medicine,* 42**,** 3395-3403.
LOFFLER, J., SASS, F. A., FILTER, S., ROSE, A., ELLINGHAUS, A., DUDA, G. N. & DIENELT, A. 2019. Compromised Bone Healing in Aged Rats Is Associated With Impaired M2 Macrophage Function. *Frontiers in Immunology,* 10.
LOI, F., CORDOVA, L. A., PAJARINEN, J., LIN, T. H., YAO, Z. & GOODMAN, S. B. 2016. Inflammation, fracture and bone repair. *Bone,* 86**,** 119-30.
LOPES, R. L., BORGES, T. J., ZANIN, R. F. & BONORINO, C. 2016. IL-10 is required for polarization of macrophages to M2-like phenotype by mycobacterial DnaK (heat shock protein 70). *Cytokine,* 85**,** 123-129.
LU, P. F., TAKAI, K., WEAVER, V. M. & WERB, Z. 2011. Extracellular Matrix Degradation and Remodeling in Development and Disease. *Cold Spring Harbor Perspectives in Biology,* 3.
LUO, K. 2017. Signaling Cross Talk between TGF-beta/Smad and Other Signaling Pathways. *Cold Spring Harb Perspect Biol,* 9.
LV, H. H., LIU, J. Y., ZHEN, C. X., WANG, Y. J., WEI, Y. P., REN, W. H. & SHANG, P. 2021. Magnetic fields as a potential therapy for diabetic wounds based on animal experiments and clinical trials. *Cell Proliferation,* 54.
MAHER, E. R., AFNAN, M. & BARRATT, C. L. 2003. Epigenetic risks related to assisted reproductive technologies: epigenetics, imprinting, ART and icebergs? *Hum Reprod,* 18**,** 2508-11.

MAKOWSKI, M., SILVA, I. C., PAIS DO AMARAL, C., GONCALVES, S. & SANTOS, N. C. 2019. Advances in Lipid and Metal Nanoparticles for Antimicrobial Peptide Delivery. *Pharmaceutics,* 11.

MALONE, A. M. D., ANDERSON, C. T., TUMMALA, P., KWON, R. Y., JOHNSTON, T. R., STEARNS, T. & JACOBS, C. R. 2007. Primary cilia mediate mechanosensing in bone cells by a calcium-independent mechanism. *Proceedings of the National Academy of Sciences of the United States of America,* 104**,** 13325-13330.

MAN, Z. T., SHA, D., SUN, S., LI, T., LI, B., YANG, G., ZHANG, L. B., WU, C. S., JIANG, P., HAN, X. J. & LI, W. 2016. In Vitro Bioactivity Study of RGD-Coated Titanium Alloy Prothesis for Revision Total Hip Arthroplasty. *Biomed Research International,* 2016.

MARSELL, R. & EINHORN, T. A. 2011. The biology of fracture healing. *Injury,* 42**,** 551-5.

MARTIN, T. J. & RODAN, G. A. 2008. Intercellular Communication during Bone Remodeling. *Osteoporosis, Vols I and Ii, 3rd Edition***,** 547-560.

MARTINEZ-RONDANELLI, A., MARTINEZ, J. P., MONCADA, M. E., MANZI, E., PINEDO, C. R. & CADAVID, H. 2014. Electromagnetic stimulation as coadjuvant in the healing of diaphyseal femoral fractures: a randomized controlled trial. *Colombia Medica,* 45**,** 67-71.

MARTINI, F., PELLATI, A., MAZZONI, E., SALATI, S., CARUSO, G., CONTARTESE, D. & DE MATTEI, M. 2020. Bone Morphogenetic Protein-2 Signaling in the Osteogenic Differentiation of Human Bone Marrow Mesenchymal Stem Cells Induced by Pulsed Electromagnetic Fields. *Int J Mol Sci,* 21.

MARUYAMA, M., RHEE, C., UTSUNOMIYA, T., ZHANG, N., UENO, M., YAO, Z. & GOODMAN, S. B. 2020. Modulation of the Inflammatory Response and Bone Healing. *Front Endocrinol (Lausanne),* 11**,** 386.

MASYUK, A. I., MASYUK, T. V. & LARUSSO, N. F. 2008. Cholangiocyte primary cilia in liver health and disease. *Developmental Dynamics,* 237**,** 2007-2012.

MATHIEU, P. S. & LOBOA, E. G. 2012. Cytoskeletal and focal adhesion influences on mesenchymal stem cell shape, mechanical properties, and differentiation down osteogenic, adipogenic, and chondrogenic pathways. *Tissue Eng Part B Rev,* 18**,** 436-44.

MCGLASHAN, S. R., JENSEN, C. G. & POOLE, C. A. 2006. Localization of extracellular matrix receptors on the chondrocyte primary cilium. *J Histochem Cytochem,* 54**,** 1005-14.

MEDINA-GOMEZ, C., CHESI, A., HEPPE, D. H. M., ZEMEL, B. S., YIN, J. L., KALKWARF, H. J., HOFMAN, A., LAPPE, J. M., KELLY, A., KAYSER, M., OBERFIELD, S. E., GILSANZ, V., UITTERLINDEN, A. G., SHEPHERD, J. A., JADDOE, V. W. V., GRANT, S. F. A., LAO, O. & RIVADENEIRA, F. 2015. BMD Loci Contribute to Ethnic and Developmental Differences in Skeletal Fragility across Populations: Assessment of Evolutionary Selection Pressures. *Molecular Biology and Evolution,* 32**,** 2961-2972.

MENZL, I., LEBEAU, L., PANDEY, R., HASSOUNAH, N. B., LI, F. W., NAGLE, R., WEIHS, K. & MCDERMOTT, K. M. 2014. Loss of primary cilia occurs early in breast cancer development. *Cilia,* 3**,** 7.

METSEMAKERS, W. J., HANDOJO, K., REYNDERS, P., SERMON, A., VANDERSCHOT, P. & NIJS, S. 2015. Individual risk factors for deep infection and compromised fracture healing after intramedullary nailing of tibial shaft fractures: a single centre experience of 480 patients. *Injury,* 46**,** 740-5.

MILLS, L., TSANG, J., HOPPER, G., KEENAN, G. & SIMPSON, A. H. 2016. The multifactorial aetiology of fracture nonunion and the importance of searching for latent infection. *Bone Joint Res,* 5**,** 512-519.
MILLS, L. A., AITKEN, S. A. & SIMPSON, A. 2017. The risk of non-union per fracture: current myths and revised figures from a population of over 4 million adults. *Acta Orthop,* 88**,** 434-439.
MILLS, L. A. & SIMPSON, A. H. 2013. The relative incidence of fracture non-union in the Scottish population (5.17 million): a 5-year epidemiological study. *BMJ Open,* 3.
MILY, A., KALSUM, S., LORETI, M. G., REKHA, R. S., MUVVA, J. R., LOURDA, M. & BRIGHENTI, S. 2020. Polarization of M1 and M2 Human Monocyte-Derived Cells and Analysis with Flow Cytometry upon Mycobacterium tuberculosis Infection (Sep, 10.3791/61807, 2020). *Jove-Journal of Visualized Experiments*.
MONTEITH, G. R., PREVARSKAYA, N. & ROBERTS-THOMSON, S. J. 2017. The calcium-cancer signalling nexus. *Nature Reviews Cancer,* 17**,** 367-380.
MORONI, M., SERVIN-VENCES, M. R., FLEISCHER, R., SANCHEZ-CARRANZA, O. & LEWIN, G. R. 2018. Voltage gating of mechanosensitive PIEZO channels. *Nature Communications,* 9.
MUKHERJEE, S., KOLB, M. R., DUAN, F. & JANSSEN, L. J. 2012. Transforming growth factor-beta evokes Ca2+ waves and enhances gene expression in human pulmonary fibroblasts. *Am J Respir Cell Mol Biol,* 46**,** 757-64.
MUNOZ, J., AKHAVAN, N. S., MULLINS, A. P. & ARJMANDI, B. H. 2020. Macrophage Polarization and Osteoporosis: A Review. *Nutrients,* 12.
MURRAY, P. J. 2017. Macrophage Polarization. *Annu Rev Physiol,* 79**,** 541-566.
MUTTIGI, M. S., HAN, I., PARK, H. K., PARK, H. & LEE, S. H. 2016. Matrilin-3 Role in Cartilage Development and Osteoarthritis. *International Journal of Molecular Sciences,* 17.
MUTUA, V. & GERSHWIN, L. J. 2021. A Review of Neutrophil Extracellular Traps (NETs) in Disease: Potential Anti-NETs Therapeutics. *Clin Rev Allergy Immunol,* 61**,** 194-211.
MYKYTYN, K. & ASKWITH, C. 2017. G-Protein-Coupled Receptor Signaling in Cilia. *Cold Spring Harbor Perspectives in Biology,* 9.
NICHOLSON, J. A., MAKARAM, N., SIMPSON, A. & KEATING, J. F. 2021. Fracture nonunion in long bones: A literature review of risk factors and surgical management. *Injury,* 52 Suppl 2**,** S3-S11.
NICKEL, J., TEN DIJKE, P. & MUELLER, T. D. 2018. TGF-beta family co-receptor function and signaling. *Acta Biochimica Et Biophysica Sinica,* 50**,** 12-36.
NORIEGA-LUNA, B., SABANERO, M., SOSA, M. & AVILA-RODRIGUEZ, M. 2011. Influence of pulsed magnetic fields on the morphology of bone cells in early stages of growth. *Micron,* 42**,** 600-7.
ORECCHIONI, M., GHOSHEH, Y., PRAMOD, A. B. & LEY, K. 2020. Macrophage Polarization: Different Gene Signatures in M1(LPS+) vs. Classically and M2(LPS-) vs. Alternatively Activated Macrophages (vol 10, 1084, 2019). *Frontiers in Immunology,* 11.
ORRU, V., STERI, M., SOLE, G., SIDORE, C., VIRDIS, F., DEI, M., LAI, S., ZOLEDZIEWSKA, M., BUSONERO, F., MULAS, A., FLORIS, M., MENTZEN, W. I., URRU, S. A., OLLA, S., MARONGIU, M., PIRAS, M. G., LOBINA, M., MASCHIO, A., PITZALIS, M., URRU, M. F., MARCELLI, M., CUSANO, R., DEIDDA, F., SERRA, V., OPPO, M., PILU, R., REINIER, F., BERUTTI, R., PIREDDU, L., ZARA, I., PORCU, E., KWONG, A., BRENNAN, C., TARRIER, B., LYONS, R., KANG, H. M., UZZAU, S., ATZENI, R., VALENTINI, M., FIRINU,

D., LEONI, L., ROTTA, G., NAITZA, S., ANGIUS, A., CONGIA, M., WHALEN, M. B., JONES, C. M., SCHLESSINGER, D., ABECASIS, G. R., FIORILLO, E., SANNA, S. & CUCCA, F. 2013. Genetic variants regulating immune cell levels in health and disease. *Cell,* 155**,** 242-56.

PATIL, S. & MONTGOMERY, R. 2006. Management of complex tibial and femoral nonunion using the Ilizarov technique, and its cost implications. *J Bone Joint Surg Br,* 88**,** 928-32.

PAUN, I. A., POPESCU, R. C., CALIN, B. S., MUSTACIOSU, C. C., DINESCU, M. & LUCULESCU, C. R. 2018. 3D Biomimetic Magnetic Structures for Static Magnetic Field Stimulation of Osteogenesis. *Int J Mol Sci,* 19.

PAUTKE, C., SCHIEKER, M., TISCHER, T., KOLK, A., NETH, P., MUTSCHLER, W. & MILZ, S. 2004. Characterization of osteosarcoma cell lines MG-63, Saos-2 and U-2OS in comparison to human osteoblasts. *Anticancer Research,* 24**,** 3743-3748.

PELAEZ, D., ARITA, N. & CHEUNG, H. S. 2012. Extracellular signal-regulated kinase (ERK) dictates osteogenic and/or chondrogenic lineage commitment of mesenchymal stem cells under dynamic compression. *Biochem Biophys Res Commun,* 417**,** 1286-91.

PENG, H. R., USAS, A., OLSHANSKI, A., HO, A. M., GEARHART, B., COOPER, G. M. & HUARD, J. 2005. VEGF improves, whereas sFlt1 inhibits, BMP2-induced bone formation and bone healing through modulation of angiogenesis. *Journal of Bone and Mineral Research,* 20**,** 2017-2027.

PENG, L. H., FU, C. Y., WANG, L., ZHANG, Q., LIANG, Z. J., HE, C. Q. & WEI, Q. 2021. The Effect of Pulsed Electromagnetic Fields on Angiogenesis. *Bioelectromagnetics,* 42**,** 250-258.

PIGNOLO, R. J., LAW, S. F. & CHANDRA, A. 2021. Bone Aging, Cellular Senescence, and Osteoporosis. *Jbmr Plus,* 5.

PORTA, C., RIMOLDI, M., RAES, G., BRYS, L., GHEZZI, P., DI LIBERTO, D., DIELI, F., GHISLETTI, S., NATOLI, G., DE BAETSELIER, P., MANTOVANI, A. & SICA, A. 2009. Tolerance and M2 (alternative) macrophage polarization are related processes orchestrated by p50 nuclear factor kappa B. *Proceedings of the National Academy of Sciences of the United States of America,* 106**,** 14978-14983.

PREVO, B., SCHOLEY, J. M. & PETERMAN, E. J. G. 2017. Intraflagellar transport: mechanisms of motor action, cooperation, and cargo delivery. *Febs Journal,* 284**,** 2905-2931.

QUARLES, L. D., YOHAY, D. A., LEVER, L. W., CATON, R. & WENSTRUP, R. J. 1992. Distinct proliferative and differentiated stages of murine MC3T3-E1 cells in culture: an in vitro model of osteoblast development. *J Bone Miner Res,* 7**,** 683-92.

RAGGI, F., PELASSA, S., PIEROBON, D., PENCO, F., GATTORNO, M., NOVELLI, F., EVA, A., VARESIO, L., GIOVARELLI, M. & BOSCO, M. C. 2017. Regulation of Human Macrophage M1-M2 Polarization Balance by Hypoxia and the Triggering Receptor Expressed on Myeloid Cells-1. *Frontiers in Immunology,* 8.

RAHMAN, M. S., AKHTAR, N., JAMIL, H. M., BANIK, R. S. & ASADUZZAMAN, S. M. 2015. TGF-beta/BMP signaling and other molecular events: regulation of osteoblastogenesis and bone formation. *Bone Res,* 3**,** 15005.

RANADE, S. S., QIU, Z. Z., WOO, S. H., HUR, S. S., MURTHY, S. E., CAHALAN, S. M., XU, J., MATHUR, J., BANDELL, M., COSTE, B., LI, Y. S. J., CHIEN, S. & PATAPOUTIAN, A. 2014. Piezo1, a mechanically activated ion channel, is

required for vascular development in mice. *Proceedings of the National Academy of Sciences of the United States of America,* 111**,** 10347-10352.
RAO, X., HUANG, X., ZHOU, Z. & LIN, X. 2013. An improvement of the 2^(-delta delta CT) method for quantitative real-time polymerase chain reaction data analysis. *Biostat Bioinforma Biomath,* 3**,** 71-85.
RAVETTO, A., WYSS, H. M., ANDERSON, P. D., DEN TOONDER, J. M. & BOUTEN, C. V. 2014. Monocytic cells become less compressible but more deformable upon activation. *PLoS One,* 9**,** e92814.
REBL, H., FINKE, B., IHRKE, R., ROTHE, H., RYCHLY, J., SCHROEDER, K. & NEBE, B. J. 2010. Positively Charged Material Surfaces Generated by Plasma Polymerized Allylamine Enhance Vinculin Mobility in Vital Human Osteoblasts. *Advanced Engineering Materials,* 12**,** B356-B364.
REEVES, E. P., LU, H., LORTAT-JACOB, H., MESSINA, C. G. M., BOLSOVER, S., GABELLA, G., POTMA, E. O., WARLEY, A., ROES, J. & SEGAL, A. W. 2002. Killing activity of neutrophils is mediated through activation of proteases by K+ flux. *Nature,* 416**,** 291-297.
REITER, J. F. & LEROUX, M. R. 2017. Genes and molecular pathways underpinning ciliopathies. *Nat Rev Mol Cell Biol,* 18**,** 533-547.
REMEDIOS, A. 1999. Bone and bone healing. *Vet Clin North Am Small Anim Pract,* 29**,** 1029-44, v.
ROMANELLO, M., PADOAN, M., FRANCO, L., VERONESI, V., MORO, L. & D'ANDREA, P. 2001. Extracellular NAD(+) induces calcium signaling and apoptosis in human osteoblastic cells. *Biochem Biophys Res Commun,* 285**,** 1226-31.
ROSS, C. L., SIRIWARDANE, M., ALMEIDA-PORADA, G., PORADA, C. D., BRINK, P., CHRIST, G. J. & HARRISON, B. S. 2015. The effect of low-frequency electromagnetic field on human bone marrow stem/progenitor cell differentiation. *Stem Cell Res,* 15**,** 96-108.
SAFARI, M., JADIDI, M., BAGHIAN, A. & HASANZADEH, H. 2016. Proliferation and differentiation of rat bone marrow stem cells by 400 mu T electromagnetic field. *Neuroscience Letters,* 612**,** 1-6.
SALASZNYK, R. M., KLEES, R. F., WILLIAMS, W. A., BOSKEY, A. & PLOPPER, G. E. 2007. Focal adhesion kinase signaling pathways regulate the osteogenic differentiation of human mesenchymal stem cells. *Experimental Cell Research,* 313**,** 22-37.
SASAKI, F., HAYASHI, M., MOURI, Y., NAKAMURA, S., ADACHI, T. & NAKASHIMA, T. 2020. Mechanotransduction via the Piezo1-Akt pathway underlies Sost suppression in osteocytes. *Biochem Biophys Res Commun,* 521**,** 806-813.
SATERNOS, H., LEY, S. & ABOUALAIWI, W. 2020. Primary Cilia and Calcium Signaling Interactions. *International Journal of Molecular Sciences,* 21.
SATO, K. & TAKAYANAGI, H. 2006. Osteoclasts, rheumatoid arthritis, and osteoimmunology. *Current Opinion in Rheumatology,* 18**,** 419-426.
SCHAFFLER, M. B., CHEUNG, W. Y., MAJESKA, R. & KENNEDY, O. 2014. Osteocytes: Master Orchestrators of Bone. *Calcified Tissue International,* 94**,** 5-24.
SCHEMITSCH, E. H., BHANDARI, M., GUYATT, G., SANDERS, D. W., SWIONTKOWSKI, M., TORNETTA, P., WALTER, S. D., ZDERO, R., GOSLINGS, J. C., TEAGUE, D., JERAY, K., MCKEE, M. D. & STUDY TO PROSPECTIVELY EVALUATE REAMED INTRAMEDULLARY NAILS IN PATIENTS WITH TIBIAL FRACTURES, I. 2012. Prognostic factors for

predicting outcomes after intramedullary nailing of the tibia. *J Bone Joint Surg Am,* 94**,** 1786-93.
SCHWARTZ, E. A., LEONARD, M. L., BIZIOS, R. & BOWSER, S. S. 1997. Analysis and modeling of the primary cilium bending response to fluid shear. *Am J Physiol,* 272**,** F132-8.
SCOLARO, J. A., SCHENKER, M. L., YANNASCOLI, S., BALDWIN, K., MEHTA, S. & AHN, J. 2014. Cigarette smoking increases complications following fracture: a systematic review. *J Bone Joint Surg Am,* 96**,** 674-81.
SEEGER-NUKPEZAH, T. & GOLEMIS, E. A. 2012. The extracellular matrix and ciliary signaling. *Current Opinion in Cell Biology,* 24**,** 652-661.
SHAPOURI-MOGHADDAM, A., MOHAMMADIAN, S., VAZINI, H., TAGHADOSI, M., ESMAEILI, S. A., MARDANI, F., SEIFI, B., MOHAMMADI, A., AFSHARI, J. T. & SAHEBKAR, A. 2018. Macrophage plasticity, polarization, and function in health and disease. *J Cell Physiol,* 233**,** 6425-6440.
SHEN, X., SHEN, X., LI, B., ZHU, W. W., FU, Y., XU, R. Y., DU, Y. F., CHENG, J. & JIANG, H. B. 2021. Abnormal macrophage polarization impedes the healing of diabetes- associated tooth sockets. *Bone,* 143.
SHI, H. F., XIONG, J., CHEN, Y. X., WANG, J. F., QIU, X. S., WANG, Y. H. & QIU, Y. 2013. Early application of pulsed electromagnetic field in the treatment of postoperative delayed union of long-bone fractures: a prospective randomized controlled study. *BMC Musculoskelet Disord,* 14**,** 35.
SINGH, K., AGRAWAL, N. K., GUPTA, S. K., SINHA, P. & SINGH, K. 2016. Increased expression of TLR9 associated with pro-inflammatory S100A8 and IL-8 in diabetic wounds could lead to unresolved inflammation in type 2 diabetes mellitus (T2DM) cases with impaired wound healing. *J Diabetes Complications,* 30**,** 99-108.
SMALL, A. G., HARVEY, S., KAUR, J., PUTTY, T., QUACH, A., MUNAWARA, U., PERVEEN, K., MCPHEE, A., HII, C. S. & FERRANTE, A. 2021. Vitamin D upregulates the macrophage complement receptor immunoglobulin in innate immunity to microbial pathogens. *Communications Biology,* 4.
SONG, B., ZHAO, M., FORRESTER, J. V. & MCCAIG, C. D. 2002. Electrical cues regulate the orientation and frequency of cell division and the rate of wound healing in vivo. *Proc Natl Acad Sci U S A,* 99**,** 13577-82.
SONG, J., LIU, L., LV, L., HU, S., TARIQ, A., WANG, W. & DANG, X. 2020. Fluid shear stress induces Runx-2 expression via upregulation of PIEZO1 in MC3T3-E1 cells. *Cell Biol Int,* 44**,** 1491-1502.
SREEKUMAR, V., ASPERA-WERZ, R., EHNERT, S., STROBEL, J., TENDULKAR, G., HEID, D., SCHREINER, A., ARNSCHEIDT, C. & NUSSLER, A. K. 2018. Resveratrol protects primary cilia integrity of human mesenchymal stem cells from cigarette smoke to improve osteogenic differentiation in vitro. *Archives of Toxicology,* 92**,** 1525-1538.
STREET, J., WINTER, D., WANG, J. H., WAKAI, A., MCGUINNESS, A. & REDMOND, H. P. 2000. Is human fracture hematoma inherently angiogenic? *Clinical Orthopaedics and Related Research***,** 224-237.
SUN, W., CHI, S., LI, Y., LING, S., TAN, Y., XU, Y., JIANG, F., LI, J., LIU, C., ZHONG, G., CAO, D., JIN, X., ZHAO, D., GAO, X., LIU, Z., XIAO, B. & LI, Y. 2019. The mechanosensitive Piezo1 channel is required for bone formation. *Elife,* 8.
TAKAYANAGI, H. 2007. Osteoimmunology: shared mechanisms and crosstalk between the immune and bone systems. *Nature Reviews Immunology,* 7**,** 292-304.

TAO, D., XUE, H., ZHANG, C., LI, G. & SUN, Y. 2019. The Role of IFT140 in Osteogenesis of Adult Mice Long Bone. *J Histochem Cytochem,* 67**,** 601-611.
TASCHNER, M., BHOGARAJU, S. & LORENTZEN, E. 2012. Architecture and function of IFT complex proteins in ciliogenesis. *Differentiation,* 83**,** S12-22.
TEMIYASATHIT, S. & JACOBS, C. R. 2010. Osteocyte primary cilium and its role in bone mechanotransduction. *Ann N Y Acad Sci,* 1192**,** 422-8.
TEMIYASATHIT, S., TANG, W. J., LEUCHT, P., ANDERSON, C. T., MONICA, S. D., CASTILLO, A. B., HELMS, J. A., STEARNS, T. & JACOBS, C. R. 2012. Mechanosensing by the primary cilium: deletion of Kif3A reduces bone formation due to loading. *PLoS One,* 7**,** e33368.
TITUSHKIN, I. & CHO, M. 2011. Altered osteogenic commitment of human mesenchymal stem cells by ERM protein-dependent modulation of cellular biomechanics. *Journal of Biomechanics,* 44**,** 2692-2698.
TITUSHKIN, I. A. & CHO, M. R. 2009. Controlling cellular biomechanics of human mesenchymal stem cells. *Annu Int Conf IEEE Eng Med Biol Soc,* 2009**,** 2090-3.
TO, K., ROMAIN, K., MAK, C., KAMARAJ, A., HENSON, F. & KHAN, W. 2020. The Treatment of Cartilage Damage Using Human Mesenchymal Stem Cell-Derived Extracellular Vesicles: A Systematic Review ofin vivoStudies. *Frontiers in Bioengineering and Biotechnology,* 8.
TONNA, E. A. & LAMPEN, N. M. 1972. Electron-Microscopy of Aging Skeletal Cells .1. Centrioles and Solitary Cilia. *Journals of Gerontology,* 27**,** 316-+.
TSUKASAKI, M. & TAKAYANAGI, H. 2019. Osteoimmunology: evolving concepts in bone-immune interactions in health and disease. *Nature Reviews Immunology,* 19**,** 626-642.
TU, D. P., LIU, Z., YU, Y. K., XU, C. & SHI, X. L. 2020. Internal Fixation versus Hemiarthroplasty in the Treatment of Unstable Intertrochanteric Fractures in the Elderly: A Systematic Review and Meta-Analysis. *Orthopaedic Surgery,* 12**,** 1053-1064.
TUSCHL, H., NEUBAUER, G., SCHMID, G., WEBER, E. & WINKER, N. 2000. Occupational exposure to static, ELF, VF and VLF magnetic fields and immune parameters. *Int J Occup Med Environ Health,* 13**,** 39-50.
UZER, G., BAS, G., SEN, B., XIE, Z., BIRKS, S., OLCUM, M., MCGRATH, C., STYNER, M. & RUBIN, J. 2018. Sun-mediated mechanical LINC between nucleus and cytoskeleton regulates betacatenin nuclear access. *J Biomech,* 74**,** 32-40.
VICTORIA, G., PETRISOR, B., DREW, B. & DICK, D. 2009. Bone stimulation for fracture healing: Whats all the fuss. *Indian Journal of Orthopaedics,* 43**,** 117-120.
VIOLA, A., MUNARI, F., SANCHEZ-RODRIGUEZ, R., SCOLARO, T. & CASTEGNA, A. 2019. The Metabolic Signature of Macrophage Responses. *Frontiers in Immunology,* 10.
WAGNER, C., KAKSA, A., MULLER, W., DENEFLEH, B., HEPPERT, V., WENTZENSEN, A. & HANSCH, G. M. 2004. Polymorphonuclear neutrophils in posttraumatic osteomyelitis: cells recovered from the inflamed site lack chemotactic activity but generate superoxides. *Shock,* 22**,** 108-15.
WALMSLEY, S. R. 2019. Immune-cell function under pressure. *Nature,* 573**,** 41-42.
WANG, H., SUN, W., MA, J. Q., PAN, Y. C., WANG, L. & ZHANG, W. B. 2014. Polycystin-1 Mediates Mechanical Strain-Induced Osteoblastic Mechanoresponses via Potentiation of Intracellular Calcium and Akt/beta-Catenin Pathway. *Plos One,* 9.

WANG, H. Z. & ZHANG, X. 2017. Magnetic Fields and Reactive Oxygen Species. *International Journal of Molecular Sciences,* 18.

WANG, L., SUN, B., ZIEMER, K. S., BARABINO, G. A. & CARRIER, R. L. 2010. Chemical and physical modifications to poly(dimethylsiloxane) surfaces affect adhesion of Caco-2 cells. *J Biomed Mater Res A,* 93**,** 1260-71.

WANG, L. J., YOU, X. L., LOTINUN, S., ZHANG, L. L., WU, N. & ZOU, W. G. 2020. Mechanical sensing protein PIEZO1 regulates bone homeostasis via osteoblast-osteoclast crosstalk. *Nature Communications,* 11.

WANG, M. N., VANHOUTEN, J. N., NASIRI, A. R., JOHNSON, R. L. & BROADUS, A. E. 2013. PTHrP regulates the modeling of cortical bone surfaces at fibrous insertion sites during growth. *Journal of Bone and Mineral Research,* 28**,** 598-607.

WANG, X., WANG, Y., GOU, W., LU, Q., PENG, J. & LU, S. 2013. Role of mesenchymal stem cells in bone regeneration and fracture repair: a review. *Int Orthop,* 37**,** 2491-8.

WANG, Y. Y., XU, J. J., ZHANG, X. D., WANG, C. D., HUANG, Y., DAI, K. R. & ZHANG, X. L. 2017. TNF-alpha-induced LRG1 promotes angiogenesis and mesenchymal stem cell migration in the subchondral bone during osteoarthritis. *Cell Death & Disease,* 8.

WEI, Q. S., WANG, B., HU, H. L., XIE, C. H., LING, L., GAO, J. L. & CAO, Y. M. 2020. Icaritin promotes the osteogenesis of bone marrow mesenchymal stem cells via the regulation of sclerostin expression. *International Journal of Molecular Medicine,* 45**,** 816-824.

WILLIAMSON, S., LANDEIRO, F., MCCONNELL, T., FULFORD-SMITH, L., JAVAID, M. K., JUDGE, A. & LEAL, J. 2017. Costs of fragility hip fractures globally: a systematic review and meta-regression analysis. *Osteoporosis International,* 28**,** 2791-2800.

WITTAUER, M., BURCH, M. A., MCNALLY, M., VANDENDRIESSCHE, T., CLAUSS, M., DELLA ROCCA, G. J., GIANNOUDIS, P. V., METSEMAKERS, W. J. & MORGENSTERN, M. 2021. Definition of long-bone nonunion: A scoping review of prospective clinical trials to evaluate current practice. *Injury,* 52**,** 3200-3205.

WOLF, J. H. 1995. [Julis Wolff and his "law of bone remodeling"]. *Orthopade,* 24**,** 378-86.

WOZNIAK, W., MARKUSZEWSKI, J., WIERUSZ-KOZLOWSKA, M. & WYSOCKI, H. 2004. Neutrophils are active in total joint implant loosening. *Acta Orthop Scand,* 75**,** 549-53.

WU, J., GOYAL, R. & GRANDL, J. 2016. Localized force application reveals mechanically sensitive domains of Piezo1. *Nat Commun,* 7**,** 12939.

WU, M., CHEN, G. & LI, Y. P. 2016. TGF-beta and BMP signaling in osteoblast, skeletal development, and bone formation, homeostasis and disease. *Bone Res,* 4**,** 16009.

XIE, Y. F., SHI, W. G., ZHOU, J., GAO, Y. H., LI, S. F., FANG, Q. Q., WANG, M. G., MA, H. P., WANG, J. F., XIAN, C. J. & CHEN, K. M. 2016. Pulsed electromagnetic fields stimulate osteogenic differentiation and maturation of osteoblasts by upregulating the expression of BMPRII localized at the base of primary cilium. *Bone,* 93**,** 22-32.

XU, J., LIU, J., GAN, Y., DAI, K., ZHAO, J., HUANG, M., HUANG, Y., ZHUANG, Y. & ZHANG, X. 2020. High-Dose TGF-beta1 Impairs Mesenchymal Stem Cell-Mediated Bone Regeneration via Bmp2 Inhibition. *J Bone Miner Res,* 35**,** 167-180.

YAN, J. L., ZHOU, J., MA, H. P., MA, X. N., GAO, Y. H., SHI, W. G., FANG, Q. Q., REN, Q., XIAN, C. J. & CHEN, K. M. 2015. Pulsed electromagnetic fields promote osteoblast mineralization and maturation needing the existence of primary cilia. *Molecular and Cellular Endocrinology,* 404**,** 132-140.

YODER, B. K., HOU, X. Y. & GUAY-WOODFORD, L. M. 2002. The polycystic kidney disease proteins, polycystin-1, polycystin-2, polaris, and cystin, are co-localized in renal cilia. *Journal of the American Society of Nephrology,* 13**,** 2508-2516.

YONEDA, M., SUZUKI, H., HATANO, N., NAKANO, S., MURAKI, Y., MIYAZAWA, K., GOTO, S. & MURAKI, K. 2019. PIEZO1 and TRPV4, which Are Distinct Mechano-Sensors in the Osteoblastic MC3T3-E1 Cells, Modify Cell-Proliferation. *Int J Mol Sci,* 20.

YONG, Y., MING, Z. D., FENG, L., CHUN, Z. W. & HUA, W. 2016. Electromagnetic fields promote osteogenesis of rat mesenchymal stem cells through the PKA and ERK1/2 pathways. *Journal of Tissue Engineering and Regenerative Medicine,* 10**,** E537-E545.

YU, V. W. C., SAEZ, B., COOK, C., LOTINUN, S., PARDO-SAGANTA, A., WANG, Y. H., LYMPERI, S., FERRARO, F., RAAIJMAKERS, M. H. G. P., WU, J. Y., ZHOU, L., RAJAGOPAL, J., KRONENBERG, H. M., BARON, R. & SCADDEN, D. T. 2015. Specific bone cells produce DLL4 to generate thymus-seeding progenitors from bone marrow. *Journal of Experimental Medicine,* 212**,** 759-774.

YUAN, J., XIN, F. & JIANG, W. X. 2018. Underlying Signaling Pathways and Therapeutic Applications of Pulsed Electromagnetic Fields in Bone Repair. *Cellular Physiology and Biochemistry,* 46**,** 1581-1594.

YUAN, X. & YANG, S. 2016. Primary Cilia and Intraflagellar Transport Proteins in Bone and Cartilage. *J Dent Res,* 95**,** 1341-1349.

YUAN, X. & YANG, S. Y. 2015. Cilia/Ift protein and motor-related bone diseases and mouse models. *Frontiers in Bioscience-Landmark,* 20**,** 515-555.

YUE, J. B. & MULDER, K. M. 2001. Transforming growth factor-beta signal transduction in epithelial cells. *Pharmacology & Therapeutics,* 91**,** 1-34.

ZARAGOZA, C., MARQUEZ, S. & SAURA, M. 2012. Endothelial mechanosensors of shear stress as regulators of atherogenesis. *Current Opinion in Lipidology,* 23**,** 446-452.

ZHANG, B. Y., ZHANG, T. T., WANG, G. P., WANG, G., CHI, W. F., JIANG, Q. & ZHANG, C. M. 2015. GSK3 beta-Dzip1-Rab8 Cascade Regulates Ciliogenesis after Mitosis. *Plos Biology,* 13.

ZHANG, F., WANG, H. S., WANG, X. F., JIANG, G. M., LIU, H., ZHANG, G., WANG, H., FANG, R., BU, X. Z., CAI, S. H. & DU, J. 2016. TGF-beta induces M2-like macrophage polarization via SNAIL-mediated suppression of a pro-inflammatory phenotype. *Oncotarget,* 7**,** 52294-52306.

ZHANG, G., LI, X., WU, L. & QIN, Y. X. 2021. Piezo1 channel activation in response to mechanobiological acoustic radiation force in osteoblastic cells. *Bone Res,* 9**,** 16.

ZHANG, R., LIANG, Y. & WEI, S. 2018. M2 macrophages are closely associated with accelerated clavicle fracture healing in patients with traumatic brain injury: a retrospective cohort study. *J Orthop Surg Res,* 13**,** 213.

ZHANG, Y., YAN, J., XU, H., YANG, Y., LI, W., WU, H. & LIU, C. 2018. Extremely low frequency electromagnetic fields promote mesenchymal stem cell migration by increasing intracellular Ca(2+) and activating the FAK/Rho GTPases signaling pathways in vitro. *Stem Cell Res Ther,* 9**,** 143.

ZHAO, Z. X., LI, Y. F., WANG, M. J., ZHAO, S., ZHAO, Z. H. & FANG, J. 2020. Mechanotransduction pathways in the regulation of cartilage chondrocyte homoeostasis. *Journal of Cellular and Molecular Medicine,* 24**,** 5408-5419.

ZHOU, T., GAO, B., FAN, Y., LIU, Y., FENG, S., CONG, Q., ZHANG, X., ZHOU, Y., YADAV, P. S., LIN, J., WU, N., ZHAO, L., HUANG, D., ZHOU, S., SU, P. & YANG, Y. 2020. Piezo1/2 mediate mechanotransduction essential for bone formation through concerted activation of NFAT-YAP1-ss-catenin. *Elife,* 9.

ZIEGLER, P., NUSSLER, A. K., WILBRAND, B., FALLDORF, K., SPRINGER, F., FENTZ, A. K., ESCHENBURG, G., ZIEGLER, A., STOCKLE, U., MAURER, E., ATESCHRANG, A., SCHROTER, S. & EHNERT, S. 2019. Pulsed Electromagnetic Field Therapy Improves Osseous Consolidation after High Tibial Osteotomy in Elderly Patients-A Randomized, Placebo-Controlled, Double-Blind Trial. *Journal of Clinical Medicine,* 8.

ZIEGLER, P., NUSSLER, A. K., WILBRAND, B., FALLDORF, K., SPRINGER, F., FENTZ, A. K., ESCHENBURG, G., ZIEGLER, A., STOCKLE, U., MAURER, E., ATESCHRANG, A., SCHROTER, S. & EHNERT, S. 2019. Pulsed Electromagnetic Field Therapy Improves Osseous Consolidation after High Tibial Osteotomy in Elderly Patients-A Randomized, Placebo-Controlled, Double-Blind Trial. *J Clin Med,* 8.

ZURA, R., MEHTA, S., DELLA ROCCA, G. J. & STEEN, R. G. 2016. Biological Risk Factors for Nonunion of Bone Fracture. *JBJS Rev,* 4.

ZURA, R., XIONG, Z., EINHORN, T., WATSON, J. T., OSTRUM, R. F., PRAYSON, M. J., DELLA ROCCA, G. J., MEHTA, S., MCKINLEY, T., WANG, Z. & STEEN, R. G. 2016. Epidemiology of Fracture Nonunion in 18 Human Bones. *JAMA Surg,* 151**,** e162775.

7. Declaration of the contribution of others

I, Yangmengfan Chen, declare that this submitted doctoral thesis was written by myself under the guidance of PD Dr. Sabrina Ehnert. Only manuscripts on which I was the first author and the main person involved in the planning, performance, data analysis, and writing of the manuscripts were included in this thesis. Neither the whole thesis nor part of this thesis have been submitted for the application of any degree. All of the work in this thesis is mine, except for the references.

7.1 Exposure to 16 Hz Pulsed Electromagnetic Fields Protects the Structural Integrity of Primary Cilia and Associated TGF-β Signaling in Osteoprogenitor Cells Harmed by Cigarette Smoke.

CHEN, Y., ASPERA-WERZ, R. H., MENGER, M. M., FALLDORF, K., RONNIGER, M., STACKE, C., HISTING, T., NUSSLER, A. K. & EHNERT, S. 2021. Exposure to 16 Hz Pulsed Electromagnetic Fields Protect the Structural Integrity of Primary Cilia and Associated TGF-beta Signaling in Osteoprogenitor Cells Harmed by Cigarette Smoke. Int J Mol Sci, 22.

The conceptualization of this study was performed by PD Dr. Sabrina Ehnert;

The methodology was designed and developed by Mr. Yangmengfan Chen under the guidance of Dr. Romina Aspera-Werz, and PD Dr. Sabrina Ehnert;

The software was authorized by Dr. Michael Ronniger, Prof. Dr. Andreas K. Nüssler, and Prof. Dr. Tina Histing;

Study validation, formal analyses, and investigation were performed by Mr. Yangmengfan Chen, and PD Dr. Sabrina Ehnert;

Resources were provided by Dr. Maximilian M. Menger, Mr. Karsten Falldorf, Prof. Dr. Andreas K. Nüssler, and Prof. Dr. Tina Histing;

Data curation was performed by Dr. Christina Stacke, and PD Dr. Sabrina Ehnert;

The original draft was prepared by Mr. Yangmengfan Chen under the guidance of PD Dr. Sabrina Ehnert;

Review and editing were performed by all authors;

Data visualization was performed by Dr. Michael Ronniger and PD Dr. Sabrina Ehnert;

Supervision was provided by Prof. Dr. Andreas K. Nüssler and Dr. Sabrina Ehnert;

Project administration was authorized by Prof. Dr. Andreas K. Nüssler;

Funding was acquired by Prof. Dr. Andreas K. Nüssler and PD Dr. Sabrina Ehnert.

7.2 Modulation of Macrophage Activity by Pulsed Electromagnetic Fields in the Context of Fracture Healing

CHEN, Y., MENGER, M. M., BRAUN, B. J., SCHWEIZER, S., LINNEMANN, C., FALLDORF, K., RONNIGER, M., WANG, H., HISTING, T., NUSSLER, A. K. & EHNERT, S. 2021. Modulation of Macrophage Activity by Pulsed Electromagnetic Fields in the Context of Fracture Healing. Bioengineering (Basel), 8.

The conceptualization of the study was performed by PD Dr. Sabrina Ehnert;

The methodology was designed and developed by Mr. Yangmengfan Chen, Dr. Caren Linnemann, Dr. Michael Ronniger, and PD Dr. Sabrina Ehnert;

The software was authorized by PD Dr. Benedikt J. Braun, Prof. Dr. Hongbo Wang, Prof. Dr. Andreas K. Nüssler, and Prof. Dr. Tina Histing;

Study validation, formal analyses, and investigation were performed by Mr. Yangmengfan and in part by Sara Schweizer;

The resources were provided by Dr. Maximilian M. Menger, Mr. Karsten Falldorf, Prof. Dr. Hongbo Wang, Prof. Dr. Andreas K. Nüssler, and Prof. Dr. Tina Histing;

Data curation was performed by PD Dr. Sabrina Ehnert;

The original draft was prepared by Mr. Yangmengfan Chen and Dr. Sabrina Ehnert;

Review and editing were performed by all authors;

Data visualization was performed by Mr. Yangmengfan Chen under the guidance of PD Dr. Sabrina Ehnert;

Supervision was provided by PD Dr. Sabrina Ehnert, and Prof. Dr. Andreas K. Nüssler;

Project administration was authorized by Prof. Dr. Andreas K. Nüssler;

Funding was acquired by Prof. Dr. Andreas K. Nüssler and PD Dr. Sabrina Ehnert.

08th July, 2022, Tübingen

Yangmengfan Chen

8. Acknowledgments

It is my great honor to express my wholehearted appreciation to all participants who are involved in this project, especially in the difficult corona situation.

My deepest thanks go firstly to my supervisor PD Dr. Sabrina Ehnert who provided me with numerous suggestions and patient guidance during my whole 3 years of study at the Siegfried Weller Institute (SWI). Sabrina devoted considerate care and efforts to refine my idea and polish my manuscript, even though she has lots of work to do. It is my great honor to learn from her diligent, serious, and rigorous spirits, her influence and selfless support treasure my whole life.

Importantly, my sincere gratitude goes to Prof. Andreas K. Nüssler for his kindly care, selfless instruction, valuable inspiration, and profound knowledge. Prof. Nüssler gave me the precious offer to be a Ph.D. student at Tübingen University 3 years ago. And I will never forget that Prof. Nüssler spend lots of time encouraging me, instructing me, and helping me. Prof. Nüssler is the most important person in my career.

I appreciate Dr. Caren Linnemann, Dr. Romina H. Aspera-Werz, Dr. Victor Häussling, Dr. Jonas Mück, Dr. Marc Ruoß, Ms. Helen Rinderknecht, Ms. Regina Breinbauer, Ms. Bianca Braun for, Ms. Sara Schweizer, and Mrs. Svetlana Gasimova for their cheerful cooperation in the lab.

Great thanks to my Ph.D. committee members Prof. Ralf Kemkemer, Prof. Fabian Springer, and Dr. Inka Montero, for their valuable suggestions, warm-hearted help, and kindly guidance.

I would like to express my thanks to Dr. Michael Ronniger, Dr. Christina Stacke, and Mr. Karsten Falldorf who provided me with lots of technical support for the ELF-PEMF system.

Thanks to my Chinese community at the SWI, Dr. Tao Chen, Dr, Sheng Zhu, Dr. Zi Li, Mr. Huizhi Guo, Mr. Chao Liu, and Mr. Xiaowei Huang. I will never forget the happy time we spent together. Great thanks to Dr. Chao Lu and Dr. Weidong Weng, not only for the happy memories but also for their countless suggestions and encouragement when I needed them.

Special thanks to my girlfriend Ms. Yichen Dai, who accompanied me for almost 3 years in Tübingen. I will be waiting for you in China.

I also like to express my appreciation to my country and China Scholarship Council because they allowed me to study abroad and covered all my living expenses.

In the end, I would express my thanks to my parents for their selfless support and understanding.

9. Annex

9.1 Ethics statement

All experiments that needed human tissues were strictly performed according to the 1964 Helsinki declaration and its latest amendment. The blood samples were isolated from healthy volunteers with a signed consent agreement. Corresponding ethical votes (541/2016BO2 approved 09.08.2016) were agreed by the Ethics Committee of the University Clinic Tübingen.

9.2 Proof of agreement of all authors with a statement of contributions

EBERHARD KARLS
UNIVERSITÄT
TÜBINGEN

Faculty of Medicine

Declaration of contributions

Herewith I, Yangmengfan Chen declare, that I have contributed to the major part of the following publication:
Modulation of Macrophage Activity by Pulsed Electromagnetic Fields in the Context of Fracture Healing
The authors contributed to the publications as indicated in the following table (indicated in %):

Contribution	Yangmengfan Chen	Maximilian M. Menger	Benedikt J. Braun	Sara Schweizer	Caren Linnemann	Karsten Falldorf	Michael Ronniger	Hongbo Wang	Tina Histing	Andreas K. Nüssler	Sabrina Ehnert
Conceptualization											100%
Methodology	25%				25%		25%				25%
Software			20%				20%	20%	20%	20%	
Validation											100%
Formal analyses	100%										
Investigation	50%			50%							
Resources		10%				10%	10%	10%	30%	30%	
Data curation											100%
Original draft preparation	50%										50%
Review and editing	8%	8%	8%	8%	8%	8%	8%	8%	8%	8%	20%
Visualization	30%						30%				40%
Supervision										50%	50%
Project administration										100%	
Funding acquisition										50%	50%

Signature of the doctoral candidate:

[redacted]

As supervisor, I agree with the declarations by the candidate:

[redacted]

As corresponding author, I agree with the declarations by the candidate: (S E)

[redacted]

As co-authors, we agree to the declarations above:

[redacted]

[Maximilian M. Menger] [Benedikt J. Braun] [Sara Schweizer] [Caren Linnemann] [Karsten Falldorf]

[redacted]

[Michael Ronniger] [Hongbo Wang] [Tina Histing] [Andreas K. Nüssler]

Version: August 2020

2

EBERHARD KARLS
UNIVERSITÄT
TÜBINGEN

Faculty of Medicine

Declaration of contributions

Herewith I, Yangmengfan Chen declare, that I have contributed to the major part of the following publication:
Exposure to 16 Hz Pulsed Electromagnetic Fields Protect the Structural Integrity of Primary Cilia and Associated TGF-β Signaling in Osteoprogenitor Cells Harmed by Cigarette Smoke
The authors contributed to the publications as indicated in the following table (indicated in %):

Contribution	Yangmengfan Chen	Romina H. Aspera-Werz	Maximilian M. Menger	Karsten Falldorf	Michael Ronniger	Christina Stacke	Tina Histing	Andreas K. Nüssler	Sabrina Ehnert
Conceptualization									100%
Methodology	25%	25%			25%				25%
Software					40%		30%	30%	
Validation									100%
Formal analyses	100%								
Investigation	100%								
Resources			20%	20%	20%		20%	20%	
Data curation						50%			50%
Original draft preparation	50%								50%
Review and editing	10%	10%	10%	10%	10%	10%	10%	10%	20%
Visualization	30%				30%				40%
Supervision								50%	50%
Project administration								100%	
Funding acquisition								50%	50%

Signature of the doctoral candidate:

[redacted]

As supervisor, I agree with the declarations by the candidate:

[redacted]

As corresponding author, I agree with the declarations by the candidate: (prof. Nüssler)

[redacted]

As co-authors, we agree to the declarations above:

[redacted]

[Romina H. Aspera-Werz] [Maximilian M. Menger] [Karsten Falldorf]

[redacted]

[Michael Ronniger] [Christina Stacke] [Tina Histing] [Sabrina Ehnert]

Version: August 2020